Master's thesis

NTNU
Norwegian University of Science and Technology
Faculty of Natural Sciences
Department of Biotechnology and Food Science

Alexander Mika Hannasvik

Marine sponges from the Trondheim fjord: Exploration of biomass and sulfated polysaccharides

Master's thesis in Biotechnology (MBIOT5)
Supervisor: Finn L. Aachmann
Co-supervisor: Leesa J. Klau
May 2023

NTNU
Norwegian University of
Science and Technology

Alexander Mika Hannasvik

Marine sponges from the Trondheim fjord: Exploration of biomass and sulfated polysaccharides

Master's thesis in Biotechnology (MBIOT5)
Supervisor: Finn L. Aachmann
Co-supervisor: Leesa J. Klau
May 2023

Norwegian University of Science and Technology
Faculty of Natural Sciences
Department of Biotechnology and Food Science

NTNU
Norwegian University of
Science and Technology

Preface

This master project was conducted at the Department of Biotechnology and Food Science at the Norwegian University of Science and Technology (NTNU) from August 2022 till May 2023. The thesis is mainly based on findings from marine sponges from the Trondheim fjord. Those being *Antho dichotoma, Geodia barretti*, *Mycale lingua,* and *Phakellia ventilabrum*. A lot of work was also done on structural elucidation of enzymatically degraded fucoidan fractions from the brown algae *Macrocystis pyrifera*. This was in connection with a different project and can be found under the Additional contributions chapter.

Acknowledgements

Firstly, I would like to thank my supervisor Professor Finn L. Aachmann for giving me the opportunity to be part of his research group and always providing invaluable advice. Working in a group with such a wealth of knowledge has been both inspiring and motivating. As the project was on the exploratory side of research, it could at times be difficult to realize where to focus my efforts. Therefore, I am extremely grateful to my co-supervisor Leesa J. Klau for sharing her knowledge and always taking the time to answer any question I might have.

I am also grateful to Turid Rustad and her research group for kindly providing me with enzymes and helping me perform a total amino acid analysis. Thanks to fellow master student Tara for teaching me C-PAGE and collaboration on NMR spectroscopy of fucoidan samples. This project would not be possible without the sponge material provided by Alexander Wentzel and Francesca Di Bartolomeo from SINTEF Industry Dept of Biotechnology and Nanomedicine. So, a big thank you to Alexander and Francesca for giving me the opportunity to work with what in my mind are fascinating and under-appreciated animals.

Finally, a thank you to friends and family who have encouraged me throughout my time at NTNU.

Abstract

Sponges are sedentary animals believed to be the last common ancestor of all living animals and among the first multicellular animals to emerge. Sponges contain unique proteoglycans which are essential for cell aggregation, these proteoglycans are aptly named aggregation factors. Connected to a central protein are high molecular weight polysaccharides (~200 kDa) with sulfated residues. The sulfate esters mediate aggregation with adjacent aggregation factors through interactions with calcium ions. Aggregation factors are species specific, both in chemical composition and three-dimensional structure. As sulfated polysaccharides like heparin and fucoidans display useful bioactivities, sulfated polysaccharides from sponges have gathered interest. One example of bioactivity displayed by sulfated polysaccharides from sponges is aggregation factor polysaccharides from the sponge *Microciona prolifera*, which was found to inhibit replication of human immunodeficiency virus (HIV).

The objectives for this thesis were twofold, firstly was the exploration of sponge biomass. Work was centered around four species of marine sponges from the Trondheim fjord, those being *Antho dichotoma*, *Geodia barretti*, *Mycale lingua*, and *Phakellia ventilabrum*. These were sampled by cooperators from SINTEF Industry Dept of Biotechnology and Nanomedicine under the MARBLES project. Explored biomass parameters included water and ash contents, elemental content, neutral monosaccharide profiles, and total amino acid profiles. Each analysis revealed variations in biomass composition across the species. Some similarities were observed, such as a much higher glycine/arginine, glutamic acid, and aspartic acid content than what is normally observed in other proteins. This is likely due to a large proportion of sponge biomass being composed of a type of collagen called spongin, which is rich in glycine. High glutamic acid and aspartic acid levels might be explained by a large amount of aggregation factors, as aggregation factors from the sponge *Microciona parthena* have been reported to contain unusually high amounts of these amino acids.

The second objective for this thesis was to develop a protocol for extraction of sulfated polysaccharides from sponge aggregation factors and to elucidate their structures using NMR spectroscopy. Three main methods were used to extract polysaccharides. The structure of a polysaccharide obtained by utilizing calcium chloride as precipitant was elucidated using two-

dimensional NMR experiments. Extracts from *Antho dichotoma*, *Geodia barretti*, *Mycale lingua*, and *Phakellia ventilabrum* all contained α-1,4-glucans, likely energy-storage polysaccharides and not aggregation factor polysaccharides. None of the methods yielded samples which could be used to elucidate the structure of aggregation factor polysaccharides. Further analysis of the polysaccharide extracts using carbohydrate polyacrylamide gel electrophoresis revealed that all α-1,4-glucan containing samples apart from one, had an ionic component to it. One explanation could be presence of uronic acids or sulfate esters, which has been found in glycogen from the species *Aplysina fulva*. An extract made based using cetylpyridinium chloride as precipitant had a darker color than other samples after the electrophoresis, indicating a higher content of ionic components. While it is possible some of the extracts contained sulfated polysaccharides, further purification would be required to obtain a sample suitable for NMR spectroscopy.

In addition to the work on marine sponges, NMR spectroscopy was performed on fucoidan oligomers from the brown algae *Macrocystis pyrifera*. Two fractions of enzymatically degraded fucoidan obtained by size-exclusion chromatography were analyzed. The first fraction contained 2,4-disulfated-L-fucose monomers. The second fraction contained 2,4- and 3-sulfated-L-fucose units, some of which were 1→3 linked.

Sammendrag

Svamper er fastsittende dyr som antas å være den siste felles stamfar til alle levende dyr og blant de aller første flercellede dyrene til å oppstå. Svamper inneholder unike proteoglykaner som er nødvendige for celleaggregering, disse har fått det passende navnet aggregasjonsfaktorer. Festet til et sentralt protein er polysakkarider med høy molekylvekt (~200 kDa) og sulfaterte monosakkarider. Sulfatesterne medierer aggregasjon med andre nærliggende aggregasjonsfaktorer gjennom interaksjoner med kalsiumioner. Aggregasjonsfaktorer er artsspesifikke, både i kjemisk sammensetning og tredimensjonal struktur. Ettersom sulfaterte polysakkarider som heparin og fukoidan har vist nyttige bioaktiviteter har det også oppstått interesse for sulfaterte polysakkarider fra svamper. Et eksempel på bioaktivitet funnet hos sulfaterte polysakkarider fra svamper er aggregasjonsfaktorpolysakkarider fra svampen *Microciona prolifera*, som inhiberte replikasjon av humant immunsvikt-virus (HIV).

Målene for dette prosjektet var todelte, første mål var utforskning av svampers biomasse. Arbeidet var sentrert rundt fire marine svamper fra Trondheimsfjorden, *Antho dichotoma*, *Geodia barretti*, *Mycale lingua*, og *Phakellia ventilabrum*. Disse ble samlet av samarbeidspartnere fra SINTEF industri, avdeling for bioteknologi og nanomedisin i forbindelse med prosjektet MARBLES. Utforskede biomasseparametere inkluderer vann og askeinnhold, grunnstoffinnhold, nøytrale monosakkarid-profiler, og totale aminosyre-profiler. Hver analyse avdekte variasjoner av biomassesammensetning på tvers av artene. Noen likheter ble observert, eksempelvis et mye høyere glysin/arginin, glutaminsyre, og asparaginsyre-innhold enn hva som vanligvis observeres i andre proteiner. Dette kommer trolig av et høyt «spongin» innhold i svamper. Spongin er en type kollagen og er i likhet med annet kollagen rikt på glysin. Høyt glutaminsyre og asparaginsyre-innhold kan forklares av et høyt aggregasjonsfaktorinnhold, ettersom aggregasjonsfaktorer fra svampen *Microciona parthena* har vist seg å ha uvanlig høyt innhold av disse aminosyrene.

Det andre målet for prosjektet var å utvikle en protokoll for ekstraksjon av sulfaterte polysakkarider fra svampers aggregasjonsfaktorer, og avklare deres struktur ved å bruke NMR-spektroskopi. Tre sentrale metoder ble benyttet for å ekstrahere polysakkarider. Strukturen til et polysakkarid ekstrahert ved å benytte kalsiumklorid som utfellingsmiddel ble avklart ved å bruke

todimensjonale NMR-eksperiment. Ekstrakter fra *Antho dichotoma*, *Geodia barretti*, *Mycale lingua*, og *Phakellia ventilabrum* inneholdte α-1,4-glukaner, trolig energilagringspolysakkarider og ikke aggregasjonsfaktorpolysakkarider. Ingen av metodene ga prøver som kunne benyttes til å strukturavklare aggregasjonsfaktorpolysakkarider. Videre analyser med karbohydrat-polyakrylamid-gelelektroforese avslørte at alle prøvene med α-1,4-glukaner, med unntak av en, hadde ioniske egenskaper. En mulig forklaring kan være innhold av uronsyrer eller sulfatestere som har blitt funnet i glykogen fra svampen *Aplysina fulva*. Et ekstrakt basert på å bruke cetylpyridiniumklorid som utfellingsmiddel, hadde en mørkere farge enn andre prøver etter elektroforese. Dette indikerte et høyere innhold av ioniske stoffer. Det er mulig noen av ekstraktene inneholdte sulfaterte polysakkarider, men at videre rensing er nødvendig for å oppnå et ekstrakt som kan analyseres med NMR-spektroskopi.

I tillegg til arbeidet i forbindelse med marine svamper ble NMR-spektroskopi utført på fukoidan oligomerer fra brunalgen *Macrocystis pyrifera*. To fraksjoner med enzymatisk nedbrutt fukoidan separert med størrelseseksklusjonskromatografi ble analysert. Den første fraksjonen inneholdte 2,4-sulfaterte-L-fukose monomerer. Den andre fraksjonen inneholdte 2,4- og 3-sulfaterte-L-fukose enheter. Noen av disse var 1→3 bundet.

Symbols and abbreviations

μ	Magnetic moment of nucleus
A	Area of electrode in cm^2
AF	Aggregation factor
Ara	Arabinose
B_0	Flux density of static magnetic field
B_1	Flux density of transmitted magnetic field
c_0	Initial concentration of analyte in mol/cm^3
CAS	Chemical abstracts service number
COSY	Correlation spectroscopy
C-PAGE	Carbohydrate polyacrylamide gel electrophoresis
CPC	Cetylpyridinium chloride
D	Diffusion coefficient of analyte in cm^2/s
D[1]	Relaxation delay
DP	Degree of polymerization
DS	Number of dummy scans
DW	Dry weight
E	Energy of nucleus
EDTA	Ethylenediaminetetraacetic acid
F	The faraday constant
Fuc	Fucose
Gal	Galactose
Glc	Glucose
H2BC	Heteronuclear 2-bond correlation
HexNac	N-acetylated hexose
HexUA	Hexuronic acid
HIV	Human immunodeficiency virus
HMBC	Heteronuclear multiple bond correlation
HPAEC-PAD	High performance anion-exchange chromatography / pulsed amperometric detection
HPLC	High-performance liquid chromatography
HSQC	Heteronuclear single quantum coherence
HSQC-TOCSY	Heteronuclear single quantum coherence - Total correlation spectroscopy

i	Current in ampere
I	Angular momentum quantum number of atomic nuclei
IP-COSY	In phase correlation spectroscopy
M_0	Macroscopic magnetization
M_z	Longitudinal magnetization
$M_{y'}$	Transverse magnetization
Man	Mannose
MWCO	Molecular weight cut-off
NMR	Nuclear magnetic resonance
NOESY	Nuclear Overhauser effect spectroscopy
NS	Number of scans
OPA	*o*-Phthalaldehyde
P	Angular momentum of nuclei
Py	Pyruvate
RO	Reverse osmosis
ROESY	Rotating frame nuclear Overhauser effect spectroscopy
SP	Sulfated polysaccharide
TD	Time domain, size of free induction decay
TEMED	Tetramethylethylenediamine
TOCSY	Total correlation spectroscopy
WW	Wet weight

Table of Contents

1 Introduction

1.1 The biology of sponges

Sponges are sessile filter-feeding animals found in both marine and freshwater environments. There are approximately 8,550 scientifically classified species with great diversity in both morphology and strategies for surviving in their environments. While most sponges obtain food and oxygen by constantly filtering water through their bodies, other strategies have emerged. *Spongilla lacustris,* a freshwater sponge, obtains a substantial portion of its oxygen and carbon from symbiotic photosynthesizing green algae (1). Some marine sponges in the family *Cladorhizidae* have evolved to completely forgo filter feeding as a strategy. To survive in nutrient-poor environments these sponges have become carnivores, capturing small crustaceans using hook-shaped spicules (2).

In general sponges are quite simple organisms, lacking true tissues, specialized organs, and mostly lacking any form of symmetry. Along with being among the simplest animals they are also among the oldest. Exactly how old is a much-debated topic. Some researchers claim a 600-million-year-old fossil resembling modern sponges is the oldest evidence we have (3), while one Canadian scientist presents 890-million-year-old calcified vermiform microstructures as possible evidence for early sponges (4). They are often said to be the oldest animals on earth, the sister group of all other animal lineages. Recent phylogenomic research claims that this role does not belong to sponges, but comb jellies of the *Ctenophora* phylum (5). These claims however have not gone unchallenged (6). Due to their simple structure and placement on the phylogenetic tree, sponges are interesting organisms to turn to when studying the emergence of multicellular animals.

1.2 Aggregation factors – aggregating proteoglycans

Every multicellular animal requires some mechanism to maintain their multicellular morphologies. Most animals possess a layer of tightly packed polarized cells called epithelial cells. These cells are held together by cell junctions consisting of proteins and is only one of many strategies for cell-cell adhesion (7).

It has long been known that sponges dissociate under poor conditions, and reassociate when conditions are favorable (8). The key to this behavior is their unique strategy for cell adhesion. Sponge cell aggregation is mediated by extracellular proteoglycans called aggregation factors (AFs) (9). These proteoglycans are species specific both in chemical composition and three-dimensional structure. This specificity means that sponge cells favor aggregation with cells of their own species (10). The proposed AF structure for the marine sponge *Microciona prolifera* consists of a circular protein with protruding protein arms. Each protein arm has multiple polysaccharides at ~6 kDa in size which interact with receptors on the surface of cell membranes. The central protein carries larger polysaccharides (~200 kDa), which interact with similar polysaccharides on adjacent AFs (10). Figure 1 shows the proposed structure of *Microciona prolifera* AFs. The AFs of *Terpios zeketi* and *Haliclona oculata* do not share the circular structure of *Microciona prolifera* AFs, but seem to have a more linear backbone (11).

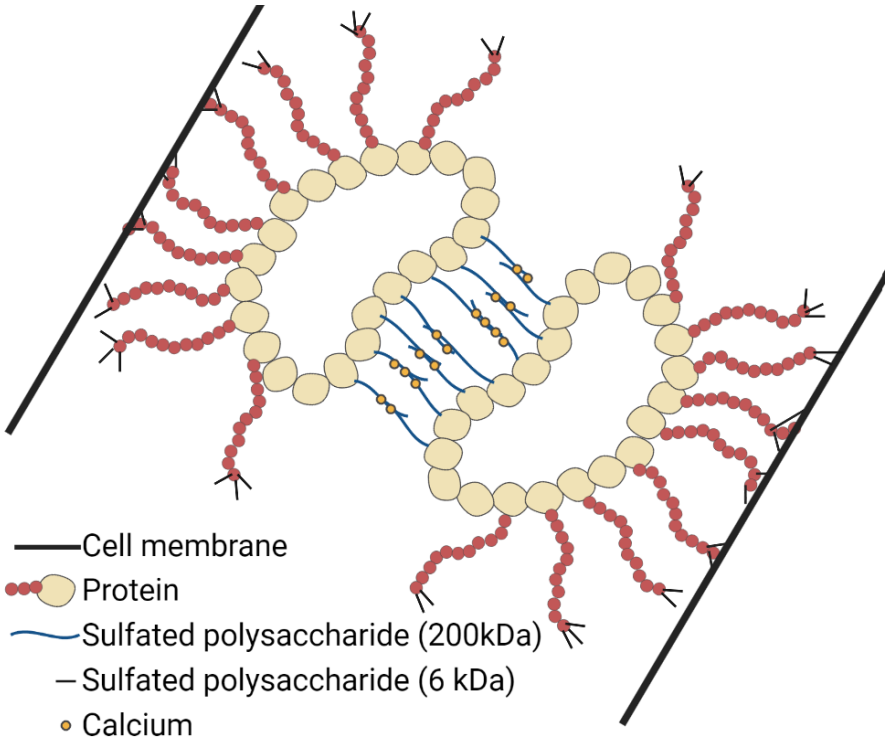

Figure 1: Proposed structure of aggregation factor proteoglycans from the marine sponge *Microciona prolifera*. Illustration based on research by Vilanova, E. *et al.* (12).

The aggregation of sponge cells is mediated by the larger polysaccharides connected to the central protein of the AFs. This self-interaction mechanism is calcium-dependent and mediated by sulfate groups on the polysaccharides of adjacent AFs (12). Sponges that live in calcium-poor

environments, such as the freshwater species *Spongilla alba*, have evolved to require less calcium to aggregate than marine species (13).

1.3 Structure and bioactivity of sulfated polysaccharides

Sulfated polysaccharides (SPs) are sugar molecules modified with negatively charged sulfate groups, making the polysaccharide a polyanion. The degree of sulfation, position of sulfate groups, monosaccharide residues, glycosidic bonds, branching, size, and other chemical modifications are all parameters which can vary among SPs (14). This gives rise to an almost endless number of unique SP structures.

SPs are found in the animal kingdom (15), among marine macroalgae (16), in cyanobacteria (17), freshwater plants (18), and has even been found in archaea (19). In addition to being represented in all domains of life, SPs can also be engineered from non-sulfated polysaccharides, by chemical sulfation (14). A brief list of the some naturally occurring SPs is represented in Table 1.

Table 1: Sulfated polysaccharides and their sources.

Sulfated polysaccharide	Source
Chondroitin sulfate	Animal
Keratan sulfate	Animal
Dermatan sulfate	Animal
Heparan sulfate	Animal
Heparin	Animal
Carrageenan	Red seaweed
Agar	Red seaweed
Fucoidan	Brown seaweed
Ulvan	Green seaweed

Within the food industry SPs are used as thickening and gelling agents, due to the negative charge of the polymer interacting with cations in food solvents starting a gelation process. They can be used to make biodegradable food packaging, both edible and non-edible. These materials prevent the exchange of moisture and oxygen increasing shelf life. The SPs can also be combined with commercial polymers enhancing the materials properties (20).

Perhaps the most important trait of many SPs is their many bioactivities. Defined in the broadest sense bioactivity means to have an effect in biological systems. Bioactivities displayed by SPs include anti-microbial, anti-viral, anti-oxidative, immuneactivation and suppression, and anti-coagulation to mention a few (14). Heparin, a SP found in the connective tissue of all mammals, is widely used as an anticoagulant in clinical medicine. By enhancing the activity of the glycoprotein antithrombin and the protein heparin cofactor II, heparin inhibits thrombin, an enzyme which converts soluble fibrinogen into insoluble fibrin. Fibrin, which is a protein, is polymerized and together with platelets lead to clotting of blood (21).

Fucoidans are SPs found in the cell wall of brown seaweeds from the *Phaeophyceae* class. Common to all fucoidans is the presence of sulfated L-fucose residues, with some variation of other sugar residues. Fucoidan from *Laminaria hyperborea* has been found to consist of 97.8 ± 0.2 % fucose and 2.2 ± 0.2 % galactose likely having a 1→3 linked backbone with extensive branching (22). Like heparin, some fucoidans display anticoagulant bioactivities (23). Other bioactivities include antiviral (24), antimicrobial (25), and anti-inflammatory (26).

Some studies have also been made on the bioactivity of SPs from sponge AFs. MacKenzie *et al*. found that the partially purified AF from *Microciona prolifera* inhibited replication of the human immunodeficiency virus (HIV) by binding to the glycoprotein gp120-CD4 on the virus envelope (27). Similarly, Esteves *et al.* looked at the anti-HIV activity of SPs from three different sponge species, *Erylus discophorus*, *Cliona celata*, and *Stelletta sp.*, with only the crude extracts form *Erylus discophorus* showing high anti-HIV activity (28).

Due to the complexity of SPs and their many possible configurations, it has been difficult to predict how specific changes in the polysaccharide structure will affect the bioactivities of the SPs.

1.4 The biomass composition of sponges

The biomass of any organism is a reflection of its environment and life strategy; thus, the study of an organism's biomass might give a clearer picture of its overall biology. Due to the vast number of sponge species and their morphological differences, combined with the many parameters encompassed by the term "biomass", means there is still a lot to explore.

Biomass analysis done on Antarctic sponges show that there are not only inter species variations, but large intra species variations as well. That is the case for *Tetilla leptoderma* which has been measured to have a water content between 80.2 % and 66.3 % depending on location (29). Similarly, metabolism and biomass has been found to vary with seasonal changes. Morley S. *et al.* measured the water content of *Sphaerotylus antarcticus* to 94.8 % in the summer and 71.6 % in winter. Many of the analyzed species did not display any seasonal variation, such as *Dendrilla antarctica* which had a water content of 86.9 % both in summer and winter (30).

A large portion of the biomass of many sponges is made up by their spicules. Small structural elements made of either calcium carbonate or silica. Spicules come in a variety of shapes and sizes, which are useful characteristics in sponge taxonomy (31). Small microscopic spicules in the µm range are referred to as microscleres, while larger spicules typically in the µm to mm range are referred to as megascleres. The deep-sea sponge *Monorhaphis chuni* create megascleres which reach a length of 3 m and a width of 10 mm (32). A common biomass parameter in sponge research, ash weight, is the mass percentage of the sponge which remains after removal of organic material utilizing high temperature (29). As with water content, there is a large variety in ash content. The ash content of *Dendrilla antarctica* has been measured to 16.4 %, while *Mycale acerata* has a much higher ash content at 72.5 % (30).

Water and ash content are among the most reported biomass parameters, likely due to a lack of instrument requirements and ease of measuring. There are a plethora of other parameters to look at when exploring sponge biomass, some methods for biomass analysis are presented in the following subchapters.

1.4.1 Element analysis

Knowing the proportions of certain elements in a sample can be useful in many situations. The proportion of sulfur might indicate the sulfation degree of polysaccharide samples, while nitrogen content is useful in estimating protein content of foodstuffs using an appropriate conversion factor. Element analyzer instruments can detect carbon, hydrogen, nitrogen, and sulfur in sub-µg amounts.

A dry sample packed in tin foil is combusted at temperatures reaching 1,800 °C while oxygen is introduced directly to the sample. This produces CO_2, H_2O, N_2, N_2O, NO_X, and SO_2. Excess

oxygen gas is removed, nitrogen oxides are reduced to N_2, and the sample gasses pass through selective gas separation columns. Finally, sample elements are quantified with a thermal conductivity detector (33).

1.4.2 Monosaccharide analysis

The total monosaccharide content of a sample is frequently determined by utilizing high-performance anion-exchange chromatography with pulsed amperometric detection (HPAEC-PAD). A sample is prepared by degrading all oligo- and polysaccharides into monosaccharides. This can be achieved by preforming acid hydrolysis. After hydrolysis the sample is neutralized and diluted to the desired concentration before being applied to an anion-exchange column. As the sample is mixed with a high pH mobile phase, hydroxyl groups are converted to oxyanions. These oxyanions interact with the ionic functional groups on the resin inside the column, increasing the elution time. Oxyanions on different monosaccharides interact differently with the column resin resulting in different elution rates (34). As the monosaccharides elute through the column, they are oxidized on the surface of a gold electrode. The current running through the sample is detected, giving a measure of sample concentration. Measured current is expressed by the Cottrell equation (*Eq 1.1*).

$$i = \frac{nFAc_0\sqrt{D}}{\sqrt{\pi t}} \qquad \textit{Eq 1.1}$$

Current (i) is measured in ampere and is given by number of electrons needed to oxidize one molecule of the analyte (n), the Faraday constant (F = 96,485 coulomb/mol), area of the electrode in cm^2 (A), initial concentration of the analyte in mol/cm^3 (c_0), the diffusion coefficient of the analyte in cm^2/s (D), and time in seconds (t). After detection of monosaccharides the potential of the electrode is increased to oxidize the gold surface, releasing the monosaccharides. The electrode is then "reset" by lowering potential to reduce the gold oxide back to gold (34).

1.4.3 Total amino acid analysis

Sample preparation for a total amino acid analysis share some principles with the sample preparation for a monosaccharide analysis. The polymers, protein in this case, in the sample are broken down to their constituent monomers, amino acids in the case of proteins, by acid hydrolysis. The sample is neutralized and diluted before being analyzed. High performance liquid chromatography (HPLC) works by injecting the eluent in a solvent stream through a column with a separation medium. Derivatization of amino acids before column injection is often done to aid in the separation and detection of amino acids. The chemical *o*-Phthalaldehyde (OPA) is commonly used as a derivatization agent as it reacts with primary amines above the amino acids isoelectric point in the presence of thiols. Derivatization of amino acids using OPA forms fluorescent derivatives (35). Amino acids can also be derivatized after being separated in the column, so called post-column derivatization. Detection of the eluent is achieved by using a fluorescence detector. A total amino acid analysis will detect both free amino acids and amino acids in proteins.

1.5 Extraction of sulfated sponge polysaccharides

Extracting and isolating polysaccharides can be challenging due to the complex biological systems they exist in, and the structural heterogeneity of the polysaccharides. As many polysaccharides are hydrophilic, the first step in isolating polysaccharides is often a water extraction. Hot water extractions have been used to extract SPs in seaweeds (36). Other methods include dilute alkaline solutions, organic solvents such as DMSO, and enzymolytic methods (37).

Sulfated polysaccharides have been extracted from several species of sponge with a few different methods. A brief overview of methods used to isolate AF polysaccharides from sponges can be seen in Table 2.

Table 2: Overview of extraction methods used to isolate aggregation factor sulfated polysaccharides in sponges. The table includes a shortened and simplified explanation of extraction methods used and is not a comprehensive list of all methods or sponges. This list does not include additional purification steps performed on the extracts. **Aplysina fulva* did not yield polysaccharides associated with aggregation factors, but an acidic glycogen-like polysaccharide.

Sponge Species	Extraction Method	References
Desmapsamma anchorata *Spongilla alba* *Chondrilla australiensis* *Chondrilla nucula* *Chondrilla sp.* *Aplysina fulva* * *Dysidea fragilis* *Hymeniacidon heliophila*	Protease digestion of sponge tissue, centrifugation, cetylpyridinium chloride (CPC) precipitation of polysaccharides in supernatant, centrifugation, solubilization of polysaccharides in NaCl:ethanol, ethanol precipitation, centrifugation, ethanol washing, lyophilization.	(12,13,38,39)
Myxilla rosacea	Water extraction, sonication, filtration, ultra filtration (300,000 MWCO), gel-filtration chromatography (size exclusion), dialysis, lyophilization.	(40)
Microciona prolifera	Extraction in calcium and magnesium free sea water, AFs dissociated by squeezing through a nylon cloth, centrifugation to precipitate cells, centrifugation of AFs in CsCl, ethanol washing, protease digestion.	(41)
Microciona prolifera *Halichondria panicea* *Cliona celata*	Extraction in calcium and magnesium free artificial sea water, calcium precipitation, ultracentrifugation, acid hydrolysis, collecting of oligosaccharides in ethanol fractions.	(42)

The extraction method outlined for *Desmapsamma anchorata* and other species uses the quaternary ammonium salt cetylpyridinium chloride as a precipitant. These salts form coordination compounds with acidic and high molecular weight polysaccharides. The coordination compounds have very low solubility in aqueous solutions, hence the precipitation of polysaccharides. Polysaccharides can be freed from the coordination compounds by increasing the ionic strength in

the solution. Ethanol can then be used to precipitate polysaccharides while quaternary ammonium salts stay in solution (37).

Extraction of polysaccharides from *Halichondria panicea* utilized calcium chloride as a precipitant. This method is also used in the extraction of alginates form seaweed. The binding of calcium and other divalent ions is especially strong in the G blocks of alginates. G blocks are sections of the polymer consisting exclusively of guluronic acid residues connected with axial – axial linkages. This chemistry causes unique egg-box structures in the calcium binding of alginate gels (43).

Many of the sponge polysaccharides listed in Table 2 have been examined to further understand their structure. Common to all AF SPs is sulfation of certain sugar residues, as this is crucial for cell adhesion (12). Otherwise, these polysaccharides are very heterogenous with a large variety of monosaccharides present, branching patterns, and chemical modifications. Vilanova et al. made an overview of sulfated polysaccharides from marine sponges and their structures, that overview can be seen in Table 3 (38).

Table 3: Structural components of sulfated polysaccharides extracted from marine sponges. Overview made by Vilanova *et al*. (38).

Species	**Sulfated polysaccharide**	**Reference**
Aplysina fulva	HexUA, Glc, (sulfated)	(39)
Chondrilla nucula	HexUA, Ara, Gal, Fuc, (sulfated)	(39)
Cliona celata	Sulfated HexNac, Ara Fuc	(42)
Dysidea robusta	HexUA, Ara, Gal, Fuc 4-*O*-sulfated	(39)
Halichondria panicea	Gal Py(4,6), Fuc, GlcNac *N*-sulfated	(42)
Hymeniacidon heliophila	HexUA, Gal, Fuc, (sulfated)	(39)
Microciona prolifera	Gal, Fuc, Gal Py (4,6), GlcNac *N*-sulfated	(42)
Myxilla rosacea	Glc 4,6-disulfated, Fuc 2,4-disulfated	(40)
Ophlithaspongia tenuis	HexUA, Glc, GlcNac *N*-sulfated	(44)
Suberites ficus	HexUA, GlcNac, Fuc, Man, Gal (sulfated)	(45)

1.6 NMR spectroscopy

1.6.1 Introduction to NMR theory

The following NMR theory section is based on established principles in the field. Information is found in the textbooks Basic One- and Two-Dimensional NMR Spectroscopy (5^{th} edition) and Organic Structure Determination Using 2-D NMR Spectroscopy: A Problem-Based Approach (46,47).

Nuclear magnetic resonance spectroscopy is a frequently utilized method for structural elucidation of unknown molecules, including oligo- and polysaccharides. Advantages of NMR spectroscopy include its non-destructive nature and ability to determine the stereochemistry of sample molecules. From the first NMR experiments on liquid samples in 1946 developed by Felix Bloch and Edward Mills Purcell to the state of the field today, a lot has changed but the principles are the same.

Central to NMR is the angular momentum quantum number of atomic nuclei (I), more commonly referred to as nuclear spin. For nuclei with an even mass number and even number of neutrons, which is the case for carbon-12 ($^{12}_{6}\mathrm{C}$), the spin number $I = 0$. The value of I can be any integer or half-integer between 0 and 8 depending on the nucleus. Nuclear spin gives rise to an intrinsic angular momentum (P) of nuclei, which is proportional to the magnetic moment of the nucleus (μ). As magnetic moment is required to obtain an NMR signal this means that nuclei with $I = 0$, such as carbon-12, are undetectable by NMR. For nuclei to be visible in NMR they must have a non-zero spin. A nucleus in a static magnetic field B_0 applied along the z-axis will precess about the axis in $2I+1$ different orientations. Therefore, a nucleus with $I = ½$ will precess in two orientations, one parallel to the magnetic field and one anti-parallel to the magnetic field. The sum of the z-components of all precessing nuclei gives rise to macroscopic magnetization M_0 (see Figure 2). Macroscopic magnetization is central to signal acquisition; this will be explained later.

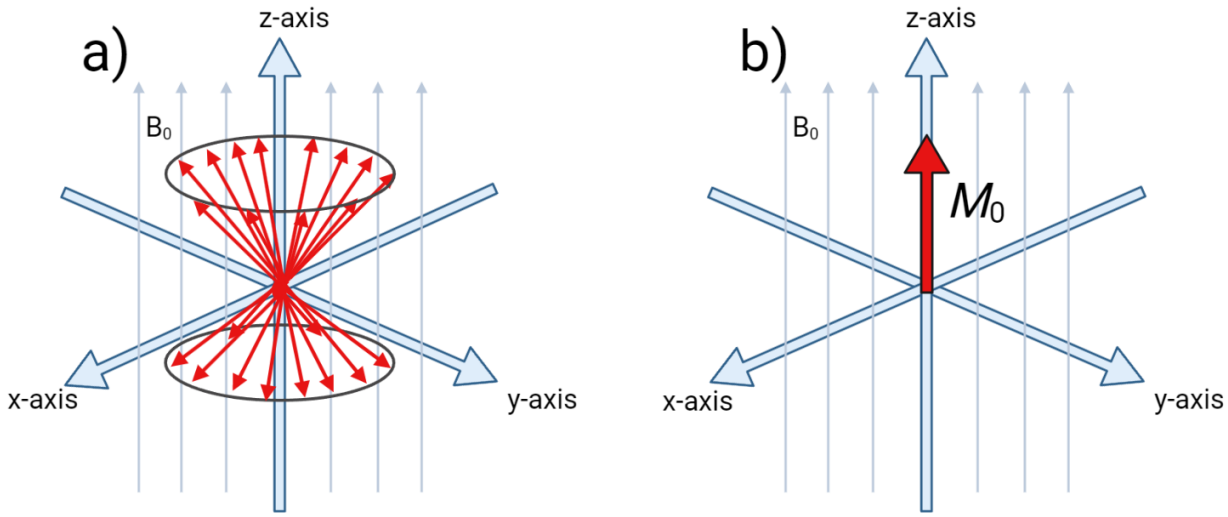

Figure 2: a) Nuclei with nuclear spin number ½ precessing parallel and anti-parallel to the magnetic field B_0. **b)** the sum of precessing nuclei gives rise to macroscopic magnetization M_0.

The precession of nuclei also corresponds to energy states called nuclear Zeeman levels. Each unique orientation corresponds to a Zeeman level. Nuclei with I = ½, such as protons, have two energy states, one parallel (lower energy state) and one anti-parallel (higher energy state) to the magnetic field. There is a slight excess of spin states in the lower energy state. To utilize NMR spectroscopy there needs to be a difference in the populations of energy states. To increase the difference in population levels one can either increase the flux capacity of the magnetic field or lower temperature. To detect signals, a transition between energy levels must be induced. This is achieved by irradiating the sample with an additional magnetic field. The result is absorption of energy for dipoles going from a lower to a higher energy level, and emission of energy for dipoles going from a higher to a lower energy level. If the populations of energy states are equal the absorption and emission of energy is equal and no signal is observed, the system is said to be saturated. An orthogonally applied B_1 pulse from the x-axis ($90^{\circ}_{x'}$) reduces the z-component of the macroscopic magnetization (M_z) and increases its y-component ($M_{y'}$) due to a fraction of nuclear dipoles precessing about the z-axis in phase. After the pulse is switched off relaxation happens, and the magnetization moment returns to its equilibrium position and $M_{y'}$ approaches zero. The effect of a $90^{\circ}_{x'}$ pulse is illustrated in Figure 3.

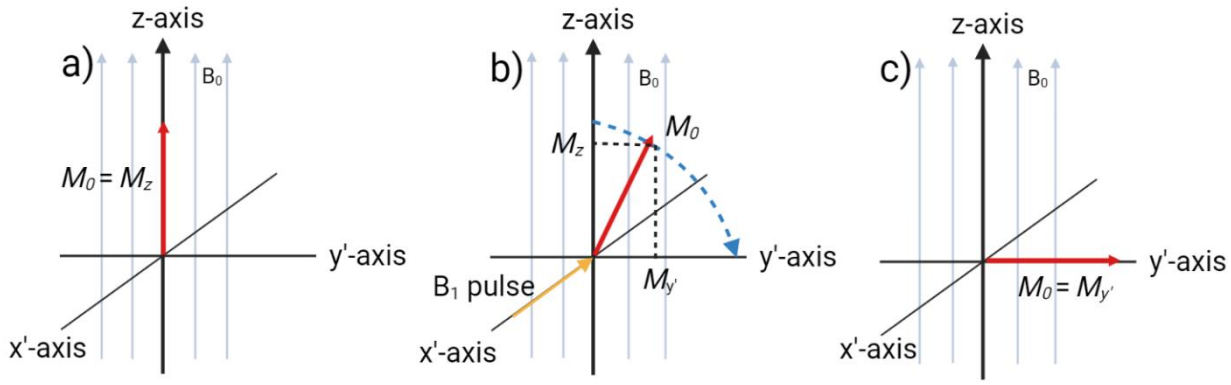

Figure 3: a) A nucleus is held in a static magnetic field B_0, and its macroscopic magnetization (M_0) is aligned along the z-axis. **b)** When a 90° radiofrequency pulse is used to irradiate the nucleus, the macroscopic magnetization is tipped towards the xy-plane. **c)** After the 90° pulse all longitudinal magnetization has disappeared from the z-axis, instead there is transverse magnetization along the y-axis. After the radiofrequency transmitter has been turned off relaxation happens, and the macroscopic magnetization will be realigned along the z-axis (returns to a).

The signal of NMR spectroscopy is recorded by a receiver coil with its axis along the y-direction. Meaning a signal proportional to $M_{y'}$ is induced in the coil. The signal recorded during the decay of transverse magnetization ($M_{y'}$) gives a time domain spectrum showing amplitude as function of time. As a time domain spectrum of more than one signal quickly becomes difficult to analyze, a mathematical operation known as Fourier transformation is used to derive a spectrum in the frequency domain. These frequency spectra are analyzed to derive information from a sample. Chemically non-equivalent nuclei appear at different frequencies in a spectrum. The nuclei are said to have chemical shifts. The chemical shift is obtained by dividing the frequency difference between the sample and an internal standard by the frequency of the internal standard. The frequency difference is commonly only a few hundred Hz, while the frequency of the internal standard is typically several hundred MHz. Chemical shift values are as a result given as parts per million (ppm).

Since nuclei in molecules are surrounded by electrons and other atoms, the effective magnetic field at the nuclei is less than the static magnetic field B_0. This phenomenon is known as shielding. Chemically non-equivalent nuclei are shielded differently; therefore, signals of these nuclei appear at different chemical shifts. In general, shielding increases with number of electrons. The protons of CH_4 will be more shielded (have a lower chemical shift) than the protons of CH_3Cl due to

chloride being more electronegative than carbon and decreasing electron density around the protons. The effect is even more pronounced for CH_2Cl_2 and $CHCl_3$.

Another property that can be visualized using NMR spectroscopy is spin-spin coupling, a through-bond effect between different nuclei. Considering a system with a CH group bound to a CH_2 group, the protons of the groups are affected by indirect spin-spin coupling. The z-component of the magnetic moment of each nucleus can be either parallel (↑) or anti-parallel (↓) to the magnetic field (B_0). This means the proton of the CH group is affected by the neighboring protons (of the CH_2 group) in four different combinations of magnetic moment orientations, (↑↑), (↓↑), (↑↓), and (↓↓). The two anti-parallel spin arrangements (↓↑ and ↑↓) cancel each other, giving no additional field contribution to the proton signal of the CH proton. Both parallel spin arrangements give rise to additional field contributions on each side of the signal with no additional field contributions. The result is a triplet with intensity ratios of 1:2:1 as can be seen in Figure 4. The effective magnetic field a nucleus experiences is the sum of the B_0 and any affect from neighboring nuclei. There are many other splitting patterns based on different indirect spin-spin coupling arrangements.

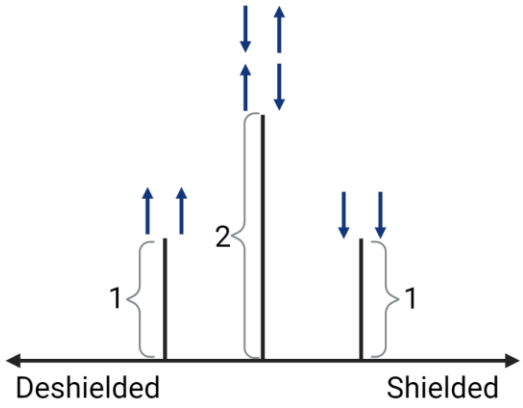

Figure 4: Example of how the signal of a proton in a ^1H spectrum is split by a neighboring CH_2 group. The four possible combinations of magnetic moment orientations of the CH_2 group, indicated by arrows, causes the signal to be split into a triplet with intensities 1:2:1.

In addition to chemical shifts and splitting patterns, other information can also be gathered from proton spectra. The area under signals in a ^1H spectrum can be calculated giving integrals. These integrals are proportional to the number of atoms and so by comparing these integrals the ratio of protons in a molecule can be found.

1.6.2 Utilization of NMR spectroscopy in structural elucidation

When elucidating the structure of complex molecules a single spectrum is in most cases insufficient. Normally a combination of one- and two-dimensional experiments are required for full elucidation of the molecular structure. In 1D experiments there is one frequency axis while 2D experiments have two frequency axes. 2D experiments can either be homonuclear, analyzing a single species of nuclei such as ^{1}H, or heteronuclear, analyzing more than one species of nuclei at the time such as ^{1}H and ^{13}C.

The ^{1}H spectrum is often the first spectrum recorded for a sample due to its useful information and short acquisition time. As mentioned in section 1.6.1, information available in a ^{1}H spectrum includes the chemical shift of protons, their splitting patterns, and integrals. In the case of oligo- and polysaccharides, integrals are useful in finding the relative abundance of different sugar residues in a sample. The chemical shift of protons in polysaccharide experiments appear in the same general regions. Anomeric signals appear in the 4.4 – 5.6 ppm region, secondary alcohol signals usually have a chemical shift of 3.0 – 4.0 ppm, and CH_3 groups on deoxy sugars are found in the 1.0 – 1.5 ppm region (48).

COSY (correlation spectroscopy) is a 2D experiment with two frequency axes for a single isotope, commonly proton, displaying through bond couplings. Using glucose as an example, the anomeric proton would correlate to the proton on position two. By analyzing correlations from the proton on position two and so on, the whole ring of a sugar residue can be identified. TOCSY (total correlation spectroscopy) is another homonuclear experiment identifying the resonances of all protons in a coupled spin-system. In the case of a polysaccharide where each sugar residue is a coupled spin-system, the experiment is especially useful. While COSY and TOCSY identify through-bond correlations, there are also through-space correlation methods. The NOESY (nuclear overhauser effect spectroscopy) and ROESY (rotating-frame nuclear overhauser effect spectroscopy) experiments detect dipole-dipole interactions through space. These experiments provide correlation signals of nuclei closer than 5.0 Å apart, making the techniques useful in determining three-dimensional structure. When working with oligo- and polysaccharides through-space correlation methods help determine the glycosidic linkages.

HSQC (heteronuclear single quantum coherence) is a heteronuclear experiment with two frequency axes, commonly one for proton and one for carbon chemical shifts. Each signal

corresponds to one or more protons directly attached to a carbon. As the proton spectra for oligo- and polysaccharides can be crowded, especially in the 3.0 – 4.4 ppm region, HSQC spectra separates signals in both the proton and carbon axes making them a lot easier to distinguish. The HMBC (heteronuclear multiple-bond correlation spectroscopy) experiment is a heteronuclear correlation experiment, identifying correlations two to four bonds away ($^{2}J_{CH}$ - $^{4}J_{CH}$). In oligo- and polysaccharide samples the HMBC experiment can detect correlations through the glycosidic bond. While the HMBC spectrum is useful, distinguishing two- and three-bond correlations from each other can be challenging. This problem can be alleviated by performing a H2BC (heteronuclear 2-bond correlation) experiment, which only detects two-bond heteronuclear correlations (49). The previously mentioned TOCSY experiment can be combined with a HSQC experiment resulting in a HSQC-TOCSY spectrum. Instead of only identifying all protons within the same spin-system, HSQC-TOCSY also detects ^{13}C atoms within the spin systems.

A brief overview of information different NMR spectra can give in the case of an α-1,4-glucan is shown in Figure 5.

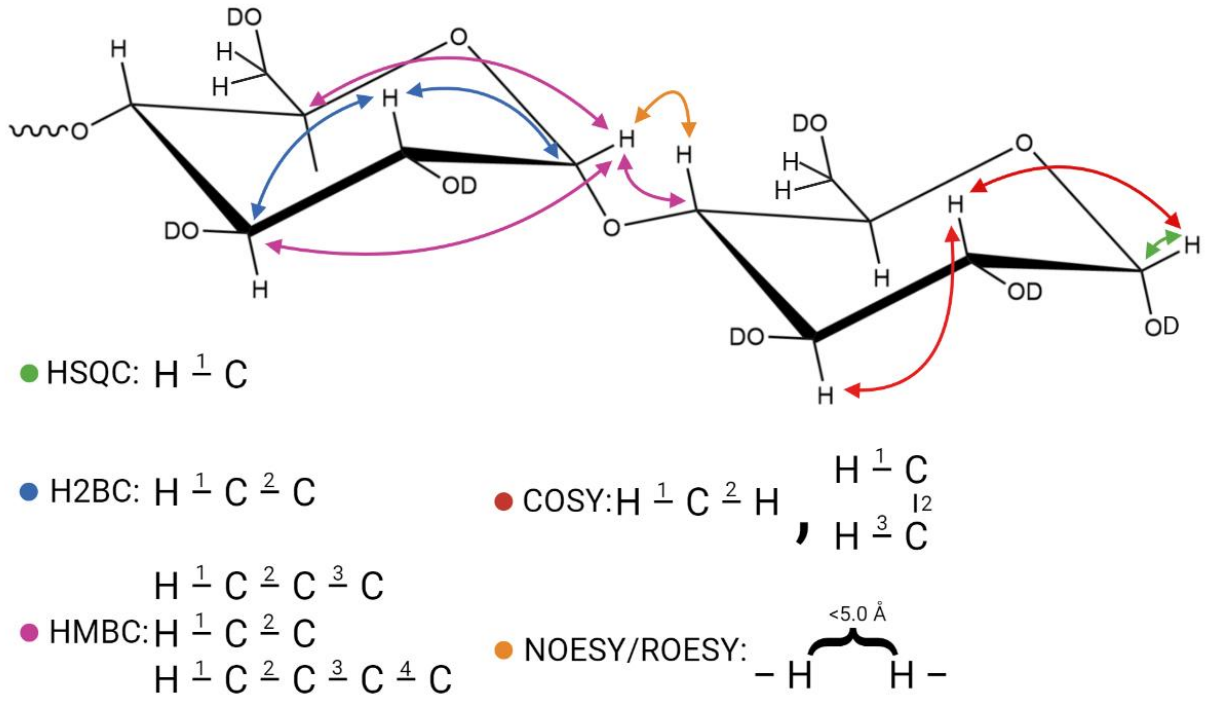

Figure 5: Overview of information obtained by heteronuclear and homonuclear 2D experiments in structural elucidation of oligo- and polysaccharides. All listed experiments are useful in determining monosaccharide structure, with HMBC and NOESY/ROESY being able to determine glycosidic linkages.

There exists many databases and computer programs to aid in the structural elucidation of sugar molecules. One such program is CASPER (50). CASPER contains chemical shift data from mono-, di-, and trisaccharides and can predict structure from experimentally obtained chemical shifts under set conditions. Additionally, it is possible to input a structure and it will predict chemical shifts for each nucleus within the molecule.

1.7 Carbohydrate-polyacrylamide gel electrophoresis – C-PAGE

Electrophoretic methods have long been used to analyze nucleic acids, proteins, and polysaccharides (51). In gel electrophoresis, samples are applied to a hydrogel, commonly made from agarose, or polyacrylamide. When an electric field is applied across the gel, sample molecules start to migrate through the gel matrix. The elution is affected by both charge and molecular size. Migration rate is proportional to charge and inverse proportional to size/molecular weight. To analyze the gel after having applied the electric field the samples need to be dyed. The characteristic bands in gel electrophoresis are achieved by using a compound that selectively binds to the substrate. Toluidine blue is a metachromatic dye which binds to acidic compounds including nucleic acids, anionic proteins, and anionic polysaccharides making the sample molecules visible in the gel (51).

Carbohydrate-polyacrylamide gel electrophoresis (C-PAGE) is a helpful method in tracking changes in a polysaccharide structure. This could be degradation of the backbone, debranching, or removal of chemical groups which affect the polysaccharide's overall charge. Degradation of a polysaccharide into smaller fragments would cause the fragments to elute farther than the undegraded polysaccharide.

2 Aim of the project

The first objective of this thesis has been to characterize the biomass composition of four species of marine sponges from the Trondheim Fjord: *Antho dichotoma*, *Geodia barretti*, *Mycale lingua*, and *Phakellia ventilabrum*. Here the following analytical methods were used: element analysis, monosaccharide analysis, and total amino acid analysis to get a profile of the sponges' element content, monosaccharide content, and amino acid content. These parameters would further the knowledge of sponge compositions and give an opportunity to compare biomass across species.

Knowledge of the biomass composition will also be beneficial when working toward the second objective, which has been to develop a protocol for extraction of sulfated aggregation factor polysaccharides in marine sponges. Knowledge from biomass analyses, such as sulfur content and monosaccharide composition, provides indications of sulfated polysaccharide content in the individual extracts investigated. Structural elucidation would be done through 1D and 2D NMR spectroscopy, a similar strategy used in achieving the final objective.

The third goal has been to learn more about sulphated polysaccharide structural elucidation using NMR spectroscopy. For this purpose, two oligomer fractions from an enzymatically degraded fucoidan of the brown algae *Macrocystis pyrifera* were studied. Fucoidans, like sponge aggregation factor polysaccharides, are marine sulfated polysaccharides. Structural characterization of fucoidan fractions was also done through 1D and 2D NMR spectroscopy.

3 Material and methods

3.1 Materials

The sponges used in this thesis were sampled and kindly provided by cooperators Alexander Wentzel and Francesca Di Bartolomeo from SINTEF Industry Dept of Biotechnology and Nanomedicine during the 2022 Sampling campaign for marine sponges in the Trondheim fjord under the EU H2020 funded project "MARBLES" (GA No. 101000392). The sampling was conducted using the R/V Gunnerus equipped with a Dynamic positioning system and a HiPap 500 unit for remotely operated underwater vehicle ROV operations. The samples were collected in the Trondheim fjord at a depth of 102.4 mt at these coordinates: 63°36'54.4"N 10°31'19.5"E.

The water used throughout this project was ultrapure water obtained by reverse osmosis from a stakpure water system. Chemicals used are listed in Table 4, instruments and equipment are listed in Table 5.

Table 4: List of all chemicals used with corresponding CAS registry number and manufacturer.

Name of chemical	CAS nr.	Manufacturer
1-Cetylpyridinium chloride monohydrate (CPC)	6004-24-6	VWR International AS
Acetic acid (CH_3COOH)	64-19-7	Acros Organics BVBA
Acrylamide	79-06-1	Sigma Aldrich Norway AS
Ammonium persulfate (APS)	7727-54-0	Sigma Aldrich Norway AS
Barium hydroxide ($Ba(OH)_2$)	17194-00-2	Sigma Aldrich Norway AS
Bis(trimethylsilyl)amine-tris(hydroxymethyl)aminomethane (Bis-tris)	6976-37-0	VWR International AS
Calcium chloride dihydrate ($CaCl_2 \cdot 2H_2O$)	10035-04-8	Sigma Aldrich Norway AS
Deuterium oxide d-99.9% (D_2O)	7789-20-0	VWR International AS
Ethanol (EtOH)	64-17-5	VWR International AS
Ethylenediaminetetraacetic acid (EDTA)	6381-92-6	Sigma Aldrich Norway AS
Glycerol	56-81-5	
Glycine	56-40-6	Thermo Fisher (Kandel) GmbH
Hydrochloric acid (HCl)	7647-01-0	Sigma Aldrich Norway AS
Papain	9001-73-4	Sigma Aldrich Norway AS
Phenol red	143-74-8	Sigma Aldrich Norway AS
Sodium chloride (NaCl)	7647-14-5	Chiron AS
Sodium hydroxide (NaOH)	1310-73-2	Nouryon Functional Chemicals B.V.
Sulfuric acid (H_2SO_4)	7664-93-9	Sigma Aldrich Norway AS
Tetramethylethylenediamine (TEMED)	110-18-9	Merck Life Science AS
Toluidine blue	92-31-9	Sigma Aldrich Norway AS

Table 5: Instruments and equipment utilized; specific model is listed along with manufacturer.

Instrument	Model	Manufacturer
Ball mill	Mixer Mill MM 400	Retsch
Dialysis tube	Spectrum™ Spectra/Por™ 3 RC Dialysis Membrane Tubing 3,500 Dalton MWCO	Fisher Scientific
Electrophoresis chamber	Mini-PROTEAN Tetra Vertical Electrophoresis Cell	Bio-Rad
Element analyzer	Vario EL cube	Elementar
Freeze dryer	Beta 1–8 LDplus Edwards E2M18 (vacuum pump)	Martin Christ Freeze Dryers
HPAEC-PAD	Dionex ISC 5000+ 4x250 mm CarboPac SA10 (main column) 4x50 SA10 (guard column) LC-20Ai (pump)	Thermo Scientific
HPLC	Dionex UltiMate® 3000 HPLC+ focused 3,9x150 mm 4 µm Nova-Pak C18 (column) Dionex UltiMate® 3000 Autosampler Dionex RF Fluorescence Detector	Thermo Scientific
NMR	800 MHz Avance III HD equipped with a 5-mm cryogenic CP-TCI z-gradient probe and SampleJet	Bruker BioSpin
NMR	600 MHz Avance III HD equipped with a 5-mm cryogenic CP-TCI z-gradient probe and SampleCase	Bruker BioSpin
NMR	600 MHz Avance NEO equipped with a 5-mm TBO z-gradient iProbe and SampleCase	Bruker BioSpin
Micronizing device	Star Burst Mini	Sugino Corp.

3.2 Measuring water content

For *G. barretti* three portions of frozen sponge material weighing ~2 g were placed in preheated crucibles and dried in an oven at 105 °C for 24 hours. The samples were cooled to room temperature in a desiccator and weighed to determine water content. For the remaining species (*A. dichotoma, M. lingua,* and *P. ventilabrum*) water content was determined by weighing tissue before and after freeze drying.

3.3 Ashing of sponge tissue

Three portions of sponge material from *G. barretti* weighing ~0.5 g dry weight (DW) was held at 550 °C for 16 hours, cooled to room temperature in a desiccator and weighed to determine ratio of organic to inorganic mass.

3.4 Element analysis of sponge tissue

A vario EL cube element analyzer was used to determine the nitrogen, carbon, hydrogen, and sulfur content of sponge tissue. Freeze dried sponge material (~0.15 g) was put in Eppendorf tubes with ten 3 mm steel balls and milled for 20 min at 20 Hz. Three parallels of 5 mg milled sponge material (six parallels for *G. barretti*) were packed in tin boats and combusted in the element analyzer. Three parallels of sulfanilic acid and two parallels of fucoidan were used as standards.

3.5 Neutral monosaccharide analysis

Sample preparation differs between *G. barretti* and the other species as the *G. barretti* samples were run at an earlier time, after which the procedure was slightly altered.

Three parallels of 20 mg milled and freeze-dried sponge material (30 mg for *G. barretti*) from each species were added to 12 mL hydrolysis tubes. Sulfuric acid (0.5 mL 12 M) was added to each vial and samples were left at 30 °C for 60 min. Each sample was diluted with 2.5 mL water and left at 100 °C for 4 hours. Samples were cooled to room temperature and diluted further with 6.0 mL water. 180 µL of the hydrolysates were neutralized with 2.4 mL 0.1 M NaOH (750 µL 0.15 M $Ba(OH)_2$ for *G. barretti*) and transferred to HPLC vials. The *G. barretti* samples were diluted 1:10 before being transferred to HPLC vials. Sample concentrations before analysis for each individual sample can be seen in Appendix C.

Samples were analyzed with high-performance anion-exchange chromatography with pulsed amperometric detection (HPAEC-PAD) on a Dionex ICS 5000+ system. 25 µL sample was injected and eluted with 1 mM NaOH with flow rate 1.2 mL/min. Post column addition of 0.4 M NaOH, 0.3 mL/min, was used to adjust NaOH concentration to 80 mM during detection. Further elution parameters are shown in Table 6.

Table 6: Elution parameters for monosaccharide analysis with 4x250 mm CarboPac SA10 column on HPAEC-PAD.

Minutes	NaOH (mM)	NaAc (mM)	Purpose
0-10	1	-	Elution of neutral monosaccharides
10-17	40	400	Wash
17-25	100	-	Removal of acetate and carbonate
25-35	1	-	Equilibration

Samples were run and processed with Chromeleon 7.2 software. The results were compared with standard mixes (mannitol, fucose, arabinose, galactose, rhamnose, glucose, xylose, mannose) (0.1 – 12.5 mg/L) which were ran before and after sponge samples. As some monosaccharides were degraded during sample preparation, factors correcting for the loss of sugars are used to estimated actual monosaccharide content of samples. These correction factors can be seen in Appendix C.

3.6 Total amino acid analysis

The total amino acid content of the four sponge species was found using HPLC in collaboration with Turid Rustad's group at the department of biotechnology and food science (NTNU).

50 mg milled and freeze-dried sponge material from each species was added to a hydrolysis tube and dissolved in 1 mL 6 M HCl. Samples were hydrolyzed for 22 hours at 105 °C before being cooled to room temperature and neutralized with NaOH. Samples were filtered through a Whatman glass microfiber filter using suction. Volume was adjusted to 10 mL and samples were diluted 1:500 using water. Diluted samples were filtered through 0.22 µm filters and transferred to HPLC vials. Amino acids underwent precolumn derivatization with *o*-phthaldialdehyde before samples were analyzed on a Dionex UltiMate® 3000 HPLC+ focused instrument and detected with a Dionex RF Fluorescence Detector.

3.7 Water extraction of *G. barretti*

Two pieces of freeze-dried sponge material from *G. barretti* (2.4 g and 2.6 g) were crushed into small pieces and suspended in 40 mL water in two separate centrifuge tubes. After set time intervals the mixture was centrifuged (4,000 x g, 10 min), and supernatant was collected before the volume of the sponge mixture was adjusted back to 40 mL. Time intervals and extraction conditions are shown in Table 7.

Table 7: Conditions for water extraction of *G. barretti* tissue.

Sponge extract 1 (2.4 g piece)	Sponge extract 2 (2.6 g piece)	Extraction conditions	Time interval
SE-01.1	-	Room temp + mixing	1 h
SE-01.2	-	Room temp + mixing	1 h
SE-01.3	-	Room temp + mixing	16 h
SE-01.4	-	Room temp + mixing	1 h
SE-01.5	SE-02.1	70 °C – no mixing	1 h
SE-01.6	SE-02.2	70 °C – no mixing	1 h
SE-01.7	SE-02.3	70 °C – no mixing	16 h
SE-01.8	SE-02.4	70 °C – no mixing	1 h

Each extract was collected separately, freeze dried and weighed. A schematic overview of the water extraction can be seen in Figure 6.

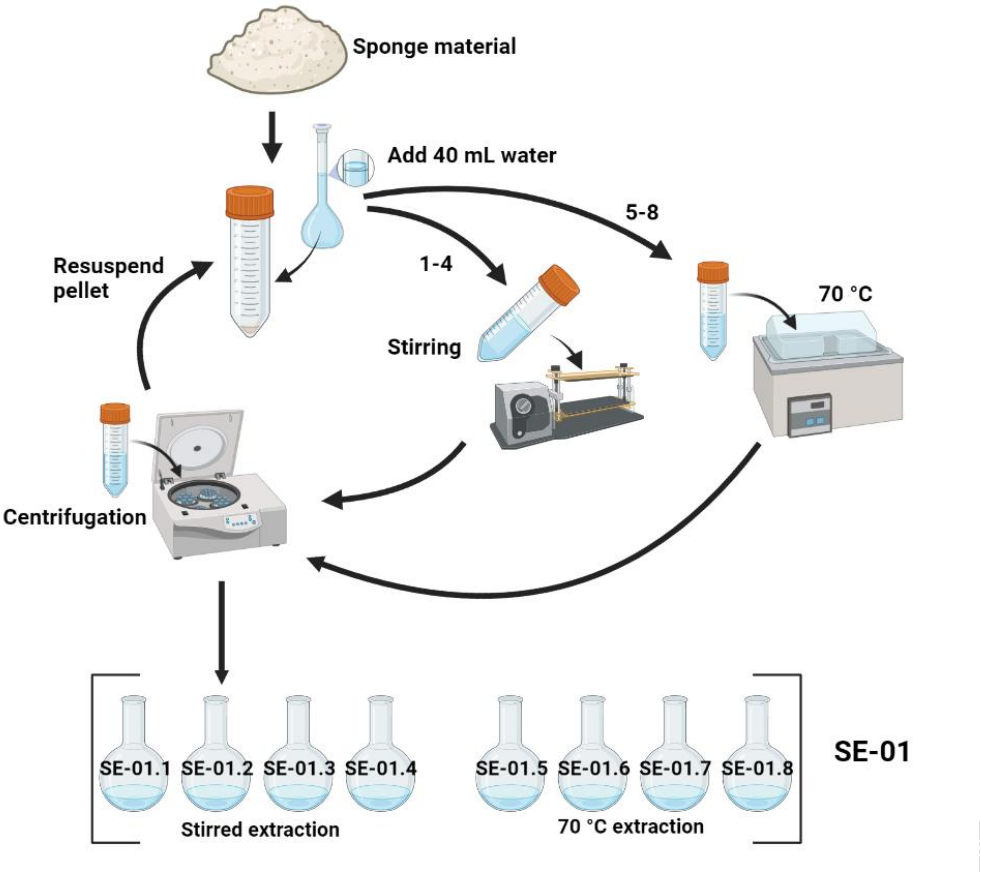

Figure 6: Schematic overview of water extraction protocol used on *G. barretti* tissue.

Fraction SE-01.3 and a sample with all eight SE-01 fractions combined were analyzed with an element analysis and a monosaccharide analysis following procedures as described in sections 3.4

and 3.5. For the monosaccharide analysis the same procedure as described for *A. dichotoma, M. lingua,* and *P. ventilabrum* was used.

3.8 Polysaccharide extractions

3.8.1 Precipitation of polysaccharides using calcium chloride

The following extraction protocol based on calcium precipitation was performed on all four species. These extracts are referred to as the Ca^{2+} extracts.

Freeze dried sponge material was crushed into small pieces, suspended in 40 mL water containing papain and incubated at 50 °C for 48 h. Sponge material and papain amounts used can be seen in Table 8.

Table 8: Sponge material (dry weight) and enzyme amounts used in polysaccharide extraction.

Species	Sponge material [mg]	Papain [mg]
Antho dichotoma	372.8	37.0
Geodia barretti	380.0	38.0
Mycale lingua	361.4	36.0
Phakellia ventilabrum	160.8	16.0

The mixtures were centrifuged (4,000 x g for 10 min at 10 °C) after incubation. Polysaccharides in the supernatants were precipitated by increasing the calcium concentration of the mixtures to 30 mM using $CaCl_2$ (176.5 mg for 40 mL supernatant). After being left at room temperature for 1 hour the calcium containing mixtures were centrifuged (4,000 x g for 10 min at 10 °C). The polysaccharide containing pellets were dissolved in 10 mL 15 mM EDTA and transferred to dialysis tubes (3,500 Da MWCO). Samples were dialyzed twice against 4 L 50 mM NaCl (18 h and 6 h) and four times against 4 L water (18 h, 6 h, 23 h, and 3 h). The volume of each sample was adjusted to 30 mL before being papain digested for a second time (5 mg papain, 50 °C for 24 h). The incubation mixtures were centrifuged (4,000 x g for 10 min). Finally, the polysaccharides in the supernatants were freeze dried and analyzed with NMR spectroscopy and C-PAGE.

3.8.2 Enzymatic digestion method

Several extractions were done on *G. barretti* before the calcium precipitation protocol was chosen as the extraction method for all four species. The first extracts performed were based on the water extracts described in section 3.7. The following protocol is referred to as the "enzymatic digestion method" as it utilizes papain and no specific method for polysaccharide isolation.

Material from the water extracts of *G barretti* (SE-01, 300 mg) was dissolved in 10 mL 100 mM bis-tris buffer (pH 6.5) with 3 mg papain. The mixture was incubated at 50 °C for 24 h and dialyzed against 4 L water (3,500 Da MWCO, 1h, 1h, 20h, 20h). The sample was acid-hydrolyzed in two steps: 1) 20 mL 0.01 M HCl, 95 °C for 45 min, 2) 20 mL 0.1 M HCl, 95 °C for 45 min. After another round of dialysis (4 L water, 3,500 Da MWCO, 1h, 1h, 20h) the sample was mechanically sheared using a Star Burst Mini (10 cycles, 200 MPa) before being freeze dried.

During this extraction procedure NMR spectroscopy was utilized multiple times to understand the change in the sample. This is not included in the procedure outlined above but is shown in the schematic overview of the extraction method (see Figure 7).

3.8.3 Precipitation of polysaccharides using cetylpyridinium chloride

Sponge tissue from *G. barretti* (4.5 g) was suspended in 50 mL water, papain digested (300 mg papain, 60 °C, 24 h), and centrifuged (2,000 x g, 10 °C, 15 min). Polysaccharides in the supernatant were precipitated with 8 mL cetylpyridinium chloride (10 %). After being left at room temperature for 24 h the mixture was centrifuged (2,000 x g, 15 min). The polysaccharide-containing pellet was dissolved in 60 mL 2 M NaCl:ethanol (100:15 v/v) and precipitated with 120 mL ethanol (96 %). The mixture was left at 4 °C for 24 h before being centrifuged (2,000 x g, 15 min). The pellet was washed twice with 60 mL 80 % ethanol and once with 60 mL 96 % ethanol. The resulting 54 mg extract was dissolved in 20 mL water and papain digested a second time (9 mg papain, 60 °C, 24 h). Mixture was centrifuged (2,000 x g, 10 °C, 15 min) and dialyzed against 4 L water (3,500 Da MWCO), water was changed three times (2h, 2h, and 16h). The mixture volume was adjusted to 50 mL and sample was mechanically sheared using a Star Burst Mini (10 cycles, 200 MPa) before being freeze dried. The resulting sample was analyzed with NMR spectroscopy and C-PAGE.

The three polysaccharide extraction methods described are summarized in Figure 7.

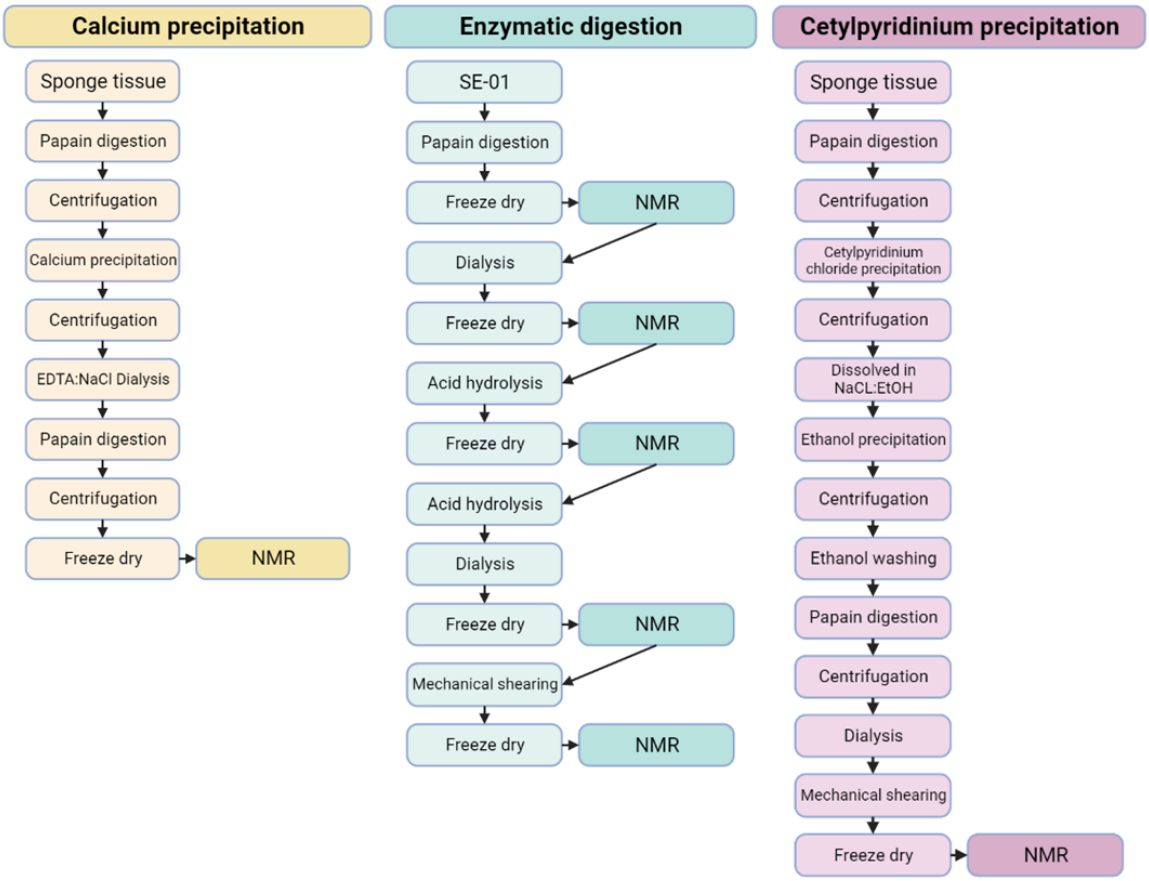

Figure 7: Schematic overview of three methods used to extract polysaccharides from marine sponges. This summary includes points in the process where the extracts were investigated with NMR spectroscopy.

3.9 NMR spectroscopy of sponge samples

NMR spectra were recorded for polysaccharide extracts from all four species obtained by calcium precipitation. The polysaccharide extracts (*A. dichotoma:* 7.6 mg, *G. barretti:*11.0 mg, *M. lingua:* 7.4 mg, *P. ventilabrum:* 8.0 mg) were dissolved in 250 µL D_2O (d-99.9 %) inside 2 mm tubes. ^1H and HSQC spectra were recorded for all four samples with number of scans = 16, size of fid for the HSQC experiments = 2048 x 256, and excitation sculpting water suppression using a Bruker Avance III HD 800 MHz instrument.

For structural elucidation of the extracted polysaccharides, spectra obtained with a *G. barretti* extract were used. The extract was obtained as described in section 3.8, using the calcium

precipitation method. An overview of experiments recorded for the structural elucidation along with some of their acquisition parameters can be seen in Table 9.

Table 9: NMR experiments performed on a polysaccharide extract from *Geodia barretti*, including acquisition parameters. All spectra recorded with a Bruker Avance III HD 800 MHz instrument. NS = number of scans, DS = dummy scans, D[1] = relaxation delay, TD = size of fid.

Experiment	Pulse program	NS	DS	D[1] [sec]	TD	Mixing time [ms]
^{1}H	zgesgp	8	2	3.0	32768	
HSQC	hsqcedetgpsisp2.3	24	16	2.0	2048 x 256	
IP-COSY	ipcosyesgp-tr	24	16	1.0	4096 x 256	
H2BC	h2bcetgpl3pr	32	16	1.0	2048 x 1024	
HSQC-TOCSY	hsqcdietgpsisp.2	16	128	2.0	2048 x 256	60
TOCSY	tocsycleanes.rw	16	128	2.2	4096 x 512	80
HMBC	hmbcetgpl3nd	32	16	2.0	2048 x 400	
NOESY	noesyesgpph	32	64	1.2	4096 x 512	80

Additional NMR experiments were performed on various samples during the development of the polysaccharide extraction protocol described in section 3.8, including NMR experiments on the enzymatic digestion extract shown in Figure 7. Those experiments were recorded on a 600 MHz Avance NEO instrument, with samples dissolved in 600 µL D_2O (99.9 %) and placed in 5 mm tubes.

The ^{1}H chemical shift of all spectra were internally referenced to residual water signal (4.80 ppm at 25 °C and 4.17 ppm at 83 °C). ^{13}C chemical shift was referenced indirectly to DSS using a ^{13}C/^{1}H frequency ratio = 0.251449530 (52). All spectra were recorded at 25 °C unless another temperature is stated. Data processed using TopSpin version 4.1.4.

3.10 Analyzing polysaccharide extracts using C-PAGE

A resolving and stacking gel solution used in casting a polyacrylamide gel was prepared according to Table 10.

Table 10: Recipe for resolving and stacking gels used in C-PAGE. Recipe is sufficient for casting two gels.

Chemical	Resolving gel (25 %)	Stacking gel (10 %)
40 % acrylamide stock	6.4 mL	0.4 mL
1 M Tris pH 6,8	-	0.4 mL
2 M Tris pH 8,8	1.3 mL	-
10 % APS stock	52.5 µL	15.6 µL
Ultrapure water	2.53 mL	2.33 mL
TEMED	5.25 µL	3.12 µL

The polyacrylamide gel was cast by pouring ~4-5 mL of the resolving gel solution and ~0.5-1 mL of the stacking gel solution into a gel cassette. A 10-well comb was inserted between the glass plates before the gel was left to set for 1 h. The gel cassette was fixed in an electrode assembly frame and placed in a gel tank surrounded by ice. Precooled running buffer was poured into both the inner and outer chamber of the setup before the 10-well comb was removed. Samples (10 µL) and loading dye (10 µL) were mixed before 10 µL of the solutions were deposited in the wells.

The composition of the running buffer and loading dye are shown below.

Running buffer (1 L):

- 3 g Tris
- 15 g glycine
- 1 L ultrapure water

Phenol red loading dye (5 mL):

- 310 µL 1 M Tris pH 6.8
- 80 µL 1 % Phenol Red
- 2 mL glycerol
- 2.61 mL ultrapure water

Samples were diluted to 1 % (w/v) concentration in water prior to mixing with the loading dye. Samples analyzed and their well positions are shown in Table 11.

Table 11: Overview of a polyacrylamide gel loaded with polysaccharide samples, two samples with polysaccharides from brown algae used as standards, and six samples of sponge polysaccharides.

Well position	Sample
1	Fucoidan (*Laminaria hyperborea*)
2	Laminarin (*Laminaria hyperborea*)
3	Ca^{2+} extract (*Antho dichotoma*)
4	Ca^{2+} extract (*Geodia barretti*)
5	Ca^{2+} extract (*Mycale lingua*)
6	Ca^{2+} extract (*Phakellia ventilabrum*)
7	SE-01 (*Geodia barretti*)
8	CPC extract (*Geodia barretti)*
9	-
10	-

Once the wells were filled, the gel was run on 100 V for 15 min followed by 200 V for 1 h. The gel was removed from the cassette, put in a petri dish, covered in a dying solution (toluidine blue), and left on a shaking pad for 20 min. The dying solution was removed and replaced with a destaining solution (0.1 % acetic acid) before being put back on the shaking pad. Destaining went on for 1 h with the destaining solution being replaced every 20 min.

4 Results

4.1 Water and ash measurements reveal high water content

The water content of all four sponge species and ash content of *G. barretti* is summarized in Table 12. Water content estimated by freeze-drying was completed for one replicate, and water content estimated using drying was completed in triplicate. The water content ranged from ~75 – 89 %. With measurements of water and ash content it was estimated that 9.8 ± 0.5 % of the total weight of *G. barretti* (wet weight) was organic matter. Due to material constraints ash content was only estimated for the one species.

Table 12: Measured water content of tissue from marine sponges. Water content of A. dichotoma, M. lingua, and P. ventilabrum estimated by freeze-drying for one replicate. Water content of *G. barretti* estimated by drying in triplicate. Ash content estimated by incineration in triplicate. DW = dry weight, WW = wet weight. Uncertainty given in standard deviation, n = 3.

Species	Water content [%]	Ash content (of WW) [%]	Organic matter (of WW) [%]
Antho dichotoma	81.3	-	-
Geodia barretti	75.4 ± 2.4	14.8 ± 2.5	9.8 ± 0.5
Mycale lingua	88.7	-	-
Phakellia ventilabrum	89.2	-	-

4.2 Comparable element content across species except for *A. dichotoma*

The nitrogen, carbon, hydrogen, and sulfur content of all four sponge species was found using a vario EL cube element analyzer. Element content of sponge dry weight was estimated to be within the following ranges, nitrogen: ~3.8 – 6.7 %, carbon: ~15.0 – 27.9 %, hydrogen: ~2.8 – 4.6 %, and sulfur ~0.5 – 2.7 %. *A. dichotoma* had the highest content of all measured elements apart from sulfur where *M. lingua* had the highest content. *G. barretti*, *M. lingua*, and *P. ventilabrum* had comparable levels of all elements apart from sulfur. Results from the analysis can be seen in Figure 8.

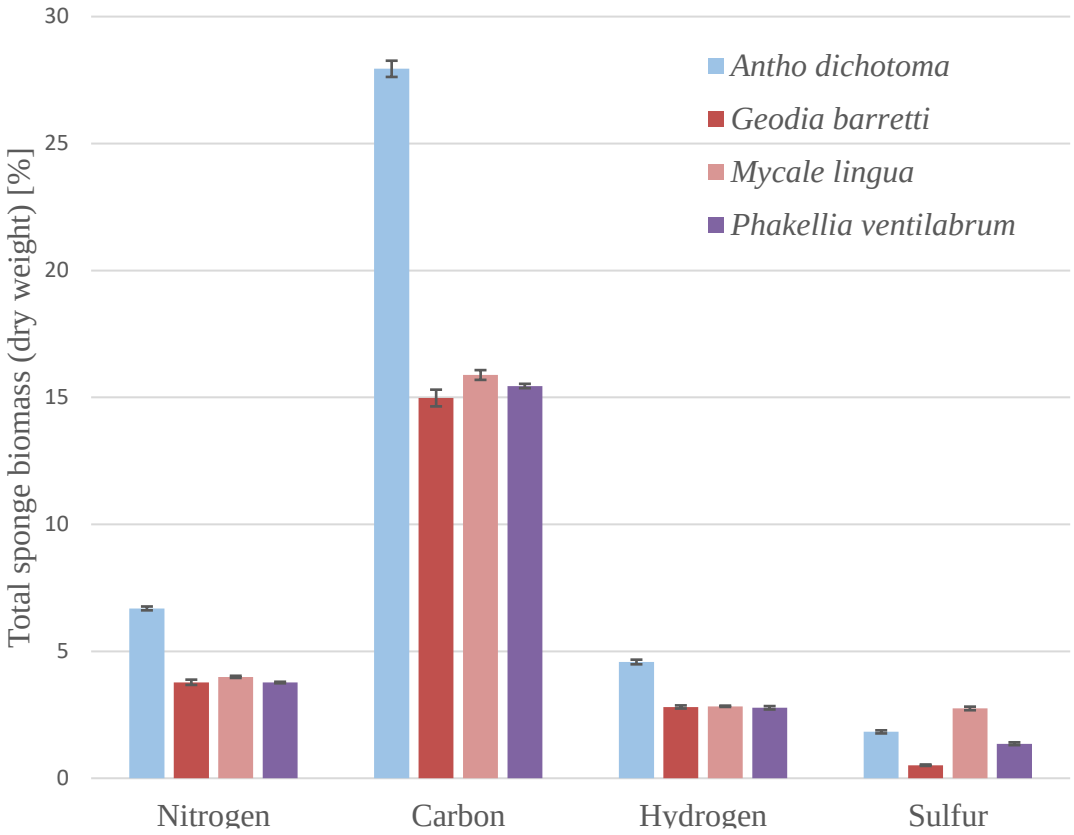

Figure 8: Total content of nitrogen, carbon, hydrogen, and sulfur of dried tissue from four species of sponge. Measurements done using a vario EL cube element analyzer. Error bars indicate standard deviation based on three measurements (six for *G. barretti*).

Nitrogen content is used in the food industry to calculate protein content of products. An appropriate conversion factor based on previous experimental data is applied to the nitrogen content. There is no such conversion factor for sponges. Table 13 contains a few different conversion factors which have been applied to the nitrogen content of the sponges.

Table 13: Nitrogen-to-protein conversion factors from literature applied to measured nitrogen content of marine sponges (53,54).

Source	**Conversion Factor**	**Estimated protein content (dry weight) [%]**			
		A. dichotoma	***G. barretti***	***M. lingua***	***P. ventilabrum***
Cow's milk	6.0	40.2	22.8	24.0	22.8
Soy milk	5.5	36.9	20.9	22.0	20.9
Seaweed (*S. latissima*)	3.8	25.5	14.4	15.2	14.4

Raw data form the element analysis can be found in Appendix B.

4.3 Large inter species variations in monosaccharide compositions

The neutral monosaccharide composition of all four species was found using HPAEC-PAD. As samples were hydrolyzed before analysis, the monosaccharide content includes all sugar residues from oligo- and polysaccharides in addition to free monosaccharides. The analysis is capable of detecting mannitol, fucose, arabinose, galactose, rhamnose, glucose, xylose, and mannose. Mannitol was not detected in any of the samples, and rhamnose was only detected in *G. barretti* and *M. lingua*. Other than mannitol and rhamnose, every monosaccharide was present in each species. The neutral monosaccharide content of the four species ranged from ~2.0 – 5.2 % of total dry weight. Figure 9 shows the proportion of sponge mass composed of neutral monosaccharides.

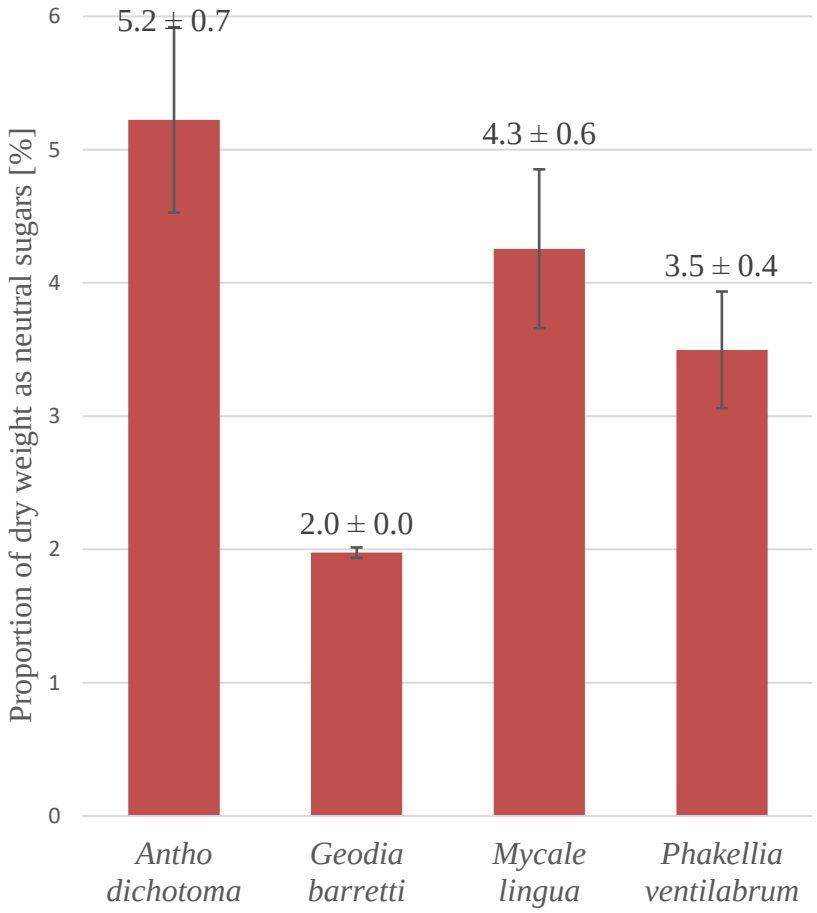

Figure 9: Proportion of sponge mass (dry weight) composed of neutral monosaccharides. Results obtained by HPAEC-PAD using a Dionex ISC 5000+ instrument with a 4x250 mm CarboPac SA 10 column. Error bars indicate standard deviation (n=3).

The monosaccharide composition of the sponges was found to vary a lot across species. Sugars such as arabinose and fucose were estimated to range from ~4 – 22 % and ~2 – 16 % of measured neutral monosaccharides respectively. Common to all four species was a relatively large amount of glucose, ~26 – 38 % of measured neutral monosaccharides. A profile of the monosaccharide content of each individual species can be seen in Figure 10.

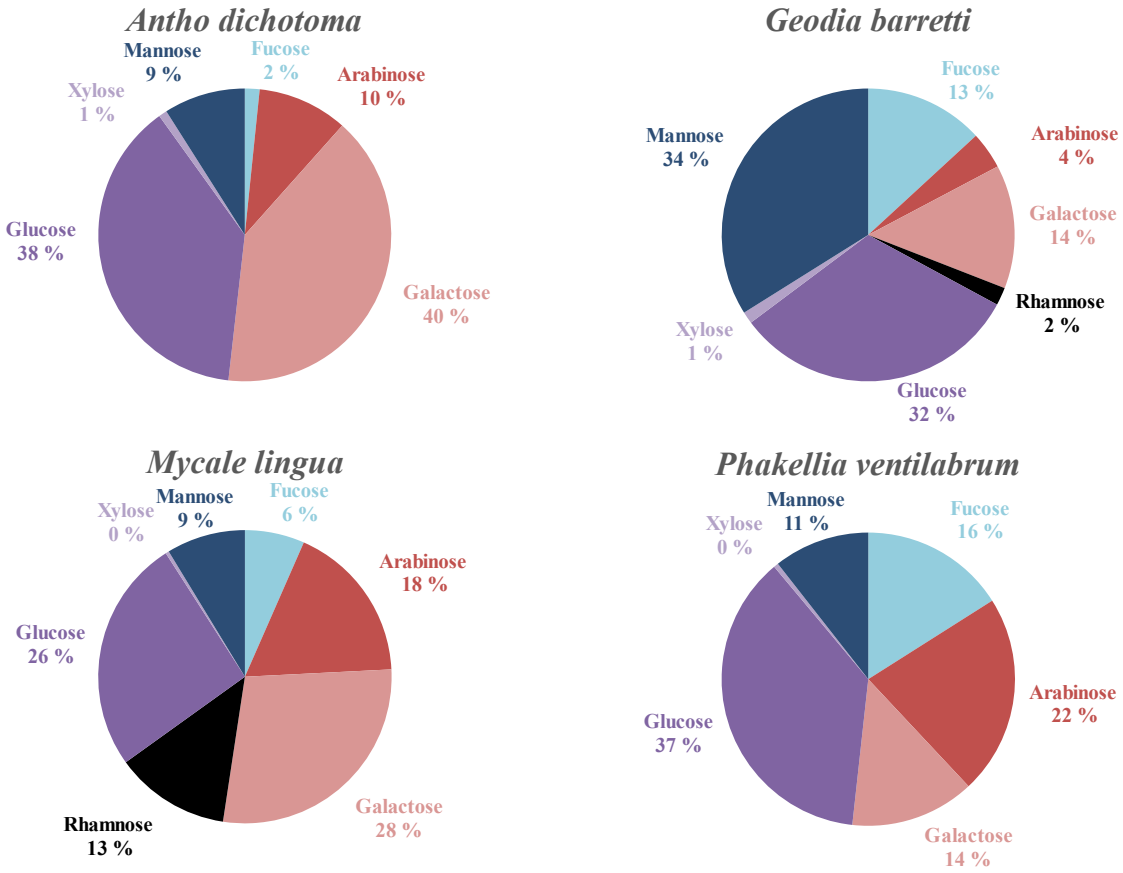

Figure 10: Total neutral monosaccharide composition of four species of sponge. Results obtained by HPAEC-PAD using a Dionex ISC 5000+ instrument with a 4x250 mm CarboPac SA 10 column. Monosaccharide degradation during sample preparation is corrected for.

Figure 11 shows a comparison of neutral monosaccharide composition between the four species.

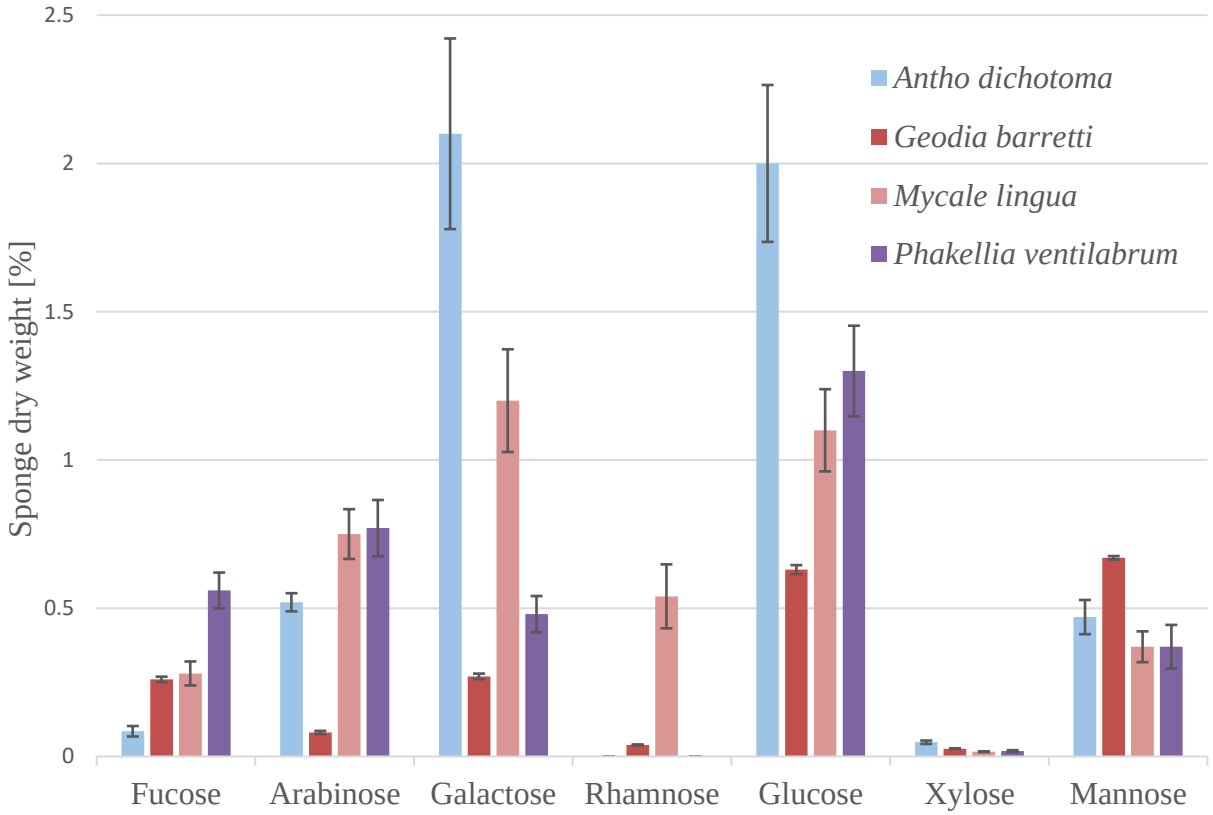

Figure 11: Total neutral monosaccharide content of four species of sponge. Results obtained by HPAEC-PAD using a Dionex ISC 5000+ instrument with a 4x250 mm CarboPac SA 10 column. Monosaccharide degradation during sample preparation is corrected for. Error bars indicate standard deviation (n=3).

Raw data from the monosaccharide analysis can be found in Appendix C along with chromatograms.

4.4 Amino acid composition of sponges differ from the average protein

As the protein in each sample was hydrolyzed, the total amino acid analysis includes amino acids in proteins and free amino acids. A total of 17 of the 20 standard proteinogenic amino acids including the non-proteinogenic amino acid aminobutyric acid (ABA) are detectable with the selected analytical method. Cysteine, proline, and tryptophan are not detected. The elution of glycine and arginine produces a single peak meaning that individual quantification of the two amino acids is not possible.

The total amino acid analysis yielded amino acid amounts relative to total amino acid content and amounts in µmol/L. The amounts in µmol/L were used to calculate the weight of each amino acid in the original sample relative to total sample weight, and by extension weight relative to the total dry weight of each sponge. Examples of the calculations can be seen in Appendix D. Following these calculations proteins and free amino acids were estimated to constitute around 15 to 22 % of total sponge biomass depending on species, as can be seen in Figure 12. Due to the coelution of glycine and arginine it is not possible to get an exact quantification of amino acid content in the sponge samples. Instead, an upper and lower value is set. The upper limit assumes the glycine/arginine peak in the chromatogram is caused exclusively by the larger arginine, while the lower limit assumes it is caused exclusively by the smaller glycine.

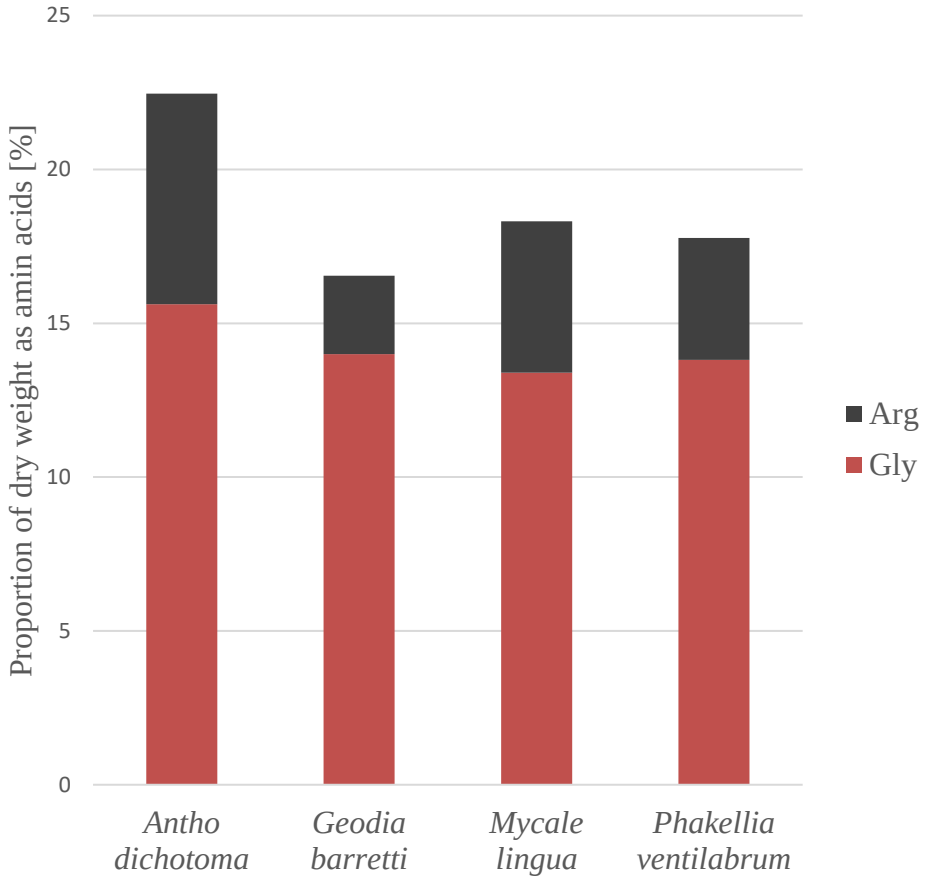

Figure 12: Total amino acid content in four species of sponge. Results obtained by HPLC using a Dionex UltiMate® 3000 HPLC+ focused instrument with a 3,9x150 mm 4 µm Nova-Pak C18 column. Due to coelution of glycine and arginine it is not possible to get an exact quantification of amino acid content. The red bar assumes there is no arginine in the sample, while the upper value assumes there is no glycine in the sample. The true value is likely to be somewhere in the gray section.

In section 4.2 three different nitrogen-to-protein conversion factors were applied to the nitrogen content of each of the four species. The highest estimates, using a factor of 6.0, gave estimated protein contents of 40.2 – 22.8 %. Using a factor of 5.0 gave estimates between 33.5 – 19 %. The smallest conversion factor of 3.8 was the most accurate, giving protein estimates of 25.5 – 14.4 %. Table 14 contains calculated nitrogen-to-protein conversion factors based on measured nitrogen content and the upper limit of measured amino acids.

Table 14: Nitrogen-to-protein conversion factors of marine sponges based on measured nitrogen and amino acid content.

Species	Nitrogen content [%]	Amino acid content [%]	Conversion factor
A. dichotoma	6.7	22.5	3.4
G. barretti	3.8	16.5	4.3
M. lingua	4.0	18.3	4.6
P. ventilabrum	3.8	17.8	4.7

A profile of amino acid composition of each species can be seen in Figure 13. The amino acids are displayed in order of most to least frequent amino acid in proteins, based on frequency of occurrence of amino acid residues in the primary structures of 1,021 unrelated proteins of known sequence (55). Since aminobutyric acid is non-proteinogenic it is sorted as least frequent.

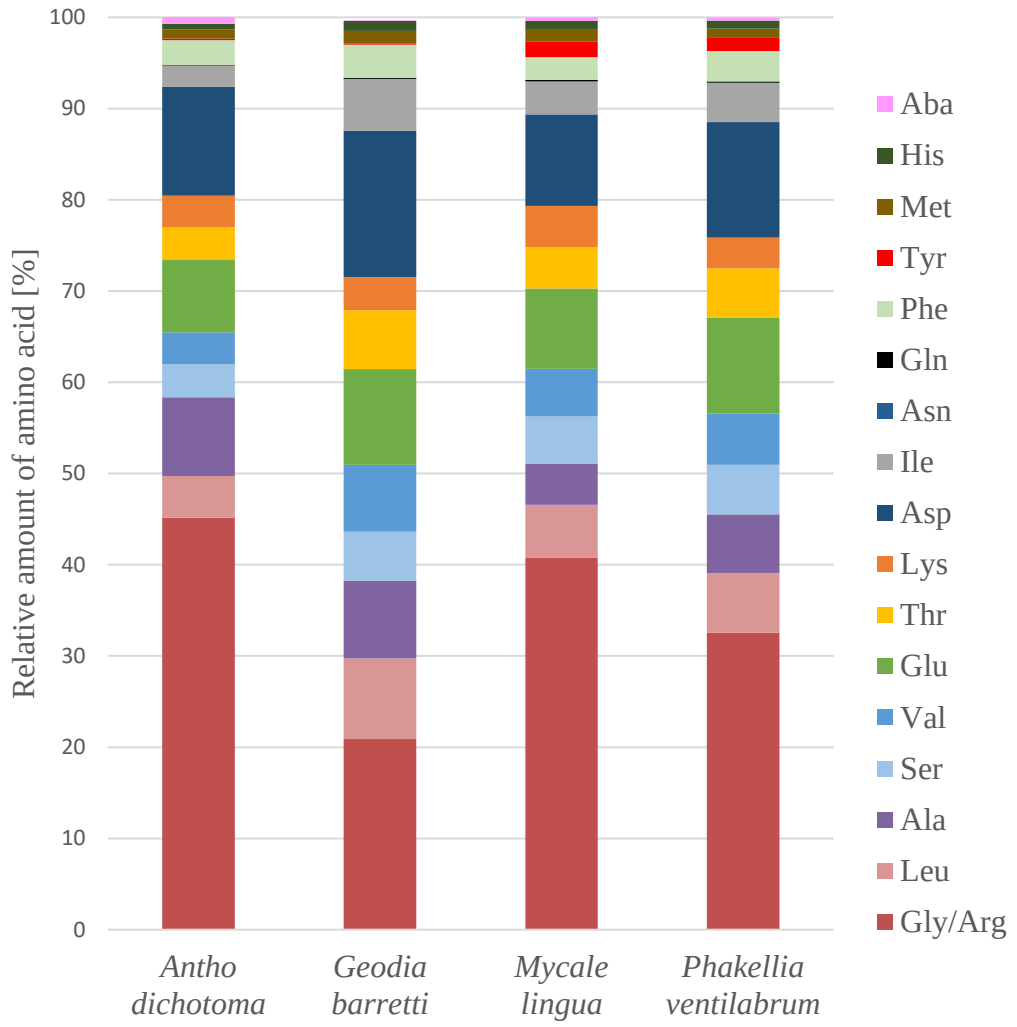

Figure 13: Total amino acid composition of four species of sponge. Results obtained by HPLC using a Dionex UltiMate® 3000 HPLC+ focused instrument with a 3,9x150 mm 4 µm Nova-Pak C18 column. Amino acids are in order of most (bottom) to least (top) frequent amino acid, based on data from the primary structure of 1,021 unrelated proteins (55).

Most amino acids were detected in comparable amount across the four species. There were some exceptions, such as glycine/arginine which ranged from ~21 – 45 %. Compared with frequencies observed in other proteins, the sponge samples had a higher glutamic and aspartic acid content, and a lot higher glycine/arginine content. For the other amino acids, the frequencies were either comparable or lower. Asparagine and glutamine were only detected in very low amounts, <0.5 % of total amino acids. Figure 14 shows a comparison of amino acid composition between the four species.

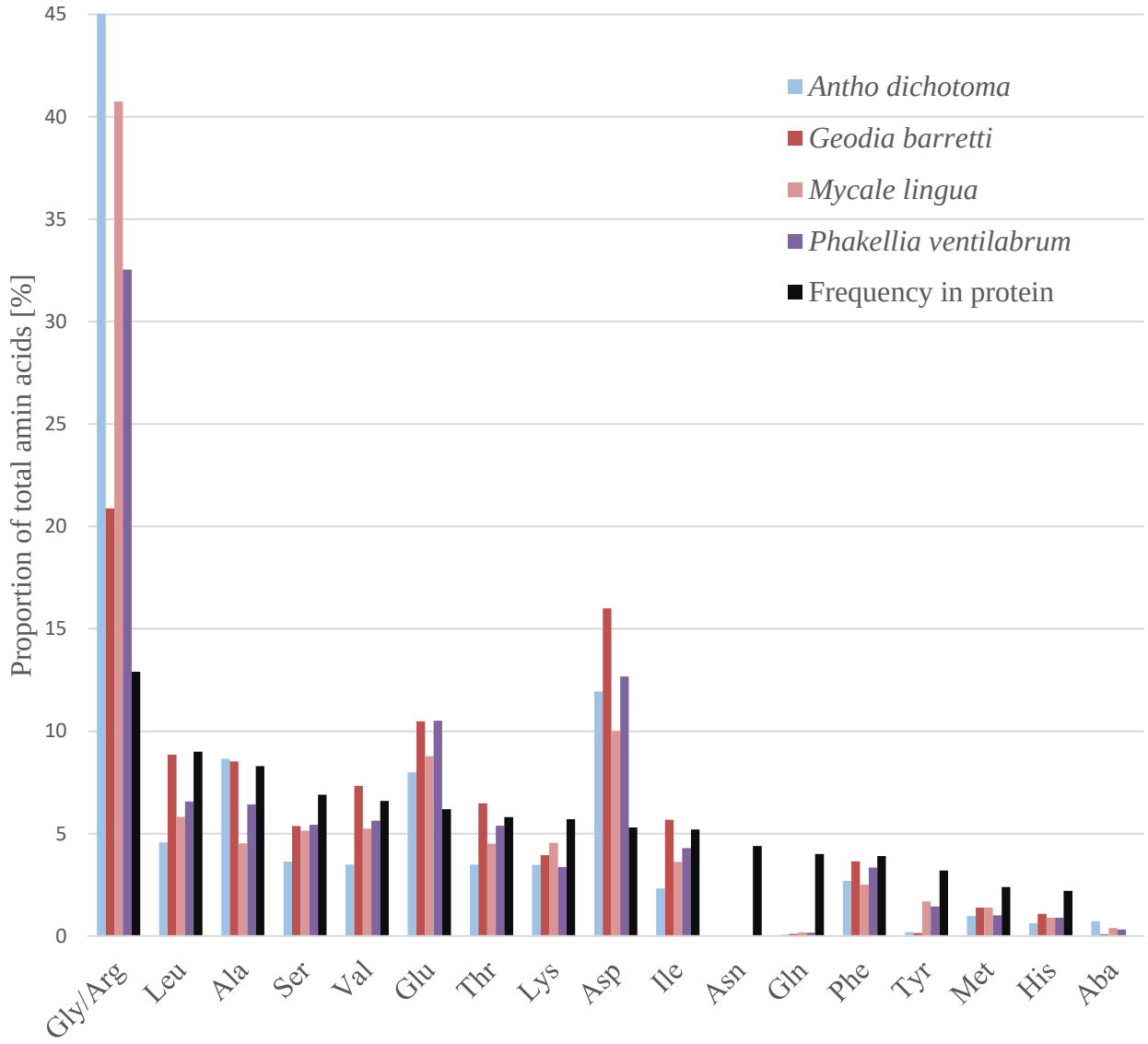

Figure 14: Total amino acid content in four species of sponge. Results obtained by HPLC using a Dionex UltiMate® 3000 HPLC+ focused instrument with a 3,9x150 mm 4 µm Nova-Pak C18 column. Amino acids are in order of most (left) to least (right) frequent amino acid in protein. Black bars indicate frequency of amino acids in proteins, based on data from the primary structure of 1021 unrelated proteins (55).

Raw data from the total amino acid analysis can be found in Appendix D.

4.5 Higher content of organic elements and monosaccharides in water extracts

The initial water extraction of *G. barretti* yielded a total of twelve fractions. Eight fractions from the first piece of tissue where the first four extractions were done in room temperature with mixing and the last four at 70 °C with no mixing (SE-01). Four fractions from the second piece where all extractions were done at 70 °C with no mixing (SE-02). Extractions were performed on two pieces of material under different conditions to compare the effect of extraction temperature. By keeping each fraction separate the yields helped determine how many volumes of water were required to obtain a substantial portion of the water-soluble part of the sample. After the first three extraction steps of SE-01, 0.95 g was obtained compared with 0.25 g from the five subsequent extraction steps. The yield from each fraction can be seen in Table 15.

Table 15: Water extracts done on *G. barretti*. Extraction conditions: Step 1-4: 40 mg water, room temp., mixing. Step 5-8: 40 mg water, 70 °C, no mixing. Each extraction step lasted 1 hour except for step 3 and 7 which lasted 16 hours. Starting material SE-01: 2.4 g DW (dry weight). Starting material SE-02: 2.6 g DW. RT = room temperature.

Step	SE-01 [Fraction]	Yield [g]	Yield [% of DW]	SE-02 [Fraction]	Yield [g]	Yield [% of DW]	Temp.	Mixing [Y/N]
1	SE-01.1	0.43	17.6	-	-	-	RT	Y
2	SE-01.2	0.13	5.5	-	-	-	RT	Y
3	SE-01.3	0.41	17.0	-	-	-	RT	Y
4	SE-01.4	0.04	1.8	-	-	-	RT	Y
5	SE-01.5	0.05	1.9	SE-02.1	0.31	12.0	70°C	N
6	SE-01.6	0.09	3.8	SE-02.2	0.18	6.8	70°C	N
7	SE-01.7	0.03	1.4	SE-02.3	0.07	2.8	70°C	N
8	SE-01.8	0.02	0.8	SE-02.4	0.04	1.7	70°C	N
Total	SE-01	1.20	49.8	SE-02	0.60	23.3		

Each subsequent step had a decreasing yield except for the longer steps 3 and 7. Mixing at room temperature had higher yields than the higher temperature extractions with no mixing. In addition to varying in weight, the extracts looked and felt different. The first fraction from both SE-01 and SE-02 were significantly darker and denser than subsequent fractions. A coarser more crystalline consistency of these fractions could be caused by a high proportion of salts washing out in the first steps. The second fractions were still a little darker and denser than following extracts. From the third fractions onward, there was little to no difference in appearance and consistency.

The composition of extract SE-01 (comprised of all sub-fractions) was investigated with an element analysis and monosaccharide analysis. In addition, sub-fraction SE-01.3 was also investigated individually as it was white in color, had a soft consistency, and a high yield. These extracts were investigated to understand the difference between the water-soluble extracts and the untreated sponge material. Figure 15 shows the nitrogen, carbon, hydrogen, and sulfur content of fraction SE-01.3 and all SE-01 fractions combined compared to *G. barretti* tissue.

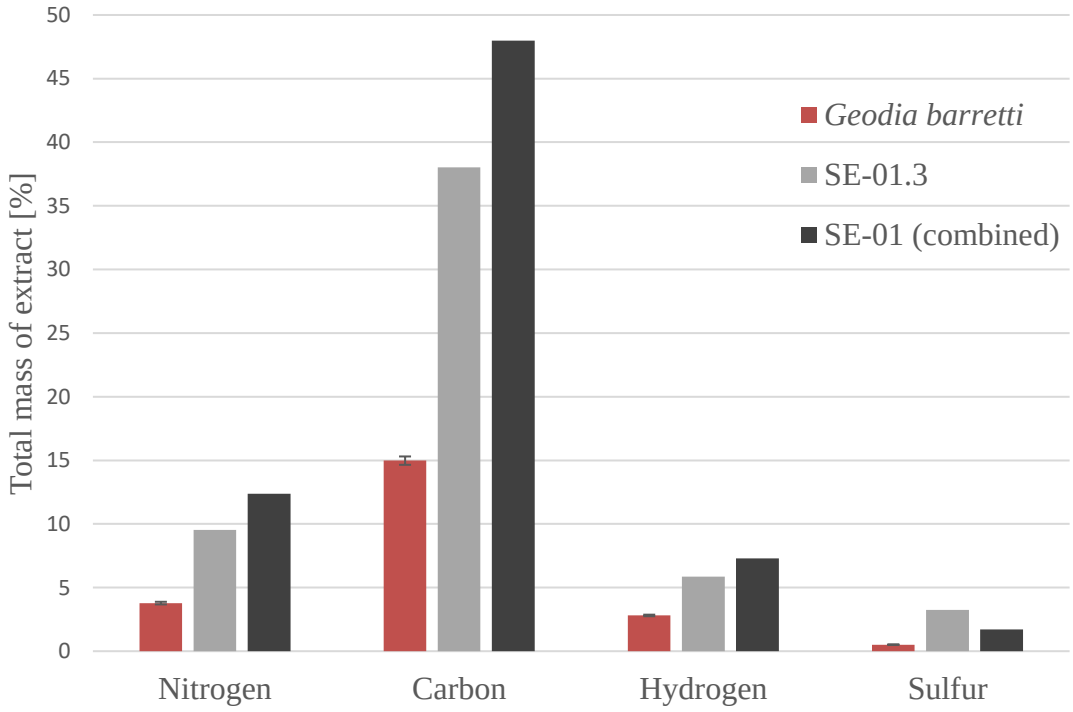

Figure 15: Total content of nitrogen, carbon, hydrogen, and sulfur in water extracts made of *Geodia barretti* compared with the whole tissue of the sponge. Measurements done using a vario EL cube element analyzer. Error bars = standard deviation, n=3.

Nitrogen, carbon, hydrogen, and sulfur levels were higher in both extracts compared to the *G. barretti* tissue. The combined SE-01 extract had a higher content of all elements except for sulfur compared with the sub-fraction SE-01.3. The neutral monosaccharide composition of fraction SE-01.3 and SE-01 fractions compared to *G. barretti* tissue can be seen in Figure 16.

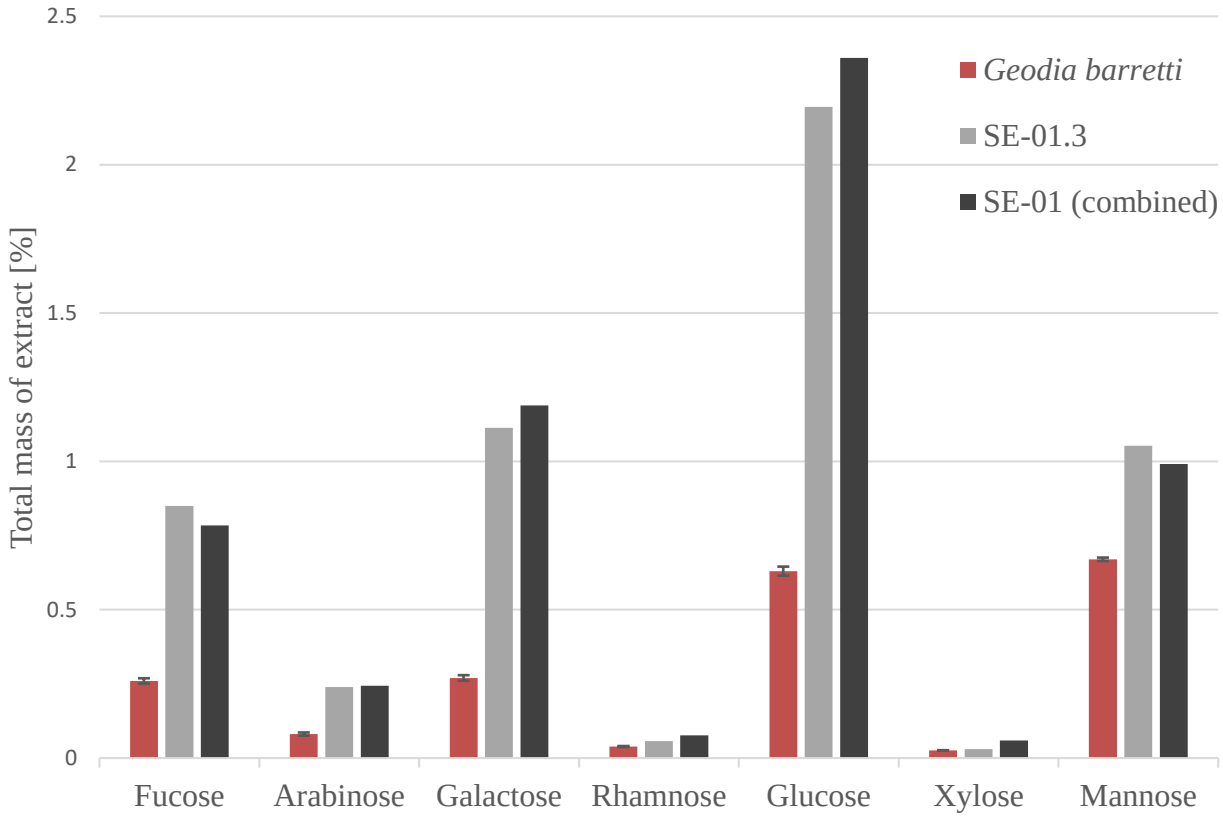

Figure 16: Total neutral monosaccharide content in water extracts made of *G. barretti* compared with the whole tissue of the sponge. Results obtained by HPAEC-PAD. Monosaccharide degradation during sample preparation is corrected for. Error bars = standard deviation, n=6.

The neutral monosaccharide content of fraction SE-01.3 was 5.5 % of its total mass and 5.7 % for the combined SE-01 fractions. Both showing an increased proportion of monosaccharides compared to the whole tissue of *G. barretti* which was composed of 2.0 % neutral monosaccharides. Raw data from both the element analysis and monosaccharide analysis of the water extracts can be found in Appendix B and Appendix C. The SE-01 water extracts were used in a polysaccharide extraction protocol based on enzyme digestion. Results from the polysaccharide extraction are presented in section 4.6.1.

4.6 NMR spectroscopy of polysaccharide extracts

4.6.1 Presence of sugars in enzymatic digestion samples

During the enzymatic digestion method, based on enzymatically digesting a previously obtained water extract (SE-01) from *G. barretti*, NMR spectra were recorded at five separate instances. 1) After papain digestion, 2) after dialysis, 3) after acid hydrolysis, 4) after acid hydrolysis and dialysis, 5) after mechanical shearing (overview can be seen in Figure 17).

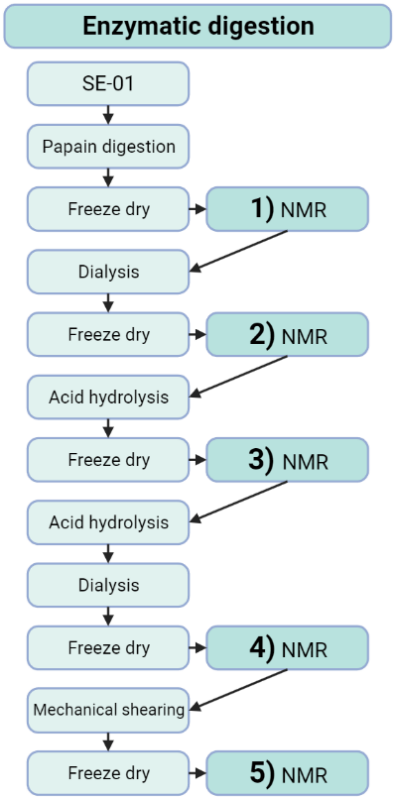

Figure 17: Overview of enzymatic digestion method used to extract polysaccharides from *G. barretti*. Each instance of NMR spectroscopy is enumerated 1-5.

The first spectra (1) were poorly resolved (^{1}H spectrum in Figure 18), with no HSQC signals, likely due to a large amount of salts leftover from the buffer used in the enzyme digestion. Due to residual buffer and water signal, picking out sugar signals in the ^{1}H spectrum was difficult. Some signals in the anomeric region (4.6 – 5.4 ppm) were observed.

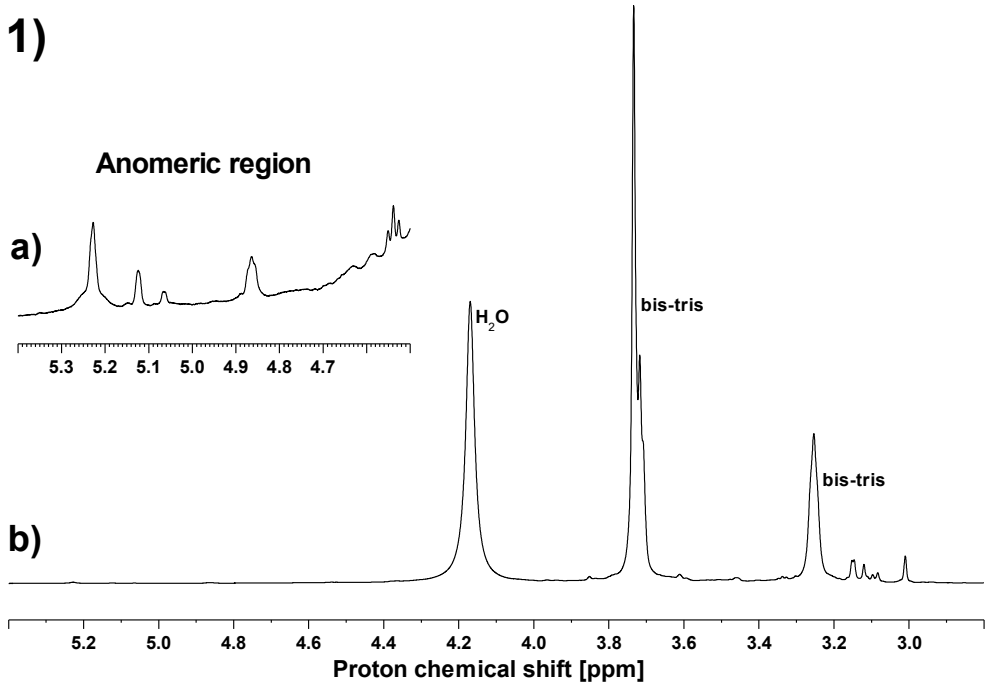

Figure 18: ^{1}H spectrum of papain digested water extract from *G. barretti*. The spectrum contains signals from leftover bis-tris buffer used in the enzymatic digestion. Region b) is a section of the larger region b) with signals intensified. Spectrum recorded at T=83°C on a 600 MHz Avance NEO instrument.

Dialyzing the sample yielded better resolved signals and a HSQC spectrum (spectrum 2) with indications of sugar signals (see Figure 19).

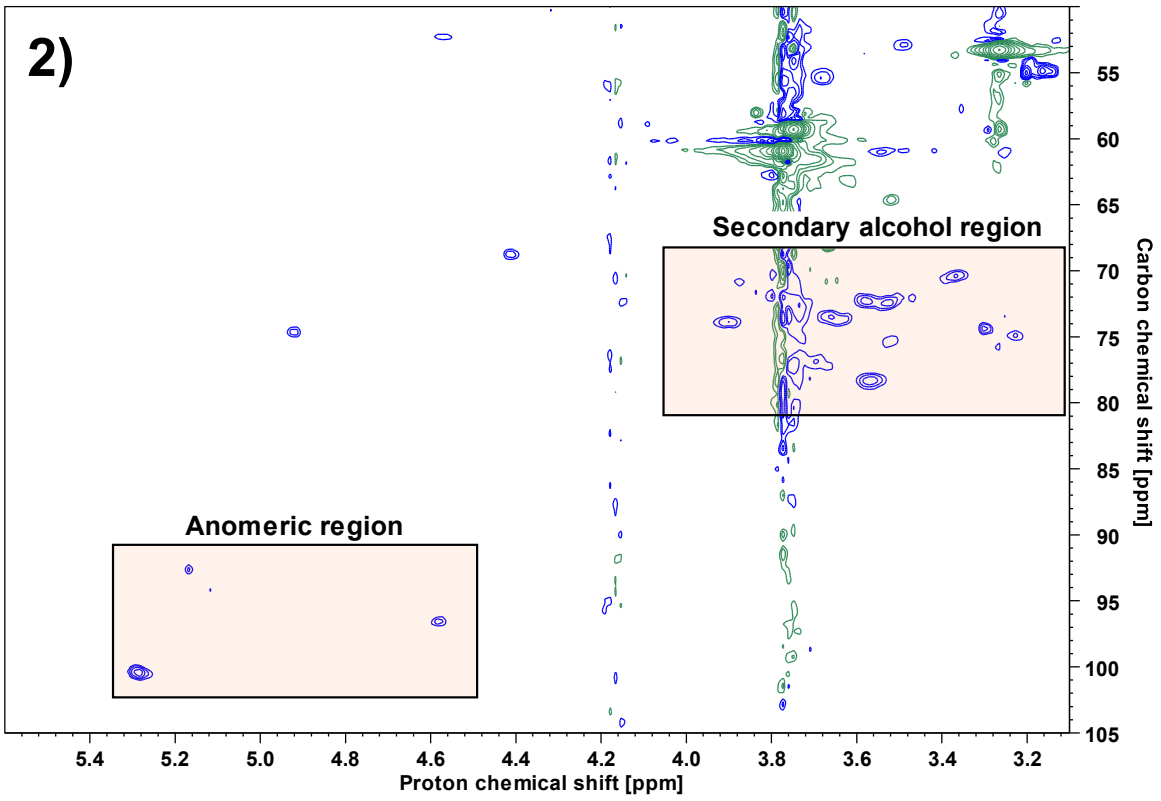

Figure 19: HSQC spectrum of papain digested and dialyzed water extract from *G. barretti*. The spectrum contains signals from leftover bis-tris buffer used in the enzymatic digestion. Spectrum recorded at T=83°C on a 600 MHz Avance NEO instrument.

The HSQC spectrum recorded after the first instance of acid hydrolysis (spectrum 3) had no detectable signals, likely due to the introduction of HCl under the hydrolysis (spectrum not included). Further acid hydrolysis and subsequent dialysis of the sample did yield a HSQC spectrum with detectable signals (spectrum 4). These signals were weaker than those obtained before the acid hydrolysis (Figure 19). The sample was mechanically sheared to obtain stronger signals. This did not yield stronger signals as the recorded spectrum (spectrum 5) had even weaker signals than spectrum 4. Spectra 4 and 5 can be seen in Figure 20.

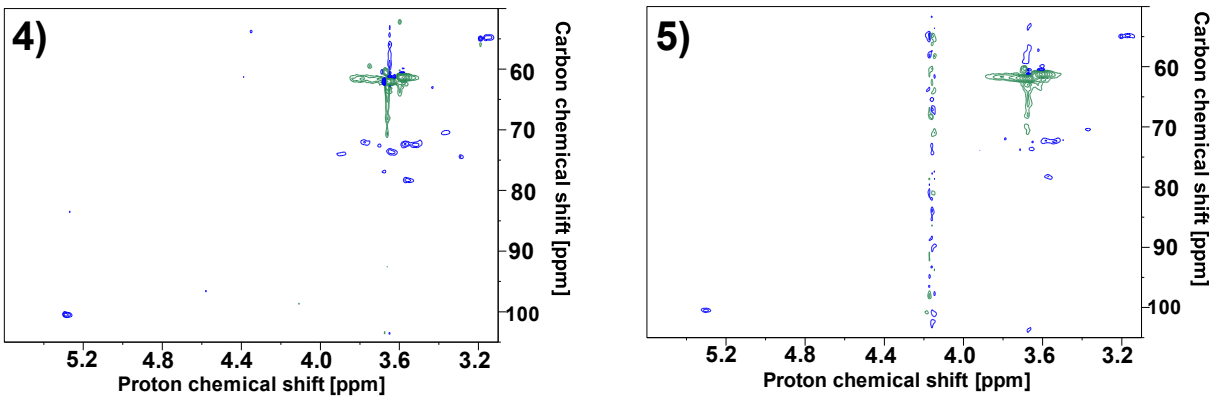

Figure 20: HSQC spectrum of papain digested, acid hydrolyzed, and dialyzed water extract from *G. barretti*. 5) The same sample after mechanical shearing 10 cycles at 200 MPa using a Star Burst Mini. Both spectra recorded at T=83°C on a 600 MHz Avance NEO instrument.

While the spectra did not improve with either acid hydrolysis or mechanical shearing, some signals did remain. Those being signals appearing in regions characteristic for sugar residues.

4.6.2 Cetylpyridinium precipitation sample possibly containing fucose

A sample was obtained by precipitating polysaccharides from *G. barretti* using cetylpyridinium chloride as a precipitant according to the method depicted in Figure 21. The method was based on protocols described in literature for extraction of sulfated sponge polysaccharides (45).

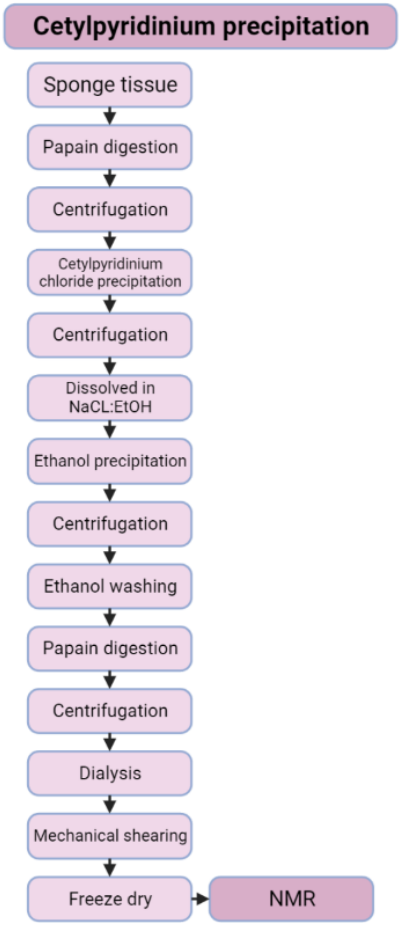

Figure 21: Overview of method used to extract polysaccharides from *G. barretti* using cetylpyridinium chloride as precipitant.

From the initial 4.5 g sponge material (DW) 22 mg sample was obtained, giving a yield of 0.49 %. The NMR sample was dark in color and opaque. Signals in the HSQC spectrum recorded of the extract had barely detectable signals. The few signals in the HSQC spectrum that were detected appeared in regions characteristic of sugars, such as signals appearing at 5.47 – 99.6 ppm and 1.26 – 18.4 ppm indicating presence of fucose in the sample. Figure 22 shows the HSQC spectrum of the cetylpyridinium precipitated extract.

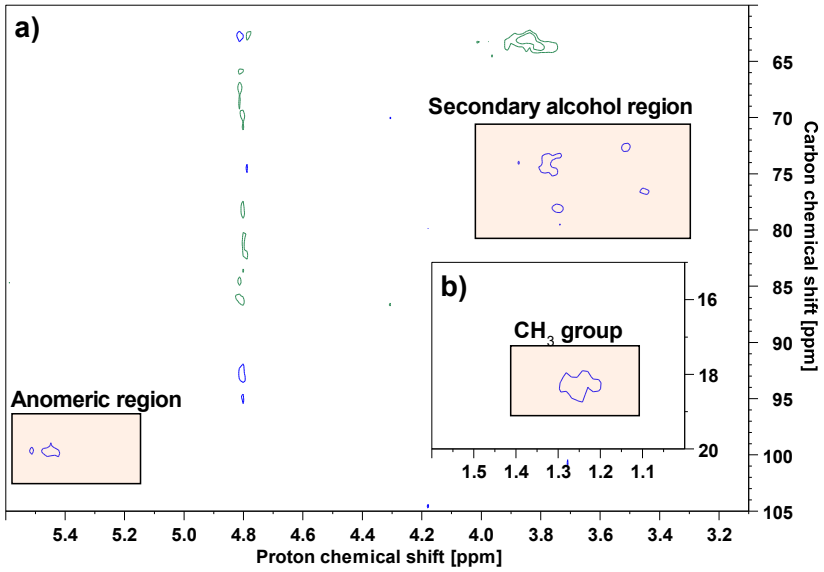

Figure 22: HSQC spectrum of cetylpyridinium chloride precipitated polysaccharide extract from *G. barretti*. Marked on the spectrum are signals appearing in regions common for polysaccharides, specifically fucose residues. Region **b)** is an inset from the same spectrum as the less shielded region **a)**. Spectrum recorded on a 600 MHz Avance NEO instrument.

4.6.3 Structural elucidation of an α-1,4-glucan in calcium precipitated extract

A polysaccharide extract from *G. barretti* obtained by calcium precipitation was used for structural elucidation. The extraction method used is depicted in Figure 23.

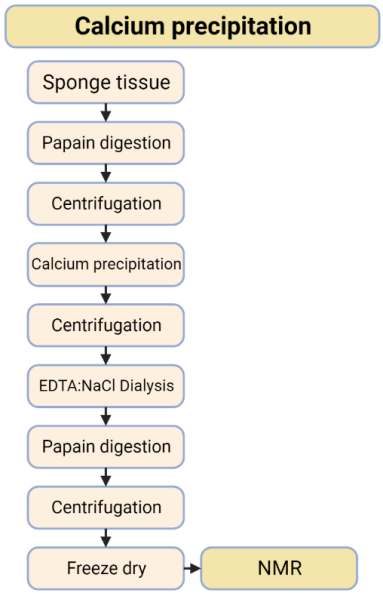

Figure 23: Overview of method used to extract polysaccharides from *G. barretti* using calcium chloride as precipitant.

One compound was identified in the sample, it was determined to be an α-1,4-glucan. Proposed structure of the polysaccharide extracted from *G. barretti* can be seen in Figure 24.

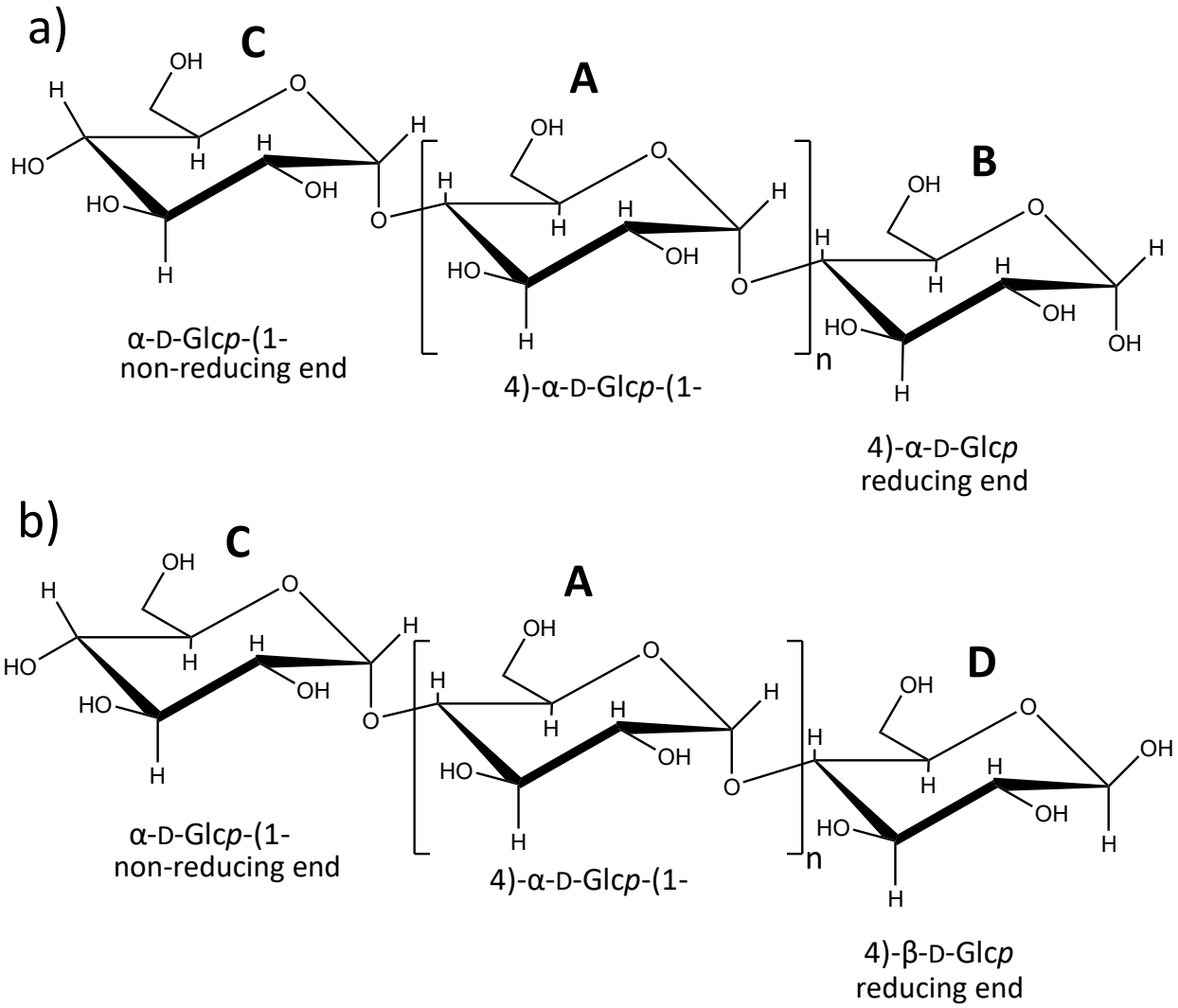

Figure 24: Proposed structure of polysaccharide extracted from the marine sponge *G. barretti*. The structures include four separate spin systems found by NMR spectroscopy. Both **a)** and **b)** is the isolated α-1,4-glucan with **a)** having an α-reducing end (B), and **b)** having a β-reducing end (D).

The proposed structures were based on four spin systems identified in the HSQC spectrum (see Figure 25) by using H2BC, HMBC, TOCSY and HSQC-TOCSY correlations. The spin systems were additionally confirmed by using IP-COSY and NOESY spectra (see Appendix E).

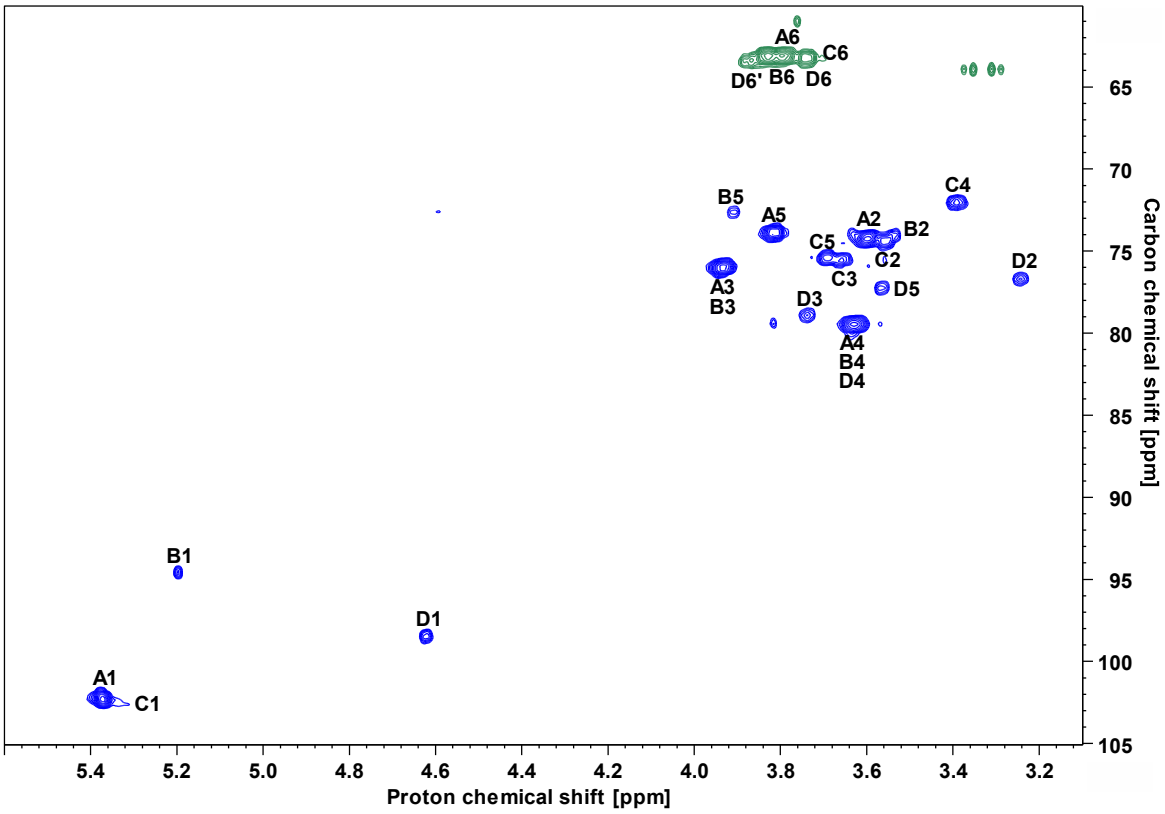

Figure 25: HSQC spectrum of a polysaccharide extract from the marine sponge *G. barretti*. Marked on the spectrum are positions within the sugar residues of the four spin systems A-D. Spectrum recorded with an 800 MHz Avance III HD instrument.

Chemical shifts of the four spin systems in Figure 25 are displayed in Table 16.

Table 16: ^{1}H and ^{13}C chemical shifts of signals in four D-Glc*p* spin systems identified in a HSQC spectrum of a polysaccharide extract from the marine sponge *G. barretti*.

Spin system	Compound	Positions and ^{1}H – ^{13}C chemical shifts [ppm]					
		1	**2**	**3**	**4**	**5**	**6**
A	4)-α-D-Glc*p*-(1-	5.37 102.3	3.60 74.3	3.93 76.0	3.63 79.5	3.82 73.9	3.79 63.1
B	4)-α-D-Glc*p*	5.20 94.6	3.54 74.0	3.93 75.9	3.63 79.5	3.82 73.9	3.79 63.1
C	α-D-Glc*p*-(1-	5.36 102.5	3.56 74.4	3.66 75.6	3.39 72.0	3.69 75.5	3.73 63.2
D	4)-β-D-Glc*p*	4.62 98.5	3.24 76.7	3.74 78.9	3.63 79.5	3.56 77.2	3.75 63.4 3.88

Most of the work with connecting signals of the individual spin systems in Figure 25 was done by analyzing correlations in the H2BC spectrum. As many signals from the HSQC spectrum are in proximity either in the proton or carbon axis, or completely overlapping, such as signals A3/B3 and A4/B4/D4, some correlations are difficult to distinguish. HMBC and TOCSY correlations were needed for complete structural elucidation. H2BC and HMBC correlations from spin system A are displayed in Table 17. H2BC and HMBC spectra can be seen in Appendix E.

Table 17: H2BC and HMBC correlations for spin system A of a polysaccharide extract from the marine sponge *G. barretti*. Position corresponding to the correlation is written in parenthesis. (-) indicates the correlation does not correspond to an identified signal within the spin system.

Position in spin system 1	**H2BC ^{13}C Correlations [ppm]**	**H2BC ^{1}H Correlations [ppm]**	**HMBC ^{13}C Correlations [ppm]**	**HMBC ^{1}H Correlations [ppm]**
A1 (5.37 – 102.3)	74.3 (C2)	3.60 (H2)	79.5 (C4)	3.93 (H3)
	-	-	76.0 (C3)	3.82 (H5)
	-	-	73.9 (C5)	3.63 (H4)
A2 (3.60 – 74.3)	76.0 (C3)	3.93 (H3)	76.0 (C3)	3.93 (H3)
A3 (3.93 – 76.0)	79.5 (C4)	3.63 (H4)	102.3 (C1)	5.37 (H1)
	-	-	79.5 (C4)	3.82 (H5)
	-	-	74.3 (C2)	3.63 (H4)
	-	-	63.1 (C6)	3.60 (H2)
A4 (3.63 – 79.5)	78.9 (-)	3.91 (-)	102.3 (C1)	5.37 (H1)
	77.2 (-)	3.82 (H5)	78.9 (-)	3.93 (H3)
	73.9 (C5)	3.74 (-)	77.2 (-)	3.87 (-)
	72.6 (-)	3.56 (-)	76.0 (C3)	3.74 (-)
	-	-	74.0 (C5)	3.56 (-)
	-	-	72.6 (-)	3.24 (-)
	-	-	63.1 (C6)	-
A5 (3.82 – 73.9)	63.1 (C6)	3.79 (H6)	102.3 (C1)	5.37 (H1)
	-	-	79.5 (C4)	3.83 (-)
	-	-	76.0 (C3)	3.79 (H6)
	-	-	72.0 (-)	3.73 (-)
	-	-		3.63 (H4)
A6 (3.79 – 63.1)	-	3.69 (-)	79.5 (C4)	3.89 (-)
	-	-	73.9 (C5)	3.63 (H4)

Assigning positions 1-4 and position 6 in spin system A was straight forward as there was only one H2BC correlation for both ^{13}C and ^{1}H. Position 5 was found by using HMBC correlations from positions 1 and 3 (see Figure 26). While position 1 does seem to have HMBC correlations to

position 4 (3.63 – 79.5 ppm), this would not be expected due to the large amount of bonds separating the nuclei. The correlation is likely to a CH group through the glycosidic bond with similar chemical shifts.

H2BC and HMBC correlations for the three remaining spin systems were identified and used to assign each position in the spin systems. Tables containing these correlations can be found in Appendix E. Like spin system A, assigning spin systems B and D was straight forward aside from position 5. As spin systems A, B, and D had overlapping position 4 signals, there were several H2BC correlations. The 5 positions were identified through HMBC correlation between positions 1 and 5 in the two spin systems. Figure 26 contains the superimposed HSQC and HMBC spectra displaying correlations used in the structural elucidation of spin systems A, B, and D.

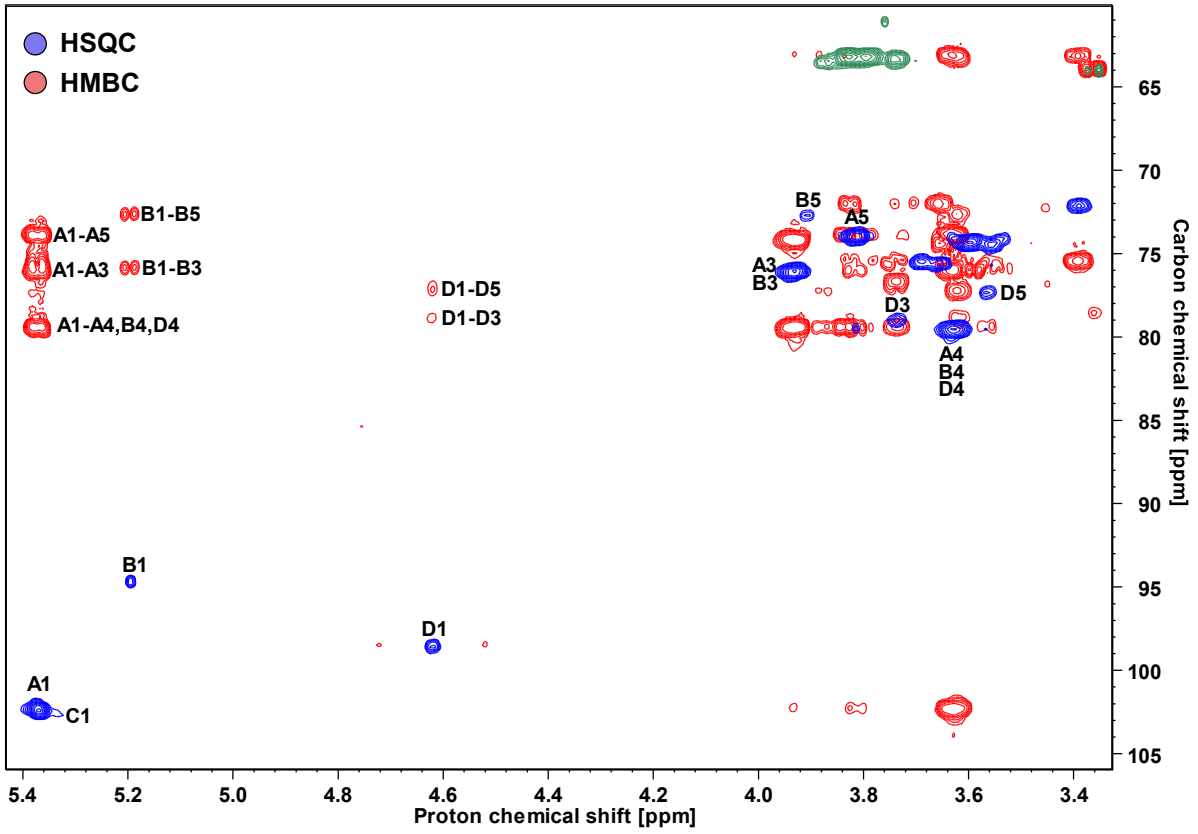

Figure 26: Superimposed HSQC and HMBC spectra of a polysaccharide extract from the marine sponge *G. barretti*. HMBC correlations used to determine position 5 in spin systems AD are labeled accordingly. Numbers correspond to position within the labeled spin system. HSQC displayed in blue, HMBC is displayed in red. Spectra recorded with an 800 MHz Avance III HD instrument.

All six positions in spin system C could be assigned with the H2BC spectrum, as there were no overlapping signals in the HSQC, which was the case for all other spin systems.

TOCSY and HSQC-TOCSY correlations were used to confirm the spin systems found using H2BC and HMBC correlations. Listed in Table 18 are correlations from position 1 for spin systems A-D. As spin systems A and C had nearly overlapping signals for position 1, their TOCSY and HSQC-TOCSY correlations were not differentiated.

Table 18: TOCSY and HSQC-TOCSY correlations for spin systems A-D of a polysaccharide extract from the marine sponge *G. barretti*. Position corresponding to the correlation is written in parenthesis. Table only includes correlations found for the 1 position of each spin system.

Position / chemical shifts [ppm]	**TOCSY Correlations [ppm]**		**HSQC-TOCSY Correlations [ppm]**
A1 (5.37 – 102.3)	3.93 (H3)	3.66 (-)	79.5 (C4)
	3.82 (H5)	3.60 (H2)	75.9 (C3)
	3.79 (H6)	3.56 (-)	74.3 (C2)
	3.73 (-)	3.39 (-)	72.0 (-)
	3.69 (-)	-	63.1 (C6)
B1 (5.20 – 94.6)	3.94 (H3)	3.61 (-)	79.6 (C4)
	3.91 (H5)	3.54 (H2)	75.9 (C3)
	3.79 (H6)	-	74.0 (C2)
	3.67 (-)	-	72.6 (C5)
	3.63 (H4)	-	-
C1 (5.36 – 102.5)	3.93 (-)	3.66 (H3)	79.5 (-)
	3.82 (-)	3.60 (-)	75.9 (-)
	3.79 (-)	3.56 (H2)	74.3 (C2)
	3.73 (H6)	3.39 (H4)	72.0 (C4)
	3.69 (H5)	-	63.1 (C6)
D1 (4.62 – 98.5)	3.88 (H6')	3.24 (H2)	78.9 (C3)
	3.75 (H6)	-	77.2 (C5)
	3.74 (H3)	-	76.7 (C2)
	3.62 (H4)	-	-
	3.56 (H5)	-	-

By using NOESY and HMBC correlations the linkages of the polysaccharides were determined to be 1→4. All observed NOESY correlations were between vicinal protons except for correlations 1 and 6 in Table 19. Correlation 1 between A1 and A4, B4, D4, corresponds to a commonly observed glycosidic linkage in nature. This is supported by the HMBC correlation between A1 and

the 4 position. Correlation 6 between A5 and D3, does not correspond to a type of glycosidic linkage which occurs in nature, and is likely a correlation between other nuclei than those listed.

Table 19: NOESY correlations for spin systems A-D of a polysaccharide extract from the marine sponge *G. barretti*.

NOESY Correlation number	NOESY Correlations [ppm]	NOESY Correlations [position]
1	5.37 – 3.63	A1 – A4/B4/D4
2	5.20 – 3.54	B1 – B2
3	4.62 – 3.24	D1 – D2
4	3.93 – 3.63	A3/B3 – A4/B4/D4
5	3.93 – 3.60	A3/B3 – A2
6	3.82 – 3.74	A5 – D3
7	3.82 – 3.63	A5 – A4/B4/D4
8	3.69 – 3.39	C5 – C4
9	3.66 – 3.56	C3 – C2

The four spin systems were determined to be pyranoses, as position 1 of all four systems were found in the anomeric region (4.4 – 5.6 ppm) and positions 2-6 were found in the secondary alcohol region (3.0 – 4.0 ppm). Additionally positions 6 were all CH_2 groups. All four spin systems were determined to be D-glucose residues by comparing chemical shifts with those reported by Agrawal P.K. (56).

Spin system A, which had the strongest signals, was determined to be α-glucose integrated in a longer chain. This can be observed as NOESY and HMBC signals revealed that the spin system was linked to adjacent residues in the 1 and 4 positions. Spin system C had an anomeric signal very close to the anomeric signal in spin system A, and a position 4 signal with significantly lower chemical than the same signal in spin system A (A4: 3.63 – 79.5 ppm, C4: 3.39 – 72.0 ppm). This indicates that spin system C is linked in the 1 position, but not in the 4 position, which is the case for non-reducing ends. The anomeric signal observed for spin system B (5.20 – 94.6 ppm) is close to the chemical shifts of α-D-glucose reported by Agrawal P.K. (5.23 – 93.0 ppm), while the anomeric signal of spin system D (4.62 – 98.5 ppm) is closer to those reported for β-D-glucose (4.64 – 96.8 ppm) (56).

CASPER was used to simulate the proposed structures seen in Figure 24. The resulting chemical shifts from the simulations were compared to the experimentally obtained chemical shifts (see

Table 20). Predicted proton shifts were largely in agreement with the experimental data, while predicted carbon shifts were ~1.5 – 2.0 ppm lower than the experimental ones.

Table 20: Computationally predicted chemical shifts of α-1,4-glucans using CASPER (50), compared with experimentally obtained chemical shifts. Difference (diff.) calculated by subtracting experimental data from the predicted data. A: 4)-α-D-Glcp-(1-, B: 4)-α-D-Glcp, C: α-D-Glcp-(1-, D: 4)-β-D-Glcp.

	A δ [ppm]	diff.	B δ [ppm]	diff.	C δ [ppm]	diff.	D δ [ppm]	diff.
H1	5.36	-0.01	5.24	+0.04	5.35	-0.01	4.65	+0.03
H2	3.64	+0.04	3.59	+0.04	3.59	+0.03	3.29	+0.05
H3	3.95	+0.02	3.97	+0.04	3.70	+0.04	3.78	+0.04
H4	3.64	+0.01	3.63	0	3.43	+0.04	3.63	0
H5	3.84	+0.02	3.95	+0.04	3.73	+0.04	3.58	+0.02
H6	3.81	+0.02	3.80	+0.01	3.77	+0.04	3.76	+0.01
	3.89	-	3.87	-	3.86	-	3.93	+0.05
C1	100.5	-1.8	92.8	-1.8	100.7	-1.8	96.7	-1.8
C2	72.5	-1.8	72.3	-1.7	72.7	-1.7	75.1	-1.6
C3	74.1	-1.9	74.0	-1.9	73.9	-1.7	77.0	-1.9
C4	78.2	-1.3	78.5	-1.4	70.4	-1.6	78.3	-1.2
C5	72.2	-1.7	71.0	-1.5	73.6	-1.9	75.5	-1.7
C6	61.5	-1.6	61.8	-1.4	61.6	-1.8	61.8	-1.6

An approximate degree of polymerization (DP) was estimated by integrating signals A1, B1, C1, and D1 from the HSQC spectrum (Figure 25). Their integrals were 1.00, 0.09, 0.13, and 0.03 respectively, indicating a DP of ~10, see Figure 27. As B1 and D1 are reducing end signals, their combined integrals should be equal to the non-reducing end integral from C1, which is observed.

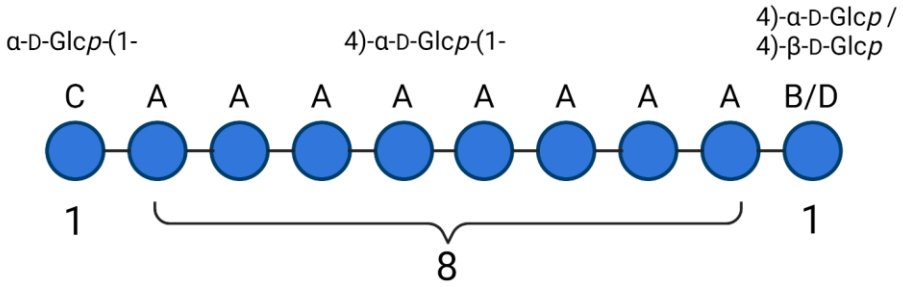

Figure 27: Estimated size of α-1,4-glucan extracted from *G. barretti* based on integrals from a HSQC spectrum containing the four spin systems A-D. Numbers correspond to integrals.

4.6.4 Calcium precipitated polysaccharide extracts from four species showing similarities

The calcium precipitation method was chosen to extract polysaccharides from all four species. The protocol was chosen ahead of the enzymatic digestion and cetylpyridinium chloride precipitation methods as it yielded the best resolved NMR spectra. Additionally, the calcium precipitation sample was not as dark and opaque as samples obtained using other methods. Yields from the Ca^{2+} extractions are summarized in Table 21.

Table 21: Starting material of sponge (DW) and extraction yield from a calcium precipitation-based polysaccharide extraction protocol.

Species	Starting material (DW) [mg]	Polysaccharide extract [mg]	Extraction yield [%]
Antho dichotoma	372.8	7.6	2.0
Geodia barretti	380.0	11.0	2.9
Mycale lingua	361.4	7.4	2.0
Phakellia ventilabrum	160.8	8.0	5.0

The polysaccharide extracts from each of the four species showed a large similarity in structure and were all determined to be α-1,4-glucans by comparing HSQC spectra. The HSQC spectra of *A. dichotoma*, *G. barretti*, *M. lingua*, and *P. ventilabrum* can be seen in Figure 28.

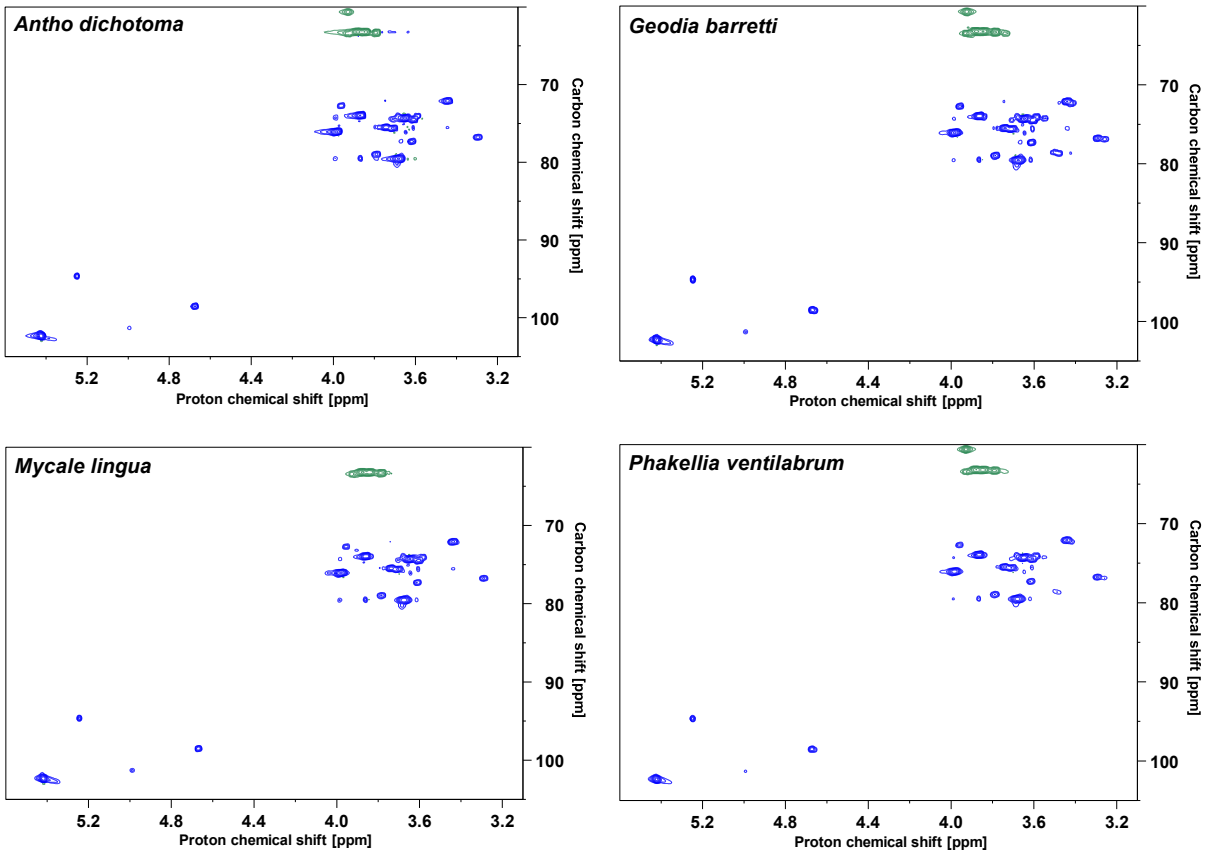

Figure 28: HSQC spectra of calcium precipitated polysaccharide extracts from marine sponges. Spectra recorded with an 800 MHz Avance III HD instrument.

Each of the four extracts were further analyzed with C-PAGE.

4.7 C-PAGE revealing charged components in most extracts

The C-PAGE method was chosen to get further insight into the structure of the polysaccharides obtained from the calcium precipitation in addition to CPC extracted polysaccharides from *G. barretti* and a crude water extract (SE-01). By using toluidine blue as a dying agent, samples containing only neutral monosaccharides should not react with the dye. If the samples contain shorter oligosaccharides these would expectedly elute through the gel. Fucoidan and laminarin were chosen as standards. As fucoidan is heavily sulfated and laminarin carries no charge, fucoidan should react with the toluidine blue while the laminarin should not react with the toluidine blue. A picture of the gel can be seen in Figure 29.

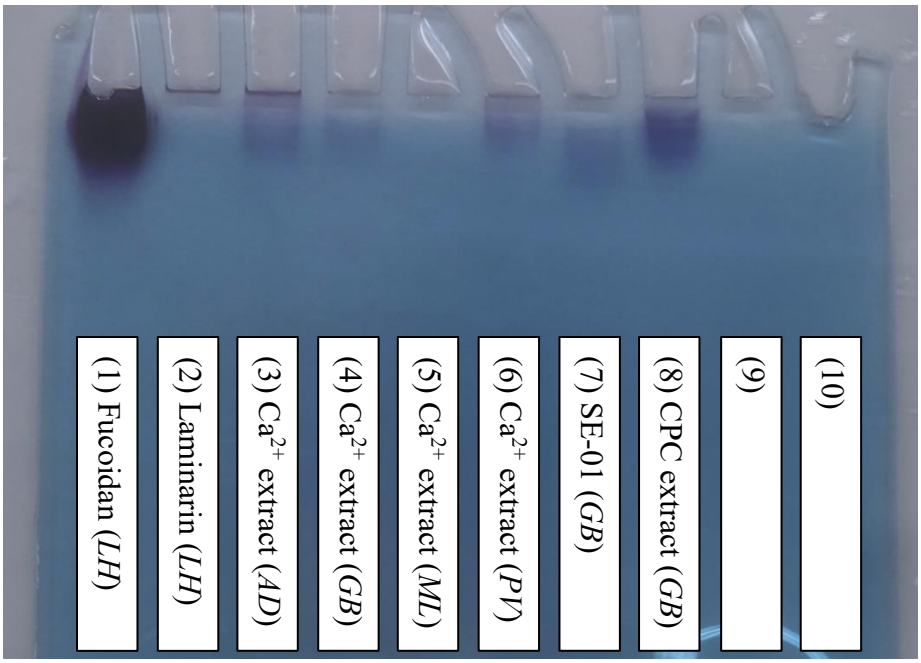

Figure 29: A polyacrylamide gel used in C-PAGE, dyed with toluidine blue. Ca^{2+} extracts are polysaccharides extracted with calcium precipitation. The CPC extract is polysaccharides extracted with cetylpyridinium chloride precipitation. SE-01 is a crude water extract. Well 9 and 10 were left empty. *LH = Laminaria hyperborea, AD =* A*ntho dichotoma, GB = Geodia barretti, ML = Mycale lingua, PV = Phakellia ventilabrum*.

The fucoidan sample in the first well clearly reacted with the toluidine blue leaving the sample a dark blue color. No coloration was observed for the laminarin sample in well nr. 2. All Ca^{2+} extracts had a blue color except for the *Mycale lingua* extract in well nr. 5. The *A. dichotoma* and *P. ventilabrum* samples (well nr. 3 and 6) had a darker shade of blue than the *G. barretti* sample in well nr. 4. Well nr. 7 containing the crude water extract (SE-01) of *G. barretti* had a slightly darker shade of blue than the Ca^{2+} extract of the same species. The most obvious reaction aside from the fucoidan sample was the CPC extract of *G. barretti* (well nr. 8). No samples seemed to elute through the gel except for sample SE-01 in well nr. 7, which seemed to elute a very short distance.

5 Discussion

5.1 Water and ash content comparable to other sponges

Most of the sample mass of each species was water weight. All species seem to have a water content in the range of what is normal for other sponges (commonly between 70-90 % (30)). As mentioned in section 1.4, water content might vary with harvesting location and season depending on species (30). Without having data from multiple specimens of varying locations and seasons, it is difficult to know exactly how accurate the measured water content of these sponges is compared to other specimens of the same species.

The ash content of *G. barretti*, which was measured to be 14.8 ± 2.5 % of WW (60.1 ± 2.8 % of its DW), coincides well with measurements recorded by Kutti *et al.* where ash content was measured to be 59.2 ± 1.1 % of its DW (57). Martins *et al*. found it to be somewhat lower at 55.1 % (58). Ashing was not completed for any of the other species due to the large amount of sponge material required. While no data was found for *A. dichotoma* and *M. lingua*, Martins *et al*. also made measurements on *P. ventilabrum* reporting that 44.4 % of its DW consists of inorganic material (58).

After the ash analysis of *G. barretti* the leftover material seemed to consist of many small rod-shaped pieces. These were likely the spicules of the sponge. As the main interest of this thesis was within the organic portion of the sponge, no further analyses were performed on the inorganic material.

5.2 Deriving useful information from element content

The element analysis revealed that the nitrogen, carbon, and hydrogen content of *G. barretti, M. lingua,* and *P. ventilabrum* is very similar. The clear outlier being *A. dichotoma* which had a higher content of nitrogen, carbon, and hydrogen compared to the other three species. One reason why this species has such a high amount of these elements (39 % of total sponge biomass combined) compared to the other species (22 – 23 % of total sponge biomass combined) could be explained by the inorganic content of the sponge. As sponges contain a large amount of spicules, which are either made of calcium carbonate ($CaCO_3$) or silica (SiO_2) the elemental composition of the spicules would not be detected with the method used, except for one carbon atom in the case of

calcium carbonate. If *A. dichotoma* contains less spicules or other inorganic material, a higher content of elements found in organic compounds would be expected. Looking at element content in comparison to organic mass instead of total dry mass might yield more comparable results.

Other than obtaining a general profile of elemental content of the selected sponges, the sulfur content was especially interesting considering the objective of extracting sulfated polysaccharides. As *G. barretti* only consisted of 0.5 % sulfur, the lowest proportion of all four species, extraction of sulfated polysaccharides would likely require a large amount of starting material to obtain a sample large enough to analyze further. *M. lingua* could be a better candidate for extraction of sulfated polysaccharides due to a sulfur content of 2.7 %, over five times the amount found in *G. barretti*. Of course, sulfur is not exclusively found in sulfated polysaccharides, but other organic molecules such as amino acids and vitamins as well. The higher sulfur levels of *M. lingua* could be explained by a higher frequency of the sulfur containing amino acids methionine and cysteine.

Nitrogen-to-protein conversion factors based on cow's milk (6.0), soy milk (5.5), and seaweed (3.8) were applied to the nitrogen content of the sponges (Table 13). Conversion factors were also estimated from measured amino acid content (Table 14). The calculated nitrogen-to-protein conversion factors obtained were *A. dichotoma*: 3.4, *G. barretti*: 4.3, *M. lingua*: 4.6, and *P. ventilabrum*: 4.7. The values used from the amino acid content were the upper limits from Figure 12 (assuming only arginine, and no glycine), as proline, cysteine, and tryptophan were not detectable. Conversion factors used for cow's milk and soy milk overestimated the protein content for each of the sponges. The conversion factor used for *S. latissima* was the most accurate, overestimating protein content of *A. dichotoma* and underestimating protein content of remaining species. Calculated conversion factors for the sponges showed a large inter-species difference (3.4 – 4.7). Obtaining a representative conversion factor across sponge species is likely difficult as their biomass composition is so varied.

5.3 Analyzing similarities and differences in monosaccharide composition

It is important to recognize the monosaccharide analysis only detects a selection of neutral monosaccharides, with other monosaccharides such as uronic acids and sialic acids going undetected.

Figure 9 shows a clear difference in neutral monosaccharide content between the four species with *Geodia barretti* only consisting of 2 ± 0 % neutral monosaccharides by weight while *A. dichotoma* consists of 5.2 ± 0.7 % neutral monosaccharides. When looking at element content it was speculated that *A. dichotoma* might have a lower content of inorganic matter than the other sponges. If that is the case, a higher monosaccharide content relative to total biomass would be expected. Nevertheless, *G. barretti* which consists of ~60 % inorganic matter contains a lower proportion of neutral monosaccharides than *P. ventilabrum*, which has been reported to consist of 44.4 % inorganic matter. While the ratio of organic to inorganic mass might affect sugar content, the discrepancy is likely not explained by this reason alone.

When looking at the monosaccharide profiles in Figure 10 of the different sponges, it is apparent that there is a varied distribution of monosaccharides both within and between the four species. Common to all four is a relatively large proportion of glucose, varying between 26 – 38 %. This could be linked to the energy storage of the sponges. Like other animals, sponges produce glycogen, polysaccharides consisting of α1→4 linked glucose residues (59). Calcium precipitated polysaccharide extracts from all four species were found to contain α-1,4-glucans, indicating that these polysaccharides are common in sponges. None of the species contained detectable amounts of mannitol, which was expected as mannitol is an energy storage molecule common in plants and fungi (60). While xylose was found in each species it only accounted for ~1 % of total neutral monosaccharides.

Rhamnose was detected in *G. barretti* and *M. lingua*, but not in *A. dichotoma* or *P. ventilabrum*. The rhamnose levels in the *G. barretti* sample were relatively low at 2 % of total neutral monosaccharide content, but in *M. lingua* it accounted for 13 % of sugar residues, making it the fourth most common neutral monosaccharide. This is interesting as rhamnose is not known to be synthesized or utilized by animals. While rhamnose is biosynthesized by eukaryotes such as land plants, fungi, and algae, they are ubiquitous in bacteria (61). The explanation for the high rhamnose levels in *M. lingua*, and the presence of the deoxy sugar in *G. barretti*, is likely a large number of sponge-associated bacteria which were hydrolyzed together with the sponge tissue itself.

As the focus of this thesis was on extracting AF SPs along with exploring sponge biomass, it was natural to think of these polysaccharides when looking at monosaccharide composition. Due to these polysaccharides only constituting a small portion of all monosaccharides within the sponge,

and their structural heterogeneity, it is difficult draw any conclusion from the monosaccharide analysis data alone. As can be seen in Table 3, AF SPs have been found to contain glucose, galactose, mannose, arabinose, fucose, uronic acids, and N-acetylglucosamine. All the neutral monosaccharides mentioned were present in each species.

5.4 Amino acid profiles provide information on the composition of sponges and their proteoglycans

Due to the coelution of arginine and glycine it is difficult to get an accurate measure of amino acid content of the sponges. Therefore, Figure 12 contains a range of uncertainty with a theoretical lower and upper limit. The lower limit assuming only elution of glycine and the upper limit assuming only elution of arginine. Due to these amino acids being the most abundant in each species in combination with their wide gap in molecular weight (Arg = 174 Da, Gly = 75 Da), the range of uncertainty is rather large. For *A. dichotoma* the total amino acid content is somewhere between 15.6 – 22.5 % of its DW. With both arginine and glycine being among the most abundant amino acids in proteins, 5.7 % and 7.2 % respectively (55), the sponges are likely to contain a significant amount of both amino acids.

Three of the four species (*G. barretti*, *M. lingua*, and *P. ventilabrum*) consist of very similar amounts of amino acids (13.4 – 14.0 % lower limit, 16.5 – 18.3 % upper limit), with *A. dichotoma* having the highest amino acid content. Again, considering the potential scenario of *A. dichotoma* having a lower proportion of inorganic matter, a higher proportion of amino acids would be expected.

It should be mentioned that the proportion of amino acids (as dry weight) in the sponges presented in Figure 12 is an underestimation due to proline, cysteine, and tryptophan not being detected. These three amino acids account for on average 8.1 % of total amino acids in proteins (55).

When looking at Figure 13 and Figure 14 it is clear that there are some inter species differences with respect to amino acid distributions. While the arginine/glycine content of each sponge is high, a lot higher than what would be expected for most proteins, it is much lower in *G. barretti* than the other three sponges. The high arginine/glycine levels could be partially explained by sponge collagen, often called spongin. Collagen, which is a fibrous protein central in the structure of many

connective tissues, consists in large part of glycine, proline, hydroxyproline. Extraction of collagen from the sponge *Chondrosia reinformis* revealed a collagen content of 30 % of sponge DW (62). If proline was detected with the amino acid analysis, a much higher level than what is observed among other proteins would be expected.

Since the total amino acid analysis includes not only amino acids from proteins, but free amino acids as well, comparing the results with the frequency of amino acids in proteins is not necessarily accurate. If all amino acids in the sponge samples came from proteins and sponge proteins had the same frequency of amino acids as other proteins, one would expect the bars in Figure 14 to become progressively smaller. This is observed to some degree with a few exceptions. Aspartic acid seems to be about twice as frequent in the sponge samples compared to the average frequency of proteins. Asparagine and glutamine which occur at a frequency of 4.4 % and 4.0 % in proteins (55) are nearly non-existent in the sponge samples.

As mentioned in the discussion of the element analysis, sulfur can be found in certain amino acids, those being methionine and cysteine. Since cysteine is one of the three proteinogenic amino acids not detected in the total amino acid analysis it is currently not possible to get a full picture of sulfur containing amino acids in these sponges. Methionine, which is detected, shows levels lower than those occurring in the average protein. It was speculated that the higher sulfur content of *M. lingua* could be due to sulfur containing amino acids. As methionine levels are comparable to the other species, the high sulfur content is not caused by methionine being abnormally abundant, it is however unknown if the sponge has a higher cysteine content.

When it comes to AFs, characterization of these proteoglycans in the species *Microciona parthena* revealed an amino acid content of 47 %. The amino acid composition was reported as not unusual with the exception of high aspartic and glutamic acid content (63). This fits well with the amino acid distribution data in Figure 14. Aspartic acid content was, as explained earlier, a lot higher than what would be expected from other proteins. Glutamic acid is also one of few amino acids at unusually high levels. While it is not possible to assign amino acids to specific proteins with the current data, high abundance of aggregation factors could explain why exactly these amino acids are so prominent.

Another important aspect of proteoglycans is the binding of polysaccharides to the protein. This can either be done through *N*-linked glycosylation or *O*-linked glycosylation. *N*-linked

glycosylation is the attachment of glycans to the amide nitrogen of either asparagine or glutamine residues (64). *O*-linked glycosylation is the attachment of glycans to the oxygen atom in the side chain of either serine or threonine residues (65). The sponges contained almost no asparagine or glutamine, while serine and threonine levels were comparable to those of the average protein. This suggests that the polysaccharides of the proteoglycans in the four sponges are *O*-linked.

5.5 Advantages and disadvantages of sequential water extractions

When developing a protocol for polysaccharide extraction, doing water extracts was a natural start. Water extraction is the basis of several sponge extraction protocols and extraction of polysaccharides from other biological sources, such as brown algae due to the high water solubility of carbohydrates. As shown in Table 7, extraction was done in multiple steps under two different conditions (SE-01 and SE-02). This was done to see if higher temperature significantly increased the yield, which was not observed (see Table 15). Room temperature extractions with mixing resulted in higher yields at every step, apart from extraction step two (SE-01.2 and SE-02.2). The higher yields might not be caused by the lower temperature, but the constant mixing. A water bath was used to keep temperature at 70 °C and the samples were not mixed while incubated. Therefore, it is not possible determine if higher temperature in combination with mixing would give comparable or higher yields with the current data.

Some of the freeze-dried extracts did, as mentioned in section 4.5, vary in appearance and texture. Especially extracts SE-01.1 and SE-02.1, which did not have the same soft texture and light appearance as the other extracts. Instead, their textures were rougher, and their colors were darker. This might be caused by salts, other water-soluble components, and particles being washed out in the first extraction step, causing the coarse texture of the extracts. Extract SE-01.3 had a high yield, 17 % of the sponge DW, a soft texture, and was white in color, similar to what is often observed for polysaccharides. For those reasons, extract SE-01.3 together with a mixture of all SE-01 extracts, was chosen to be further investigated with an element analysis and monosaccharide analysis.

Both SE-01.3 and SE-01 had higher content of nitrogen, carbon, hydrogen, and sulfur compared to the untreated tissue of *G. barretti*. This is likely due to the inorganic portion of the sponge

biomass having low water solubility and having a relatively low abundance of the measured elements. Interestingly, extract SE-01.3 had lower nitrogen, carbon, and hydrogen content than the SE-01 extracts, but a higher sulfur content. The increased sulfur content might indicate a higher proportion of SPs in the SE-01.3 extract.

Both extracts had a much higher sugar content than the untreated tissue. Again, this is likely due to the low water solubility of the sponge's inorganic material in combination with the high water solubility of carbohydrates. The neutral monosaccharide profiles are mostly similar, with SE-01.3 having a somewhat higher fucose and mannose content. From the overview of structural components of sulfated sponge polysaccharides in Table 3, one can see that fucose occurs frequently, especially sulfated fucose. Mannose has been found, but only in one of the ten species in the overview. Combining the results from the element analysis with the monosaccharide analysis, the increased sulfur and fucose content of fraction SE-01.3 could be due to sulfated fucose residues in AF SPs.

While the sequential water extracts of *G. barretti* did reveal useful information and could be used to obtain higher concentrations of desired compounds the method was not used in the extraction of polysaccharides from the other three species. As there was limited sponge material of *A. dichotoma*, *M. lingua*, and *P. ventilabrum*, a separation of water extracts would limit the total polysaccharides in the final extract. Instead, methods used to selectively isolate polysaccharides were chosen.

5.6 Polysaccharide extraction and NMR analysis

5.6.1 Enzymatic digestion method

The enzymatic digestion method described in section 3.8 and shown in Figure 7 was the first of the three methods to be used, hence the five instances of NMR spectroscopy. The first spectra recorded for this sample, right after the papain digestion, was a ^{1}H and an HSQC spectrum. There were some indications of sugar and amino acid signals in the ^{1}H spectrum, but this was difficult to conclude from the ^{1}H spectrum alone. No signals were observed in the HSQC spectrum, likely due to a lot of salts from the bis-tris buffer used during the enzymatic digestion. To solve that issue the sample was dialyzed, resulting in a HSQC spectrum with signals. There was still a noticeable

amount of buffer salts left in the sample, but for the first time, good indications of sugar signals were observed. While the signals were consistent with carbohydrates, there was not a great diversity among the signals observed. As AF SPs are heterogenous polysaccharides consisting of several different monosaccharides, a higher diversity of signals would be expected. These signals were instead likely to be α-1,4-glucans which were later elucidated. To hopefully observe stronger sugar signals the polysaccharides were acid hydrolyzed to reduce the molecular weight of the polysaccharides.

After the first round of acid hydrolysis the recorded HSQC spectrum had no detectable signals, this was believed to be due to the HCl used in the degradation of sample molecules. As the first acid hydrolysis was very mild, the sample was acid hydrolyzed again with harsher conditions and dialyzed to remove salts. There were clearly fewer impurities than previously, but the same signals as previously observed were present with no new signals appearing. Mechanical shearing was chosen to further degrade the polysaccharides. The resulting NMR spectra were similar to the ones previously recorded, but the signals were even weaker. At this point the sample had been enzymatically digested, hydrolyzed twice, mechanically sheared, and freeze dried a total of six times. The pursuit of better results using this sample was abandoned. The NMR analysis did reveal that water extraction of *G. barretti* does yield polysaccharides and that papain digestion of sponge proteins in a bis-tris buffer does work.

5.6.2 Calcium precipitation method

Calcium precipitation was chosen as it had previously been used to extract AFs from *Microciona prolifera*, *Halichondria panicea*, and *Cliona celata* (42). Preliminary tests were done to determine if addition of calcium would result in precipitation of polysaccharides. In addition to the use of calcium, the enzymatic digestion, which previously was done in a bis-tris buffer, was now performed unbuffered and for twice as long. As the function of the papain was to break down as many polypeptides as possible, leaving the enzymes for longer would hopefully liberate more protein-associated polysaccharides. Acid hydrolysis was not performed, as the acidic conditions could desulfate sulfated polysaccharides.

The calcium precipitation method described in section 3.8 was first performed on *Geodia barretti*. NMR experiments of the resulting extract yielded spectra with obvious sugar signals and relatively

few impurities compared with previously recorded spectra. Therefore, multiple NMR spectra were recorded to elucidate the structure of the extracted polysaccharide. Superimposing the HSQC, H2BC, and HMBC spectra made identifying four monosaccharide spin systems possible. Using the H2BC spectrum alone was not sufficient due to overlapping signals, such as position 4 in spin systems A, B, and D. The HMBC spectrum could in those cases be used to see correlations from previous positions in the same spin system.

Protons in the CH_2 group at position 6 were difficult to determine due to crowded spectra. As those protons are diastereotopic they have unique chemical shifts. The only spin system with both H6 protons assigned with certainty was the β-reducing end glucose (D). H2BC correlations from position 5 were used to find the first proton (3.75 – 63.4 ppm) and a HMBC correlation from position 4 in combination with an unassigned TOCSY correlation at 3.88 ppm were used to assign the second proton at position 6.

When comparing the experimentally obtained chemical shifts with computationally predicted chemical shifts from CASPER and reference data from Pawan K.A. (56), glucose did seem to be a good fit. As the NOESY spectrum indicated the polysaccharide was 1→4 linked, α-1,4-glucans were simulated using CASPER. These simulations had almost the exact same proton chemical shifts as the sponge polysaccharide, while predicted carbon shifts were ~1.5 – 2.0 ppm lower than experimental ones. The chemical shift discrepancy is likely due to external referencing in the ^{13}C axis. NMR spectra of compounds used in the CASPER model were externally referenced to dioxane at 67.40 ppm (50). NMR spectra recorded in this thesis were externally referenced to DSS at 0.00 ppm. Wishart *et al.* reported that dioxane in D_2O at 25 °C, relative to DSS at 0.00 ppm, has a chemical shift of 69.3 ppm (52), 1.9 ppm higher than the value used for the development of CASPER. This value fits well with the observed differences in Table 20. Estimates of size based on integrals of anomeric signals from the HSQC spectrum in Figure 25 gave a DP of 10. Two-dimensional spectra are not ideal for measuring integrals as signal intensity is not only dependent on abundance of given nuclei, but also on the magnetization through the C-H bond, therefore the result should be treated as a rough estimate.

While the method resulted in oligosaccharides, there were no indications in the NMR spectra that these oligosaccharides were sulfated. Since there was no evidence of the desired sulfated

polysaccharides, a method base on precipitation of polysaccharides with cetylpyridinium chloride was tested.

5.6.3 Cetylpyridinium chloride precipitation method

The cetylpyridinium protocol was based on a method utilized by Vilanova et al. (12) to extract AF SPs for NMR samples. When analyzing the extract with NMR spectroscopy it appeared that the sample did contain polysaccharides, but the NMR spectra had very weak signals and poorly resolved peaks. One of the few signals that did appear in the HSQC had a chemical shift of 5.45 – 100 ppm, indicating an anomeric signal. Another signal was observed at 1.24 – 18.3 ppm. This region of the spectrum is relevant for the detection of the methyl group of deoxysugars such as fucose (48).

The monosaccharide analysis did reveal that the monosaccharides in *G. barretti* were comprised of 13 % fucose. Having a polysaccharide extract with some amounts of fucose does not seem unlikely. Many of the previously analyzed SPs from sponges (Table 3) contained fucose residues, often with sulfate esters. There were however no indications of sulfated sugars in the HSQC spectrum. Since the spectra recorded for this sample were so poor, additional spectra for structural elucidation were not recorded.

Due to the poor NMR data, no indications of sulfated polysaccharides, and a sample color indicating impurities, the calcium precipitation method was chosen to extract polysaccharides from all four species ahead of the cetylpyridinium precipitation method.

5.6.4 Extraction of polysaccharides from four sponge species

Three of the four species gave comparable yields from the polysaccharide extraction, 2.0 – 2.9 % of total DW. *A. dichotoma* had a yield of 5.0 % of total DW, about twice as much as the other species. As *A. dichotoma* had a higher content of neutral monosaccharides compared with the other species, a higher polysaccharide yield was expected.

When superimposing the recorded NMR spectra of the polysaccharide extracts from the four species it was clear that each sample contained the same polysaccharides, those being α1→4 glucans. The extracted polysaccharides were likely not the sponges' AF SPs as they appeared to be non-sulfated and had no interspecies variation. Glycogen might be an explanation considering

sponges, like other animals, use glycogen for energy storage, and glycogen is an α-1,4-glucan. While glycogen is α1→6 branched, no branching was observed in the NMR spectra. Sponge glycogen has been isolated previously from *Aplysina fulva* (see Table 2) and found to consist of uronic acids and sulfate esters in addition to the more abundant glucose residues (66).

Glycogen isolated from *Aplysina fulva* was extracted using the same cetylpyridinium precipitation method used for extracting AF SPs from other sponges (66). While the initial extraction steps were described as the exact same, some of the later purification steps did vary. Polysaccharide extracts from *Chondrilla nucula*, *Dysidea fragilis*, and *Hymeniacidon heliophila* were purified using a Mono-Q-FPLC column, equilibrated with 20 mM Tris HCl buffer. Polysaccharides from *Aplysina fulva* were eluted using a DEAE-cellulose column with a pH gradient (39). This might indicate that each crude extract contained glycogen, but the purification separated out these polysaccharides.

For this thesis, those findings could mean a few things. One possibility is that the α-1,4-glucans are weakly acidic containing some amount of either uronic acids or sulfate ester, but in a low proportion making them difficult to detect using NMR experiments. A weakly acidic property would help explain why the polysaccharides precipitated out after addition of calcium, like alginates which consist exclusively of uronic acids. Performing a monosaccharide analysis capable of detecting uronic acids would have revealed whether there are uronic acids in the sample or not. Even a neutral monosaccharide analysis would be useful in seeing the glucose content in the samples. Another possibility is that the AF SPs were extracted, but in such low amounts in comparison to the α-1,4-glucans present that they went undetected. Performing anion exchange chromatography of the sample might yield polysaccharide fractions with different charge densities.

5.7 Indications of ionic polysaccharides from C-PAGE

C-PAGE was chosen as samples could be applied to a gel and would be stained and elute based on charge and size. None of the polysaccharide samples had been degraded apart from the CPC extract which had been mechanically sheared. Therefore, the undegraded extracts were not expected to elute very far through the gel due to a large molecular weight. The fucoidan sample was expected to stain easily due to a large amount of sulfate esters, while the laminarin was

expected to not be stained due to it being a neutral polysaccharide. This is exactly what was observed. Three of the four calcium precipitated polysaccharide extracts were stained with the one from *M. lingua* remained unstained. It was previously speculated that *M. lingua* contained more sulfated polysaccharides than the other species due to higher amounts of sulfur (2.75 % compared to 0.51 – 1.83 % of total DW). If that was the case, in addition to the Ca^{2+} extracts containing sulfated polysaccharides, the *M. lingua* extract would be expected to have a darker color than other Ca^{2+} extracts. It is difficult to determine if the Ca^{2+} extracts from *A. dichotoma, G. barretti*, and *P. ventilabrum* reacted with the toluidine blue due to ionic properties of the polysaccharides or ionic impurities.

The crude water extract from *G. barretti* (SE-01) both reacted with the staining agent and eluted slightly through the gel. As this sample was very crude with no purification steps, the reaction was likely due to compounds in the sample other than polysaccharides. The polysaccharide extract obtained by cetylpyridinium chloride precipitation of *G. barretti* was the sample with the darkest color aside from the fucoidan. This is a good indication that the method did precipitate acidic polysaccharides. It should be reiterated however, that the extract obtained using this method did seem to have a lot more impurities (based on opacity and color of NMR sample) than those obtained using $CaCl_2$ as the precipitant.

C-PAGE did reveal that most sponge polysaccharide extracts had an ionic component to them, whether this is due to acidic polysaccharides or impurities is not known. The CPC extract appeared to be more acidic than other extracts. Since there were some observed reactions with the toluidine blue, further analyzing the samples for either uronic acids or sulfated polysaccharides could be interesting. When extracting sulfated polysaccharides, it could appear that cetylpyridinium chloride is better suited than calcium chloride as precipitant.

6 Prospective research

Many biomass parameters were explored in the marine sponges *A. dichotoma*, *G. barretti*, *M. lingua*, and *P. ventilabrum*. In most cases the data was only based on a few measurements and sometimes on a single measurement. Therefore, additional measurements would give good insight into intraspecies variations and would allow for statistical analysis. Due to material constraints, ash content was only investigated for *G. barretti*. This simple analysis would contribute to a better understanding of the composition of these sponges.

Since the amino acid analysis could not detect cysteine, proline, and tryptophan, the amino acid profiles are somewhat incomplete. Cysteine content would be useful in understanding how much the sulfur levels of the sponges are affected by sulfur containing amino acids. A proposed explanation for the high glycine/arginine content was due to large amounts of collagen. As collagen is a protein rich in glycine and proline, the proline levels would be expected to exceed what is observed in most proteins.

While isolating glycogen was not the main objective for this thesis, it would be interesting to investigate if it contained some amounts of uronic acids and sulfate groups like the one identified from *Aplysina fulva* (39). Performing a monosaccharide analysis capable of identifying uronic acids would be the most obvious next step. Additionally, a neutral monosaccharide analysis like the one performed on the sponge tissue would give an indication of exactly how much of the sample consisted of glucose residues. Glucose was the only sugar residue identified in the NMR experiments and would therefore be expected to dominate the monosaccharide analysis.

As the aggregation factor polysaccharides were not isolated, there are improvements to be made on the extraction procedures. From the C-PAGE analysis it could look like using cetylpyridinium chloride as a precipitant instead of calcium chloride yields more sulfated polysaccharides. The best strategy would likely be to use the cetylpyridinium chloride method, increase the amount of starting material, and purify the crude extract. Purification could be achieved with ion-exchange chromatography. This would separate the polysaccharides based on charge. The less charged glycogen molecules would elute through the column faster than the sulfated polysaccharides. Structural elucidation of the polysaccharides would be done with two-dimensional NMR spectroscopy, as was done with the α-1,4-glucan identified in this thesis. Additionally, a

monosaccharide analysis would be useful in determining which residues were present, and in which proportion to each other they appeared.

After successful extraction and isolation of sulfated sponge polysaccharides it would be interesting to investigate the bioactivities of these polysaccharides. Since their structures are species specific their bioactivities would likely vary from those already investigated.

7 Additional contributions

In addition to the work done on marine sponges, efforts were made towards the structural elucidation of enzymatically degraded fucoidan fractions from the brown algae *Macrocystis pyrifera*. This was in connection with a project on fucoidan degrading enzymes. Fucoidan was degraded with the enzyme GH107 (glycoside hydrolase family 107) and a total of six fractions were generated with size exclusion chromatography. The work described here is related to NMR experiments performed on fractions 4 and 6.

Recorded spectra of fucoidan fractions 4 and 6 are listed in Table 22. The ^{1}H and ^{13}C chemical shifts of all fucoidan spectra were internally referenced to TSP (0.00 ppm). All spectra were recorded at 25 °C.

Table 22: Acquisition parameters of NMR experiments performed on enzymatically degraded fucoidan. NS = number of scans, DS = dummy scans, D[1] = relaxation delay, TD = size of fid, F = fucoidan fraction. Experiments marked 800 MHz were recorded with a Bruker Avance III HD 800 MHz instrument. Experiments marked 600 MHz were recorded with a Bruker Avance III HD 600 MHz instrument.

Expt.	Pulse program	NS	DS	D[1] [sec]	TD	Mixing time [ms]	F	Instrument [MHz]
^{1}H	zgesgp	8	2	3.0	32768		6	800
HSQC	hsqcedetgpsisp2.3	16	16	2.0	2048 x 256		6	800
IP-COSY	ipcosyesgp-tr	16	16	1.0	4096 x 256		6	800
NOESY	noesyesgpph	32	64	1.2	4096 x 512	80	6	800
^{1}H	zgesgp	8	2	3.0	32768		4	600
HSQC	hsqcedetgpsisp2.3	16	16	2.0	2048 x 512		4	600
IP-COSY	ipcosyesgp-tr	8	16	1.5	4096 x 256		4	600
H2BC	h2bcetgpl3	32	32	2.0	2048 x 1024		4	600
TOCSY	tocsycleanes.rw	16	128	2.2	4096 x 800	80	4	600
HMBC	hmbcetgpl3nd	24	32	2.0	8192 x 400		4	600
ROESY	roesyesgpph	24	16	2.0	4096 x 512	75	4	600

7.1 Fucoidan fraction 6 – structural elucidation

Two spin systems were identified in the fraction 6 sample. Those spin systems were found to be 2,4-disulfated α-L-fucose and 2,4-disulfate β-L-fucose. Structure of the identified compound can be seen in Figure 30.

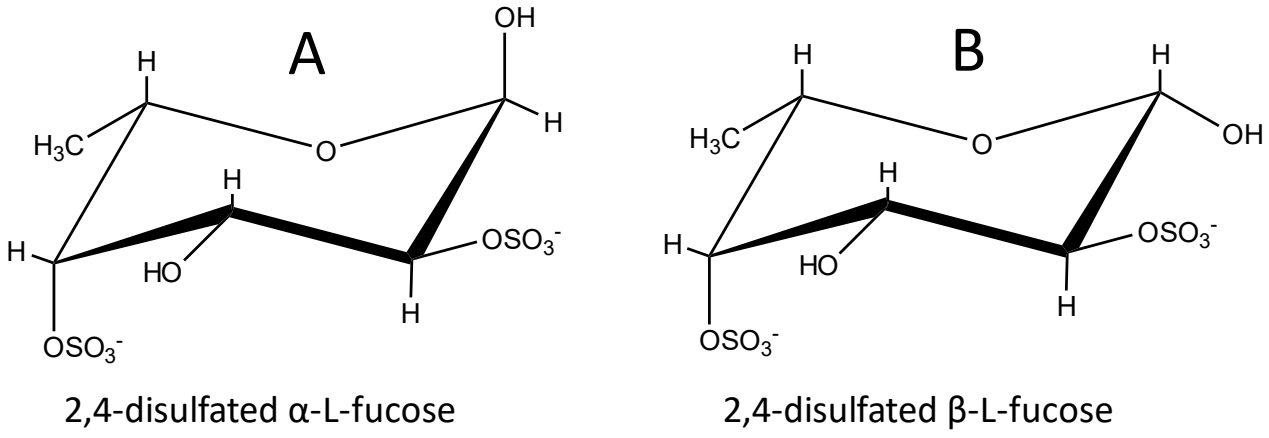

Figure 30: Proposed structure of monosaccharides from enzymatically degraded fucoidan. The two spin systems were identified by NMR spectroscopy. Compounds A and B are both 2,4-disulfated L-fucose units, the only difference being A is an α sugar and B is a β sugar.

The annotated HSQC spectrum of the monomer can be seen in Figure 31.

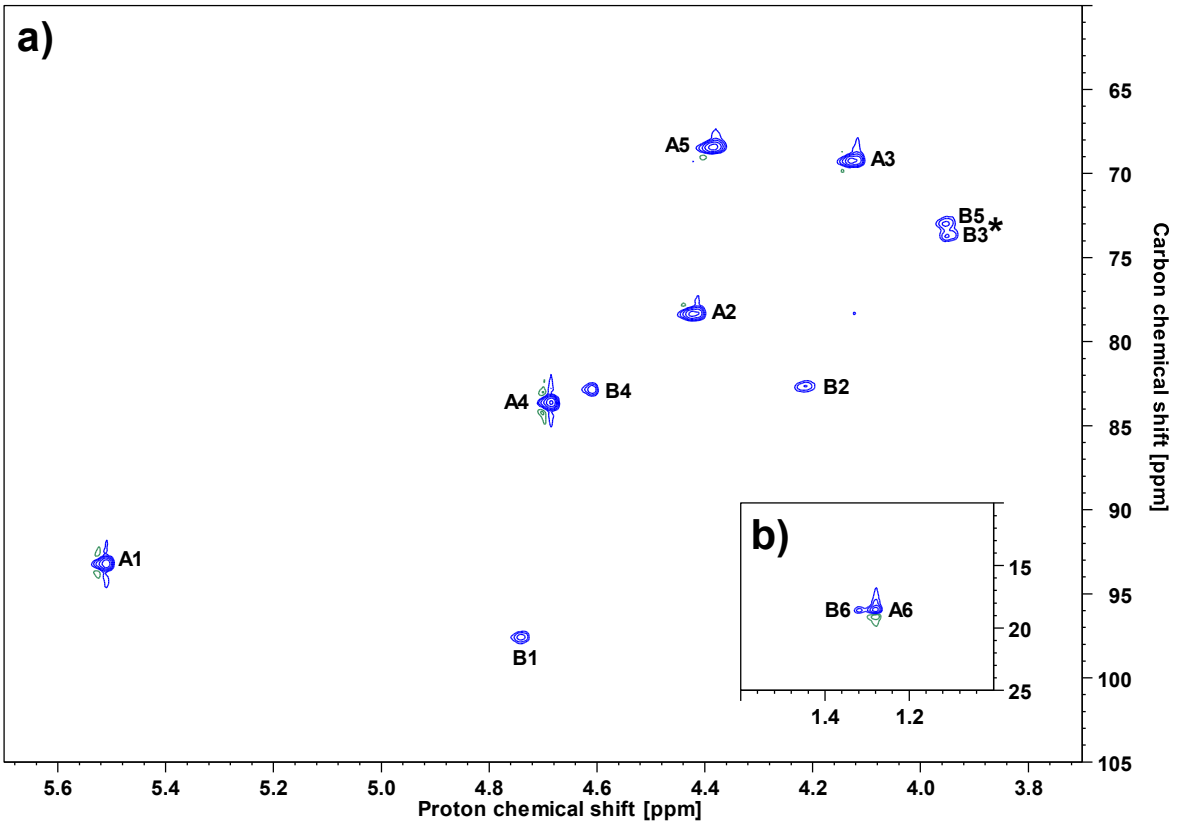

Figure 31: HSQC spectrum of an enzymatically degraded fucoidan fraction from *M. pyrifera.* Spectrum recorded with an 800 MHz Avance III HD instrument. b) is a lower shift region of spectrum a). Marked on the spectrum with numbers 1-6 are CH and CH3 groups from two spin systems (A and B). *Assignment of B3 and B5 was done with ^{1}H chemical shifts, their placement on the carbon axis is based on values from literature (67).

As positions B3 and B5 had overlapping ^{1}H chemical shifts, their positions were assigned by comparing chemical shifts with ones reported by Bezerra *et al.* (67). Their experiments showed that H3 had a higher ^{13}C chemical shift than H5 in β-fucose. Their positions could be determined by performing heteronuclear experiments such as H2BC and HMBC. Proton and carbon chemical shifts of signals identified in the HSQC spectrum can be seen in Table 23.

Table 23: ^{1}H and ^{13}C chemical shifts of signals from two spin systems identified in a HSQC spectrum of an enzymatically degraded fucoidan sample.

Spin system	Compound	Positions and ^{1}H – ^{13}C chemical shifts [ppm]					
		1	**2**	**3**	**4**	**5**	**6**
A	α-L-Fuc*p*-(2,4diSO_3^-)	5.51	4.42	4.13	4.68	4.38	1.28
		93.2	78.3	69.3	83.6	68.5	18.8
B	β-L-Fuc*p*-(2,4diSO_3^-)	4.74	4.21	3.95	4.61	3.95	1.32
		97.5	82.7	73.7	82.8	73.0	18.9

Spin systems A and B were identified by analyzing IP-COSY correlations. Correlations from both spin systems can be seen in Table 24.

Table 24: IP-COSY correlations for spin systems A and B of an enzymatically degraded fucoidan fraction. Position corresponding to the correlation is written in parenthesis.

Position	A Chemical shifts [ppm]	A COSY ^{1}H Correlations [ppm]	B Chemical shifts [ppm]	B COSY ^{1}H Correlations [ppm]
1	(5.51 – 93.2)	4.42 (H2)	(4.74 – 97.5)	4.21 (H2)
		-		3.95 (H3)
2	(4.42 – 78.3)	5.51 (H1)	(4.21 – 82.7)	4.74 (H1)
		4.13 (H3)		3.95 (H3)
3	(4.13 – 69.3)	4.68 (H4)	(3.95 – 73.0)	4.74 (H1)
		4.42 (H2)		4.61 (H4)
		-		4.21 (H2)
		-		1.32 (H6)
4	(4.68 – 83.6)	4.42 (H2)	(4.61 – 82.8)	3.95 (H3/H5)
		4.38 (H5)		-
		4.13 (H3)		-
5	(4.38 – 68.5)	4.68 (H4)	(3.95 – 73.7)	4.74 (H1)
		1.28 (H6)		4.61 (H4)
		-		4.21 (H2)
		-		1.32 (H6)
6	(1.28 – 18.8)	4.38 (H5)	(1.32 – 18.9)	3.95 (H5)

In most cases the IP-COSY correlations only corresponded to 3-bond vicinal couplings. There were some exceptions such as position A4 which had three correlations. As two of the correlations were for nuclei already identified (H2 and H3), the third correlation was likely with the proton on position 5. Position B3 had two correlations which had not yet been identified. As one signal had a low chemical shift (1.32 ppm) it was assumed to be a methyl group, and not the proton on position

4 of a monosaccharide. A correlation at 1.32 ppm for B3 was unexpected, as a correlation to the methyl group at B6 would require a 5-bond correlation. B5 was found to have a similar proton chemical shift to B3 explaining the COSY signal observed at 1.32 ppm. Likewise, COSY correlations from 3.95 ppm to H1 and H2 are likely from the B3 position, not the more separated B5 position.

The monosaccharides were determined to be fucose, as a monosaccharide analysis performed outside of this thesis found that the fucoidan had a very high proportion of fucose. Additionally, the HSQC spectrum in Figure 31 shows a methyl group in the sugar units confirming that they are 6-deoxysugars. No NOESY correlations were observed between the two spin systems, only intra-residue correlations as can be seen in Table 25. This indicates that the two systems are not linked. The chemical shifts of the assigned monomers are consistent with reducing ends, and not glycosidic linkages. Additionally, an oligo/polysaccharide sample would contain non-reducing end signals, which were not observed.

Table 25: NOESY correlations for spin systems A and B of an enzymatically degraded fucoidan sample.

NOESY Correlations A [ppm]	**NOESY Correlations A [position]**	**NOESY Correlations B [ppm]**	**NOESY Correlations B [position]**
5.51 – 4.42	A1 – A2	4.74 – 4.21	B1 – B2
5.51 – 4.13	A1 – A3	4.61 – 3.95	B2 – B3
4.42 – 4.13	A2 – A3	4.21 – 3.95	B3/B5 – B4
4.13 – 4.68	A3 – A4	4.12 – 3.95	B5 – B6
4.13 – 4.38	A3 – A5	-	-
4.38 – 1.28	A5 – A6	-	-

All identified NOESY correlations are shown in Figure 32. The correlations are shown for fucose in both $_1C^4$ and $_4C^1$ conformations.

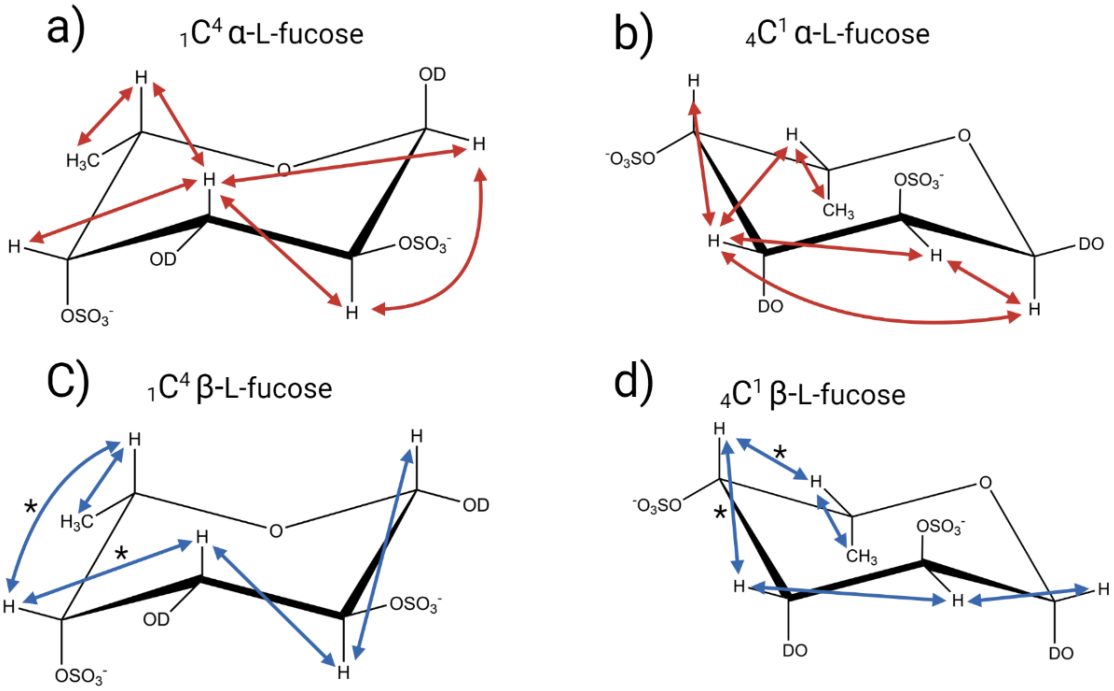

Figure 32: NOESY correlations of L-fucose monomers. *H3 and H5 of β-L-fucose had overlapping ^{1}H chemical shifts, making it difficult to distinguish between correlations from the two positions.

The fucose units were found to be 2,4-sulfated due to the chemical shifts of positions A2, A4, B2, and B4. Bezerra *et al.* reports a downfield shift of δ_H/δ_C values around 0.7/5-10 ppm at sulfation sites in fucose units (67). The experimentally obtained chemical shifts were compared with ones by Bezerra *et al.* as seen in Table 26. The comparison clearly showed that both A and B residues were sulfated at the 2 and 4 positions as these positions had ^{1}H chemical shifts 0.6 – 0.9 ppm higher and ^{13}C chemical shift 9 – 10 ppm higher than unsulfated fucose.

Table 26: Reported chemical shifts of α-L-Fuc*p* and β-L-Fuc*p* by Bezerra *et al.* compared with chemical shifts of two identified spin systems (A and B) in a fucoidan fraction from *M. pyrifera*. Difference obtained by subtracting the chemical shifts of unsulfated fucose units from the *M. pyrifera* residues (67).

	^{1}H – ^{13}C chemical shifts [ppm]			
Position	**α-L-Fuc*p***	**δ_H/δ_C diff. A**	**β-L-Fuc*p***	**δ_H/δ_C diff. B**
1	5.21 – 93.1	0.1 – 0.3	4.56 – 97.1	0.2 – 0.4
2	3.78 – 69.0	0.6 – 9.3	3.45 – 72.7	0.8 – 10.0
3	3.86 – 70.3	0.3 – -1.0	3.64 – 73.8	0.3 – -0.5
4	3.81 – 72.8	0.9 – 10.8	3.75 – 72.4	0.9 – 10.4
5	4.20 – 67.2	0.2 – 1.3	3.81 – 71.8	0.3 – 6.6
6	1.26 – 16.5	0.0 – 2.3	1.26 – 16.5	0.1 – 2.4

By annotating the ^{1}H spectrum of this fraction, a ratio of the two components was determined by integrating the A1 and B2 positions. These signals were chosen as they were the best resolved non-overlapping signals. The integrals revealed a ratio of 1.0:0.33 of α- to β-fucose. Due to the use of excitation sculpting water suppression, the signals B1, B4, and A4 were almost non-existent in the ^{1}H spectrum. The annotated ^{1}H spectrum can be seen in Figure 33.

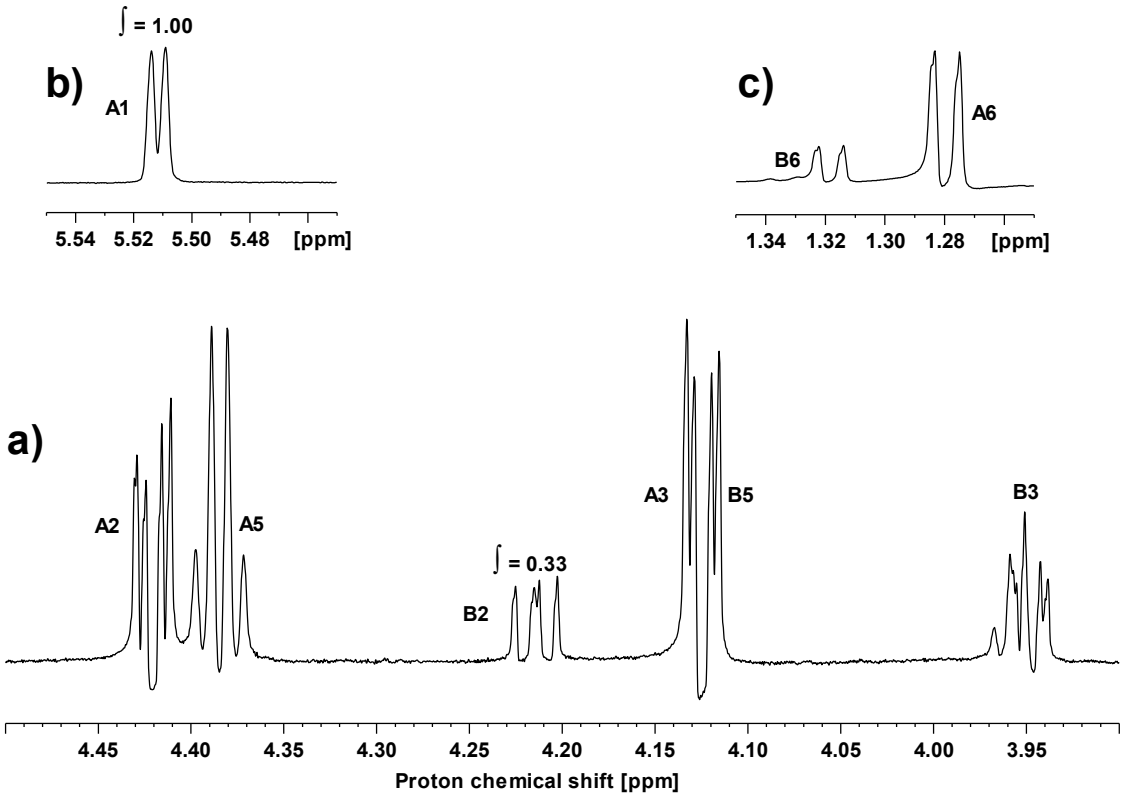

Figure 33: ^{1}H spectrum with excitation sculpting water suppression of an enzymatically degraded fucoidan fraction from *M. pyrifera.* Marked on the spectrum are signals from two spin systems (A and B). Signals B1, A4, and B4 are not included due to their low signals caused by water suppression. Regions **a)**, **b)**, and **c)** are all part of the same spectrum. Spectrum recorded with an 800 MHz Avance III HD instrument.

The IP-COSY spectrum from fraction 4 can be seen in Appendix F.

7.2 Fucoidan fraction 4 – structural elucidation

Six spin systems (A-F) were identified in the NMR spectra recorded of fraction 4. Some of the spin systems were not completely assigned. An annotated HSQC spectrum of fraction 4 with the six identified spin systems can be seen in Figure 34. Signal D1 was only identified with a ^{1}H chemical shift, meaning the ^{13}C chemical shift is undetermined.

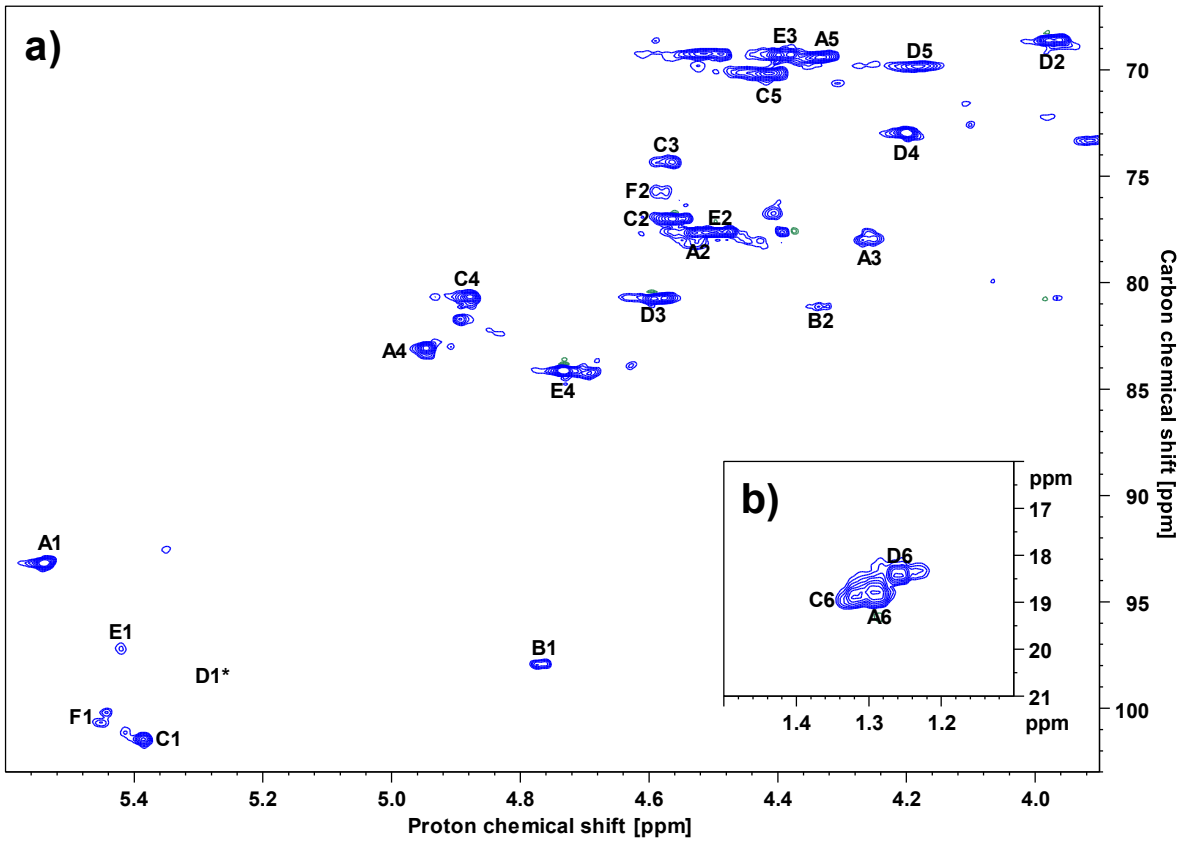

Figure 34: HSQC spectrum of an enzymatically degraded fucoidan fraction from *M. pyrifera*. **b)** is a lower shift region of spectrum **a)**. Marked on the spectrum with numbers 1-6 are CH and CH3 groups from six spin systems (A-F). Spectrum recorded with an 800 MHz Avance III HD instrument. *Signal D1 was only identified with ^{1}H chemical shift, meaning it's ^{13}C chemical shift is undetermined.

The ^{1}H and ^{13}C chemical shifts from spin systems A-F of fucoidan fraction 4 are displayed in Table 27.

Table 27: ^{1}H and ^{13}C chemical shifts of signals from six spin systems identified in a HSQC spectrum of an enzymatically degraded fucoidan sample.

Spin system	Fucose [α/β]	Positions and ^{1}H – ^{13}C chemical shifts [ppm]					
		1	**2**	**3**	**4**	**5**	**6**
A	α	5.54 93.2	4.52 77.6	4.26 78.0	4.95 83.1	4.33 69.3	1.29 18.8
B	β	4.77 97.9	4.34 81.1				
C	α	5.38 101.5	4.56 77.0	4.58 74.3	4.88 80.7	4.41 70.1	1.32 18.9
D	α	5.30 -	3.97 68.5	4.58 80.7	4.20 72.9	4.18 69.8	1.26 18.4
E	α	5.42 97.3	4.49 77.6	4.40 69.3	4.73 84.1		
F	α	5.45 100.8	4.58 75.7				

The six spin systems were assigned using a combination of correlations from H2BC, HMBC, and TOCSY spectra (these can be seen in Appendix G). Spin system A was assigned by using H2BC correlations from positions 1-4. Position A5 was found by HMBC correlations from position A1. A5 had H2BC correlations to position A6 completing the spin system. H2BC and HMBC correlations for spin system A are shown in Table 28.

Table 28: H2BC and HMBC correlations for spin system A of a fucoidan fraction from *M. pyrifera*. Position corresponding to the correlation is written in parenthesis. (-) indicates the correlation does not correspond to an identified signal within the spin system.

Position in spin system A [ppm]	**H2BC ^{13}C Correlations [ppm]**	**H2BC ^{1}H Correlations [ppm]**	**HMBC ^{13}C Correlations [ppm]**	**HMBC ^{1}H Correlations [ppm]**
A1 (5.54 – 93.2)	77.6 (C2)	4.53 (H2)	77.9 (C3)	4.33 (H5)
	-	-	69.3 (C5)	-
A2 (4.52 – 77.6)	77.9 (C3)	4.39 (-)	77.9 (C3)	4.95 (H4)
		4.26 (H3)	-	-
A3 (4.26 – 77.9)	-	4.95 (H4)	-	5.54 (H1)
		-	-	4.52 (H2)
A4 (4.95 – 83.1)	-	-	77.6 (C2)	4.33 (H5)
	-	-	-	1.29 (H6)
A5 (4.33 – 69.3)	18.8 (C6)	1.29 (H6)	93.2 (C1)	5.54 (H1)
	-	-	83.1 (C4)	4.48 (-)
	-	-	18.8 (C6)	1.29 (H6)
A6 (1.29 – 18.8)	-	4.45 (-)	84.0 (-)	4.41 (-)
	-	-	83.1 (C4)	4.33 (H5)
	-	-	69.3 (C5)	-

A similar strategy was utilized to assign the remaining 5 spin systems. H2BC and HMBC correlation tables can be seen in Appendix G. As the assignment of some spin systems were incomplete it was not possible to be certain of their exact structures. From a previous monosaccharide analysis, it is known that fucose was the dominating monosaccharide, as was the case with fraction 6, therefore it is assumed that spin systems A-F are all fucose units. Spin system B, which has an anomeric signal at 4.77 – 97.9 ppm, is likely β-fucose, while all other spin systems are α-fucose units. Their sulfation patterns were determined by comparing chemical shifts with ones reported by Bezerra *et al*., see Table 29 (67).

Table 29: Comparison of chemical shifts of six spin systems (A-F) identified in a fucoidan fraction from *M. pyrifera* and fucose chemical shift reported by Bezerra *et al*. Difference obtained by subtracting the chemical shifts of unsulfated fucose units from the *M. pyrifera* residues. Marked in blue are signals with a difference >0.6 – 6.0 ppm, caused by sulfation (67).

Position	δ_H/δ_C diff. A [ppm]	δ_H/δ_C diff. B [ppm]	δ_H/δ_C diff. C [ppm]	δ_H/δ_C diff. D [ppm]	δ_H/δ_C diff. E [ppm]	δ_H/δ_C diff. F [ppm]
1	0.3 – 0.1	0.2 – 0.8	0.2 – 8.4	0.1 – (-)	0.2 – 4.2	0.2 – 7.7
2	0.7 – 8.6	0.9 – 8.4	0.8 – 8.0	0.2 – -0.5	0.7 – 8.6	0.8 – 6.7
3	0.4 – 7.7	-	0.7 – 4.0	0.7 – 10.4	0.5 – -1.0	-
4	1.1 – 10.3	-	1.1 – 7.9	0.4 – 0.1	0.9 – 11.3	-
5	0.1 – 2.1	-	0.2 – 2.9	0.0 – 2.6	-	-
6	0.0 – 2.3	-	0.1 – 2.4	0.0 – 1.9	-	-

Fucose units A, C, and E were 2,4-sulfated. While only the first two positions of units B and F were identified they were found to be 2-sulfated. Fucose unit C was the only residue sulfated at position 3.

As the chemical shifts of anomeric positions in spin systems A and B are similar to those of α and β monomers, they are believed to be reducing end sugars. The other spin systems have higher ^{13}C chemical shifts at the anomeric position indicating a glycosidic link. Spin system D is uncertain as the ^{13}C chemical shift of anomeric carbon is unknown. A ROESY spectrum was recorded to analyze through-space correlations, hopefully revealing glycosidic bonds. The spectrum was of poor quality and is not included here. A HMBC correlation was observed between C1 and A3, revealing that spin systems C and A are 1→3 linked. This is also supported by A3 having a ^{13}C chemical shift 7.7 ppm higher than expected for an unsulfated monomer. Other signals such as C3 and F1 also had higher ^{13}C chemical shifts than expected for unliked residues indicating sites for glycosidic bonds. Figure 35 shows the HMBC correlation used to determine the glycosidic link between C1 and A3.

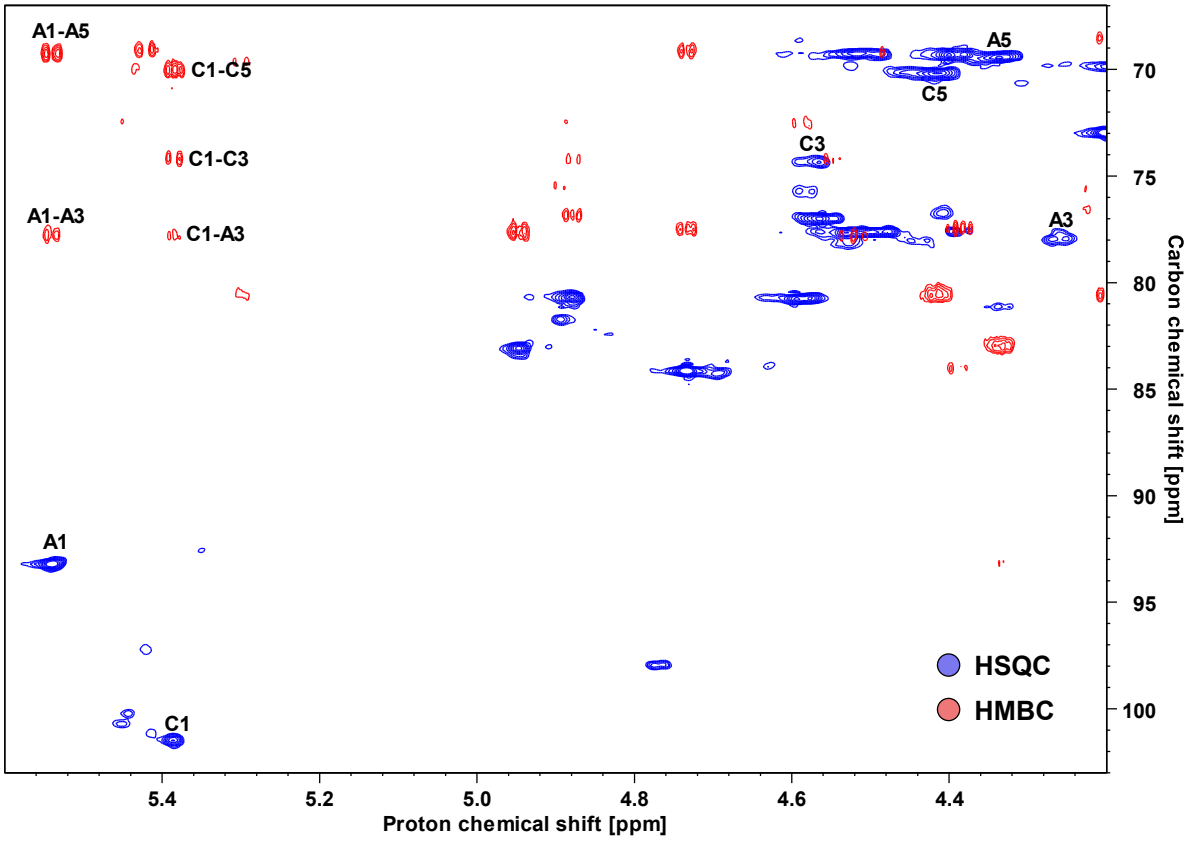

Figure 35: Superimposed HSQC and HMBC spectra of a fucoidan fraction from *M. pyrifera*. HMBC correlation used to determine 1→3 link between C1 and A3 is labeled accordingly. HSQC displayed in blue, HMBC is displayed in red. Spectra recorded with an 800 MHz Avance III HD instrument.

There were likely more glycosidic bonds that were not identified due to a poor ROESY spectrum. A better ROESY spectrum would likely help in identifying more of the unidentified glycosidic bonds.

8 Conclusion

Biomass of the sponges *Antho dichotoma*, *Geodia barretti*, *Mycale lingua*, and *Phakellia ventilabrum* was explored using several analytical techniques. All species had a high water content, (75.4 – 89.2 %), a large amount of glucose (26 – 38 % of neutral monosaccharides), and broadly the same proportions of individual amino acids. Glycine/arginine content which varied between 20.9 – 45.2 % depending on species was much higher than the 12.9 % found in the average protein. Glutamic and aspartic acid levels, 8.0 – 10.5 % and 10.0 – 16.0 %, were also higher than those of the average protein, which are 6.2 % and 5.3 % respectively. Asparagine and glutamine were barely detectable in any of the species (Asn: <0.1 %, Gln: 0.1 – 0.2 %). *Antho dichotoma* was the sponge which stood out the most with regards to biomass. It had a lot higher nitrogen, carbon, hydrogen, monosaccharide, and amino acid content than all other species, likely due to a lower proportion of inorganic material. Nitrogen content in combination with data from the total amino acid analysis was used to obtain nitrogen-to-protein conversion factors for each of the species. The calculated nitrogen-to-protein conversion factors obtained were 3.4 for *A. dichotoma*, 4.3 for *G. barretti*, 4.6 for *M. lingua*, and 4.7 for *P. ventilabrum*.

Polysaccharides were extracted from all four species utilizing a method based on precipitation using calcium chloride as precipitant with yields of 2.0 – 5.0 % of starting material. The extracts were investigated using NMR spectroscopy. HSQC spectra showed that all four extracts contained polysaccharides with similar structures. Additional two-dimensional experiments performed on a sample from *Geodia barretti* revealed that the extracts contained α-1,4-glucans with an estimated degree of polymerization of 10, likely related to energy-storage polysaccharides and not aggregation factor polysaccharides. Another polysaccharide extract from *Geodia barretti* obtained by using cetylpyridinium chloride as a precipitant was also analyzed with NMR spectroscopy. The sample yielded poorly resolved spectra, likely containing some polysaccharides and possibly 6-deoxysugars.

Polysaccharide extracts were investigated with C-PAGE. All calcium precipitated extracts apart from the one from *Mycale lingua* reacted with toluidine blue indicating the presence of some compounds with ionic properties. The cetylpyridinium chloride precipitated *Geodia barretti* extract had an even stronger reaction with toluidine blue, likely due to more ionic compounds. Fucoidan from *Laminaria hyperborea*, which was used as a sulfated standard, had a much stronger

reaction with the toluidine blue than any other sample. It is possible that aggregation factor polysaccharides were extracted in some amounts, but further purification would be necessary to obtain samples suitable for NMR spectroscopy.

Oligomer fractions of enzymatically degraded fucoidan from the brown algae *Macrocystis pyrifera* were obtained by size exclusion chromatography on a different project. Two of these fractions were analyzed using NMR spectroscopy. The first fraction contained 2,4-disulfated-L-fucose monomers. The second fraction contained 2,4- and 3-sulfated-L-fucose units. Some of the 2,4-disulfated monomers were found to be 1→3 linked using HMBC correlations. Complete elucidation of the glycosidic bonds present was not achieved due to a poor ROESY spectrum. Acquisition of a better ROESY spectrum would likely help in determining more of the glycosidic bonds.

References

1. Jensen KS, Pedersen MF. Photosynthesis by symbiotic algae in the freshwater sponge, Spongilla lacustris. Limnol Oceanogr. 1994;39(3):551–61.

2. Vacelet J, Boury-Esnault N. Carnivorous sponges. Nature. 1995 Jan;373(6512):333–5.

3. Yin Z, Zhu M, Davidson EH, Bottjer DJ, Zhao F, Tafforeau P. Sponge grade body fossil with cellular resolution dating 60 Myr before the Cambrian. Proc Natl Acad Sci. 2015 Mar 24;112(12):E1453–60.

4. Turner EC. Possible poriferan body fossils in early Neoproterozoic microbial reefs. Nature. 2021 Aug;596(7870):87–91.

5. Dunn CW, Hejnol A, Matus DQ, Pang K, Browne WE, Smith SA, et al. Broad phylogenomic sampling improves resolution of the animal tree of life. Nature. 2008 Apr;452(7188):745–9.

6. Redmond AK, McLysaght A. Evidence for sponges as sister to all other animals from partitioned phylogenomics with mixture models and recoding. Nat Commun. 2021 Mar 19;12(1):1783.

7. Abedin M, King N. Diverse evolutionary paths to cell adhesion. Trends Cell Biol. 2010 Dec 1;20(12):734–42.

8. Wilson HV. On Some Phenomena of Coalescence and Regeneration in Sponges. J Elisha Mitchell Sci Soc. 1907;23(4):161–74.

9. Weinbaum G, Burger MM. Two Component System for Surface Guided Reassociation of Animal Cells. Nature. 1973 Aug;244(5417):510–2.

10. Jarchow J, Fritz J, Anselmetti D, Calabro A, Hascall VC, Gerosa D, et al. Supramolecular Structure of a New Family of Circular Proteoglycans Mediating Cell Adhesion in Sponges. J Struct Biol. 2000 Nov 1;132(2):95–105.

11. Humphreys S, Humphreys T, Sano J. Organization and polysaccharides of sponge aggregation factor. J Supramol Struct. 1977;7(3–4):339–51.

12. Vilanova E, Santos GRC, Aquino RS, Valle-Delgado JJ, Anselmetti D, Fernàndez-Busquets X, et al. Carbohydrate-Carbohydrate Interactions Mediated by Sulfate Esters and Calcium Provide the Cell Adhesion Required for the Emergence of Early Metazoans. J Biol Chem. 2016 Apr 29;291(18):9425–37.

13. Vilanova E, Ciodaro PJ, Bezerra FF, Santos GRC, Valle-Delgado JJ, Anselmetti D, et al. Adhesion of freshwater sponge cells mediated by carbohydrate–carbohydrate interactions requires low environmental calcium. Glycobiology. 2020 Aug 20;30(9):710–21.

14. Arlov Ø, Rütsche D, Asadi Korayem M, Öztürk E, Zenobi-Wong M. Engineered Sulfated Polysaccharides for Biomedical Applications. Adv Funct Mater. 2021;31(19):2010732.

15. Medeiros GF, Mendes A, Castro RAB, Baú EC, Nader HB, Dietrich CP. Distribution of sulfated glycosaminoglycans in the animal kingdom: widespread occurrence of heparin-like compounds in invertebrates. Biochim Biophys Acta BBA - Gen Subj. 2000 Jul 26;1475(3):287–94.

16. Jiao G, Yu G, Zhang J, Ewart HS. Chemical Structures and Bioactivities of Sulfated Polysaccharides from Marine Algae. Mar Drugs. 2011 Feb 8;9(2):196–223.

17. Panoff JM, Priem B, Morvan H, Joset F. Sulphated exopolysaccharides produced by two unicellular strains of cyanobacteria, Synechocystis PCC 6803 and 6714. Arch Microbiol. 1988 Oct 1;150(6):558–63.

18. Dantas-Santos N, Gomes DL, Costa LS, Cordeiro SL, Costa MSSP, Trindade ES, et al. Freshwater Plants Synthesize Sulfated Polysaccharides: Heterogalactans from Water Hyacinth (Eicchornia crassipes). Int J Mol Sci. 2012 Jan 17;13(1):961–76.

19. Calo D, Kaminski L, Eichler J. Protein glycosylation in Archaea: Sweet and extreme. Glycobiology. 2010 Sep 1;20(9):1065–76.

20. Muthukumar J, Chidambaram R, Sukumaran S. Sulfated polysaccharides and its commercial applications in food industries—A review. J Food Sci Technol. 2021 Jul 1;58(7):2453–66.

21. Koide T. Antithrombin and Heparin Cofactor II: Structure and Functions. In: Tanaka K, Davie EW, Ikeda Y, Iwanaga S, Saito H, Sueishi K, editors. Recent Advances in Thrombosis and Hemostasis 2008. Tokyo: Springer Japan; 2008. p. 177–89.

22. Kopplin G, Rokstad AM, Mélida H, Bulone V, Skjåk-Bræk G, Aachmann FL. Structural Characterization of Fucoidan from *Laminaria hyperborea* : Assessment of Coagulation and Inflammatory Properties and Their Structure–Function Relationship. ACS Appl Bio Mater. 2018 Dec 17;1(6):1880–92.

23. Kim WJ, Kim SM, Kim HG, Oh HR, Lee KB, Lee YK, et al. Purification and Anticoagulant Activity of a Fucoidan from Korean Undaria pinnatifida Sporophyll. ALGAE. 2007 Sep 1;22(3):247–52.

24. Ponce NMA, Pujol CA, Damonte EB, Flores ML, Stortz CA. Fucoidans from the brown seaweed Adenocystis utricularis: extraction methods, antiviral activity and structural studies. Carbohydr Res. 2003 Jan 20;338(2):153–65.

25. Jun JY, Jung MJ, Jeong IH, Yamazaki K, Kawai Y, Kim BM. Antimicrobial and Antibiofilm Activities of Sulfated Polysaccharides from Marine Algae against Dental Plaque Bacteria. Mar Drugs. 2018 Sep;16(9):301.

26. Yang JW, Yoon SY, Oh SJ, Kim SK, Kang KW. Bifunctional effects of fucoidan on the expression of inducible nitric oxide synthase. Biochem Biophys Res Commun. 2006 Jul 21;346(1):345–50.

27. MacKenzie R, Newman D, Burger M, Roy R, Kuhns W. Adhesion of a viral envelope protein to a non-self-binding domain of the aggregation factor in the marine sponge Microciona prolifera. Biol Bull. 2000 Oct;199(2):209–11.

28. Esteves AIS, Nicolai M, Humanes M, Goncalves J. Sulfated Polysaccharides in Marine Sponges: Extraction Methods and Anti-HIV Activity. Mar Drugs. 2011 Jan;9(1):139–53.

29. Barthel D. Tissue composition of sponges from the Weddell Sea, Antarctica:not much meat on the bones. Mar Ecol Prog Ser. 1995;123:149–53.

30. Morley SA, Berman J, Barnes DKA, de Juan Carbonell C, Downey RV, Peck LS. Extreme Phenotypic Plasticity in Metabolic Physiology of Antarctic Demosponges. Front Ecol Evol. 2016;3.

31. Boury-Esnault N, Rutzler K. Thesaurus of Sponge Morphology. Smithson Contrib Zool. 1997;(596).

32. Wang X, Gan L, Jochum KP, Schröder HC, Müller WEG. The largest Bio-Silica Structure on Earth: The Giant Basal Spicule from the Deep-Sea Glass Sponge Monorhaphis chuni. Evid-Based Complement Altern Med ECAM. 2011;2011:540987.

33. Organic elemental analyzer vario EL cube - Elementar [Internet]. [cited 2023 Apr 12]. Available from: https://www.elementar.com/en/products/organic-elemental-analyzers/vario-el-cube

34. Mechelke M, Herlet J, Benz JP, Schwarz WH, Zverlov VV, Liebl W, et al. HPAEC-PAD for oligosaccharide analysis—novel insights into analyte sensitivity and response stability. Anal Bioanal Chem. 2017 Dec 1;409(30):7169–81.

35. Roth Marc. Fluorescence reaction for amino acids. Anal Chem. 1971 Jun 1;43(7):880–2.

36. Peasura N, Laohakunjit N, Kerdchoechuen O, Wanlapa S. Characteristics and antioxidant of Ulva intestinalis sulphated polysaccharides extracted with different solvents. Int J Biol Macromol. 2015 Nov;81:912–9.

37. Shi L. Bioactivities, isolation and purification methods of polysaccharides from natural products: A review. Int J Biol Macromol. 2016 Nov;92:37–48.

38. Custódio M, Lôbo-Hajdu G, Hajdu E, Muricy G. A novel biochemical method to distinguish cryptic species of Chondrilla (Chondrosida, Demospongiae) based on its sulfated polysaccharides. Porifera Res Biodivers Innov Sustain. 2007 Jan 1;653–9.

39. Zierer MS, Mourão PAS. A wide diversity of sulfated polysaccharides are synthesized by different species of marine sponges. Carbohydr Res. 2000 Sep 8;328(2):209–16.

40. Cimino P, Bifulco G, Casapullo A, Bruno I, Gomez-Paloma L, Riccio R. Isolation and NMR characterization of rosacelose, a novel sulfated polysaccharide from the sponge Mixylla rosacea. Carbohydr Res. 2001 Aug 3;334(1):39–47.

41. Spillmann D, Hård K, Thomas-Oates J, Vliegenthart JF, Misevic G, Burger MM, et al. Characterization of a novel pyruvylated carbohydrate unit implicated in the cell aggregation of the marine sponge Microciona prolifera. J Biol Chem. 1993 Jun;268(18):13378–87.

42. Guerardel Y, Czeszak X, Sumanovski LT, Karamanos Y, Popescu O, Strecker G, et al. Molecular Fingerprinting of Carbohydrate Structure Phenotypes of Three Porifera Proteoglycan-like Glyconectins*. J Biol Chem. 2004 Apr 9;279(15):15591–603.

43. Grant GT, Mon ER, Rees SDA. BIOLOGICAL INTERACTIONS BETWEEN POLYSACCHARtDES AND DIVALENT CATIONS: THE EGG-BOX MODEL. FEBS Lett.

44. Parish CR, Jakobsen KB, Coombe DR, Bacic A. Isolation and characterization of cell adhesion molecules from the marine sponge, Ophlitaspongia tenuis. Biochim Biophys Acta BBA - Gen Subj. 1991 Jan 23;1073(1):56–64.

45. Bucior I, Burger MM. Carbohydrate-carbohydrate interaction as a major force initiating cell-cell recognition. Glycoconj J. 2004;21(3–4):111–23.

46. Friebolin H. Basic One- and Two-Dimensional NMR Spectroscopy. 5th ed. Weinheim: WILEY-VCH; 2011.

47. Simpson JH. Organic Structure Determination Using 2-D NMR Spectroscopy: A Problem-Based Approach. Elsevier; 2008.

48. Speciale I, Notaro A, Garcia-Vello P, Di Lorenzo F, Armiento S, Molinaro A, et al. Liquid-state NMR spectroscopy for complex carbohydrate structural analysis: A hitchhiker's guide. Carbohydr Polym. 2022 Feb 1;277:118885.

49. Petersen BO, Vinogradov E, Kay W, Würtz P, Nyberg NT, Duus JØ, et al. H2BC: a new technique for NMR analysis of complex carbohydrates. Carbohydr Res. 2006 Mar 20;341(4):550–6.

50. Furevi A, Ruda A, Angles d'Ortoli T, Mobarak H, Ståhle J, Hamark C, et al. Complete 1H and 13C NMR chemical shift assignments of mono-to tetrasaccharides as basis for NMR chemical shift predictions of oligo- and polysaccharides using the computer program CASPER. Carbohydr Res. 2022 Mar 1;513:108528.

51. Dietrich CP, Dietrich SMC. Electrophoretic behaviour of acidic mucopolysaccharides in diamine buffers. Anal Biochem. 1976 Feb 1;70(2):645–7.

52. Wishart DS, Bigam CG, Yao J, Abildgaard F, Dyson HJ, Oldfield E, et al. 1H, 13C and 15N chemical shift referencing in biomolecular NMR. J Biomol NMR. 1995 Sep 1;6(2):135–40.

53. Tome D, Cordella C, Dib O, Péron C. Nitrogen and protein content measurement and nitrogen to protein conversion factors for dairy and soy protein-based foods: a systematic review and modelling analysis. World Health Organization; 2019.

54. Forbord S, Matsson S, Brodahl GE, Bluhm BA, Broch OJ, Handå A, et al. Latitudinal, seasonal and depth-dependent variation in growth, chemical composition and biofouling of cultivated Saccharina latissima (Phaeophyceae) along the Norwegian coast. J Appl Phycol. 2020 Aug 1;32(4):2215–32.

55. McCaldon P, Argos P. Oligopeptide biases in protein sequences and their use in predicting protein coding regions in nucleotide sequences. Proteins Struct Funct Bioinforma. 1988;4(2):99–122.

56. Agrawal PK. NMR Spectroscopy in the structural elucidation of oligosaccharides and glycosides. Phytochemistry. 1992 Oct 1;31(10):3307–30.

57. Kutti T, Bannister RJ, Fosså JH, Krogness CM, Tjensvoll I, Søvik G. Metabolic responses of the deep-water sponge Geodia barretti to suspended bottom sediment, simulated mine tailings and drill cuttings. J Exp Mar Biol Ecol. 2015 Dec 1;473:64–72.

58. Martins E, Rapp HT, Xavier JR, Diogo GS, Reis RL, Silva TH. Macro and Microstructural Characteristics of North Atlantic Deep-Sea Sponges as Bioinspired Models for Tissue Engineering Scaffolding. Front Mar Sci. 2021;7.

59. Boury-Esnault N. A cell type in sponges involved in the metabolism of glycogen. Cell Tissue Res. 1977 Jan 1;175(4):523–39.

60. Patel TK, Williamson JD. Mannitol in Plants, Fungi, and Plant–Fungal Interactions. Trends Plant Sci. 2016 Jun 1;21(6):486–97.

61. Wagstaff BA, Zorzoli A, Dorfmueller HC. NDP-rhamnose biosynthesis and rhamnosyltransferases: building diverse glycoconjugates in nature. Biochem J. 2021 Feb 26;478(4):685–701.

62. Swatschek D, Schatton W, Kellermann J, Müller WEG, Kreuter J. Marine sponge collagen: isolation, characterization and effects on the skin parameters surface-pH, moisture and sebum. Eur J Pharm Biopharm. 2002 Jan 1;53(1):107–13.

63. Henkart P, Humphreys S, Humphreys T. Characterization of sponge aggregation factor. Unique proteoglycan complex. Biochemistry. 1973 Jul 1;12(16):3045–50.

64. Valliere-Douglass JF, Eakin CM, Wallace A, Ketchem RR, Wang W, Treuheit MJ, et al. Glutamine-linked and Non-consensus Asparagine-linked Oligosaccharides Present in Human Recombinant Antibodies Define Novel Protein Glycosylation Motifs. J Biol Chem. 2010 May 21;285(21):16012–22.

65. Creighton TE. Proteins: Structures and Molecular properties. Second edition. 1992. 91 p.

66. Zierer MS, Vieira RP, Mulloy B, Mourão PAS. A novel acidic glycogen extracted from the marine sponge Aplysina fulva (porifera-demospongiae). Carbohydr Res. 1995 Sep 8;274:233–44.

67. Bezerra FF, Vignovich WP, Aderibigbe AO, Liu H, Sharp JS, Doerksen RJ, et al. Conformational properties of l-fucose and the tetrasaccharide building block of the sulfated l-fucan from Lytechinus variegatus. J Struct Biol. 2020 Jan 1;209(1):107407.

68. Amino Acid Structure | Amino Acid Abbreviations | Molecular Weight [Internet]. [cited 2023 Apr 18]. Available from: https://no.promega.com/resources/tools/amino-acid-chart-amino-acid-structure/

Appendices

Appendix A Water and ash content – raw data

Raw data from the water content measurements are shown in Table 30.

Table 30: Water content of sponges based on measured weight before and after drying. *A. dichotoma*, *M. lingua*, and *P. ventilabrum* were freeze dried. *G. barretti* was dried in an oven. WW = wet weight, DW = dry weight.

Sample	Sponge WW [g]	Sponge DW [g]	Sponge DW [%]	Water content [%]
Antho dichotoma	1.4336	0.2686	18.74	81.26
(1) *Geodia barretti*	2.4329	0.6800	27.95	72.05
(2) *Geodia barretti*	1.9868	0.4682	23.57	76.43
(3) *Geodia barretti*	2.3954	0.5342	22.30	77.70
Mycale lingua	3.0072	0.3413	11.35	88.65
Phakellia ventilabrum	1.6754	0.1818	10.85	89.15

Ash content measurements were only done on *G. barretti*. Measurements shown in Table 31.

Table 31: Ash content of the marine sponge *G. barretti* found by incineration of sponge material at 550 °C for 16 hours. DW = dry weight.

Sample	Sponge DW [g]	Ash-weight [g]	Ash-free DW [g]	Ash-weight [%]	Ash-free DW [%]
(1) *Geodia barretti*	0.6800	0.4281	0.2519	62.96	37.04
(2) *Geodia barretti*	0.4682	0.2806	0.1876	59.93	40.07
(3) *Geodia barretti*	0.5342	0.3060	0.2282	57.28	42.72

Appendix B Element analysis – raw data

Raw data from the element analysis of sponge tissue and water extracts is shown in Table 32.

Table 32: Element analysis data for marine sponges based on dry weight (*A. dichotoma*, *G. barretti*, *M. lingua*, and *P. ventilabrum*). SE-01.3 and SE-01 are water extracts from *G. barretti*. Measurements done using a vario EL cube element analyzer.

Sample	N area	C area	H area	S area	N [%]	C [%]	H [%]	S [%]
A. dichotoma	11409	33915	16786	820	6.68	27.93	4.619	1.879
A. dichotoma	11506	34134	16786	799	6.77	28.27	4.645	1.841
A. dichotoma	10501	31233	15058	716	6.62	27.63	4.475	1.760
G. barretti	5533	15747	9002	253	3.85	15.20	2.827	0.542
G. barretti	5580	15987	9197	253	3.81	15.15	2.833	0.532
G. barretti	6602	18720	10860	297	3.88	15.24	2.860	0.543
G. barretti	5610	16081	9409	244	3.67	14.59	2.772	0.490
G. barretti	5309	15315	8749	231	3.63	14.52	2.701	0.481
G. barretti	6026	17148	9971	253	3.84	15.16	2.857	0.496
M. lingua	6400	18362	9407	1094	4.04	16.09	2.834	2.686
M. lingua	7035	20162	10526	1251	3.96	15.71	2.810	2.737
M. lingua	7070	20308	10700	1289	3.98	15.85	2.860	2.826
P. ventilabrum	6312	18677	10016	613	3.77	15.46	2.843	1.412
P. ventilabrum	5862	17250	8948	547	3.80	15.53	2.773	1.364
P. ventilabrum	5590	16512	8445	507	3.74	15.36	2.710	1.302
SE-01.3	14544	41001	19072	1404	9.46	37.91	5.851	3.612
SE-01.3	15083	42246	19534	1140	9.59	38.15	5.845	2.862
SE-01	22945	62927	29438	844	12.39	48.13	7.329	1.785
SE-01	22017	60277	28121	743	12.34	47.86	7.281	1.629

Appendix C Monosaccharide analysis – raw data

Starting weight of samples and their final concentrations before they were analyzed are shown in Table 33.

Table 33: Starting weight of sponge samples and final concentrations used in monosaccharide analysis using HPAEC-PAD. SE-01.3 and SE-01 are water extracts from *G. barretti*.

Sample	Sample starting weight [mg]	Concentration in HPLC vials [mg/L]
(1) *Antho dichotoma*	20.1	155.81
(2) *Antho dichotoma*	19.9	154.26
(3) *Antho dichotoma*	20.0	155.04
(1) *Geodia barretti*	29.8	64.09
(2) *Geodia barretti*	30.0	64.52
(3) *Geodia barretti*	30.1	64.73
(1) *Mycale lingua*	20.0	155.04
(2) *Mycale lingua*	20.2	156.59
(3) *Mycale lingua*	20.1	155.81
(1) *Phakellia ventilabrum*	20.1	155.81
(2) *Phakellia ventilabrum*	20.0	155.04
(3) *Phakellia ventilabrum*	20.1	155.81
(1) SE-01.3	20.4	158.14
(2) SE-01.3	20.4	31.63
(1) SE-01	20.4	158.14
(2) SE-01	20.4	31.63

As some monosaccharides are degraded during sample preparation a conversion factor for each individual monosaccharide is applied to the results. This gives a more accurate estimate of monosaccharides in the original sample. Correction factors are shown in Table 34. Raw data before correction factors have been applied is displayed in Table 35, while Table 36 contains data where monosaccharide degradation during sample preparation has been corrected for.

Table 34: Factors correcting for degradation of monosaccharides during acid hydrolysis.

Monosaccharide	Correction factor
Mannitol	1.02
Fucose	1.05
Arabinose	1.11
Galactose	1.08
Rhamnose	1.09
Glucose	1.08
Xylose	1.29
Mannose	1.11

Table 35: Data from monosaccharide analysis of marine sponges. Degradation of monosaccharides during sample preparation has not been corrected for. Results obtained by HPAEC-PAD using a Dionex ISC 5000+ instrument with a 4x250 mm CarboPac SA10 column. Ad = *Antho dichotoma*, Gb = *Geodia barretti*, Ml = *Mycale lingua*, PV = *Phakellia ventilabrum*. SE-01.3 and SE-01 are water extracts from *Geodia barretti*.

Sample	Fucose [mg/l]	Fucose [% of DW]	Arabinose [mg/l]	Arabinose [% of DW]	Galactose [mg/l]	Galactose [% of DW]	Rhamnose [mg/l]	Rhamnose [% of DW]	Glucose [mg/l]	Glucose [% of DW]	Xylose [mg/l]	Xylose [% of DW]	Mannose [mg/l]	Mannose [% of DW]
(1) Ad	0.15	0.094	0.97	0.62	3.2	2.1	n.a.	n.a.	3.2	2.0	0.057	0.036	0.75	0.48
(2) Ad	0.15	0.096	0.93	0.60	3.1	2.0	n.a.	n.a.	3.0	2.0	0.059	0.038	0.74	0.48
(3) Ad	0.10	0.065	0.85	0.55	2.5	1.6	n.a.	n.a.	2.4	1.6	0.047	0.030	0.60	0.39
(1) Gb	0.17	0.27	0.055	0.085	0.18	0.29	0.026	0.041	0.42	0.65	0.015	0.023	0.43	0.67
(2) Gb	0.18	0.29	0.056	0.087	0.19	0.29	0.027	0.041	0.43	0.66	0.015	0.023	0.43	0.67
(3) Gb	0.18	0.28	0.050	0.077	0.18	0.27	0.025	0.038	0.41	0.63	0.015	0.024	0.43	0.66
(1) Ml	0.46	0.30	1.4	0.90	1.8	1.2	1.0	0.67	1.8	1.1	0.019	0.012	0.60	0.39
(2) Ml	0.36	0.23	1.2	0.74	1.4	0.92	0.74	0.47	1.4	0.89	0.016	0.010	0.46	0.29
(3) Ml	0.47	0.30	1.4	0.91	1.9	1.2	1.1	0.70	1.8	1.2	0.018	0.011	0.60	0.39
(1) Pv	0.78	0.50	1.2	0.77	0.62	0.4	n.a.	n.a.	1.6	1.0	0.016	0.010	0.46	0.29
(2) Pv	0.96	0.62	1.5	0.99	0.79	0.5	n.a.	n.a.	2.1	1.3	0.022	0.014	0.67	0.43
(3) Pv	0.85	0.54	1.4	0.87	0.68	0.4	n.a.	n.a.	1.9	1.2	0.023	0.014	0.51	0.33
(1)SE01.3	1.3643	0.863	0.4295	0.272	1.6306	1.03	0.0738	0.047	3.2458	2.05	0.0435	0.028	1.6159	1.02
(2)SE01.3	0.2615	0.827	0.0863	0.273	0.3261	1.03	0.0259	0.082	0.6451	2.04	0.0051	0.016	0.3158	1.00
(1) SE-01	1.2321	0.779	0.4524	0.286	1.7602	1.11	0.1183	0.075	3.4911	2.21	0.0677	0.043	1.5699	0.99
(2) SE-01	0.2467	0.780	0.0848	0.268	0.3444	1.09	0.0306	0.097	0.6929	2.19	0.0136	0.043	0.2878	0.91

Table 36: Data from monosaccharide analysis of marine sponges. Degradation of monosaccharides during sample preparation has been corrected for. Results obtained by HPAEC-PAD using a Dionex ISC 5000+ instrument with a 4x250 mm CarboPac SA10 column. Ad = *Antho dichotoma*, Gb = *Geodia barretti*, Ml = *Mycale lingua*, PV = *Phakellia ventilabrum*. SE-01.3 and SE-01 are water extracts from *Geodia barretti*.

Sample	Corr. Fucose [mg/l]	Corr. Fucose [% of DW]	Corr. Arabinose [mg/l]	Corr. Arabinose [% of DW]	Corr. Galactose [mg/l]	Corr. Galactose [% of DW]	Corr. Rhamnose [mg/l]	Corr. Rhamnose [% of DW]	Corr. Glucose [mg/l]	Corr. Glucose [% of DW]	Corr. Xylose [mg/l]	Corr. Xylose [% of DW]	Corr. Mannose [mg/l]	Corr. Mannose [% of DW]
(1) Ad	0.15	0.094	0.85	0.55	3.5	2.3	n.a.	n.a.	3.4	2.2	0.078	0.050	0.78	0.50
(2) Ad	0.15	0.097	0.82	0.53	3.4	2.2	n.a.	n.a.	3.3	2.1	0.082	0.053	0.77	0.50
(3) Ad	0.10	0.065	0.75	0.49	2.7	1.7	n.a.	n.a.	2.6	1.7	0.065	0.042	0.62	0.40
(1) Gb	0.159	0.248	0.053	0.083	0.177	0.277	0.025	0.039	0.406	0.634	0.017	0.026	0.43	0.67
(2) Gb	0.172	0.266	0.055	0.085	0.181	0.281	0.026	0.040	0.416	0.644	0.017	0.026	0.43	0.67
(3) Gb	0.167	0.258	0.049	0.075	0.170	0.263	0.024	0.037	0.396	0.611	0.017	0.027	0.43	0.66
(1) Ml	0.46	0.30	1.2	0.79	2.0	1.3	0.92	0.59	1.9	1.2	0.026	0.017	0.63	0.40
(2) Ml	0.36	0.23	1.0	0.65	1.6	1.0	0.66	0.42	1.5	0.96	0.022	0.014	0.48	0.31
(3) Ml	0.47	0.30	1.3	0.80	2.0	1.3	0.97	0.62	1.9	1.2	0.024	0.016	0.63	0.40
(1) Pv	0.78	0.50	1.1	0.68	0.67	0.43	n.a.	n.a.	1.7	1.1	0.022	0.014	0.48	0.31
(2) Pv	0.96	0.62	1.4	0.87	0.85	0.55	n.a.	n.a.	2.2	1.4	0.030	0.019	0.70	0.45
(3) Pv	0.85	0.55	1.2	0.77	0.73	0.47	n.a.	n.a.	2.0	1.3	0.031	0.020	0.54	0.34
(1)SE01.3	1.372	0.868	0.378	0.239	1.760	1.113	0.066	0.042	3.483	2.202	0.060	0.038	1.684	1.065
(2)SE01.3	0.263	0.832	0.076	0.240	0.352	1.113	0.023	0.073	0.692	2.188	0.007	0.022	0.329	1.040
(1) SE-01	1.239	0.784	0.398	0.252	1.899	1.201	0.105	0.067	3.746	2.369	0.094	0.059	1.636	1.034
(2) SE-01	0.248	0.784	0.075	0.236	0.372	1.175	0.027	0.086	0.744	2.351	0.019	0.059	0.300	0.948

Chromatograms from the monosaccharide analysis of sponge samples are shown in the following figures. Figure 36: *A. dichotoma*, Figure 37: *G. barretti*, Figure 38: *M. lingua*, and Figure 39: *P. ventilabrum*. Concentrations for the different levels of standard mixes are shown in Table 37.

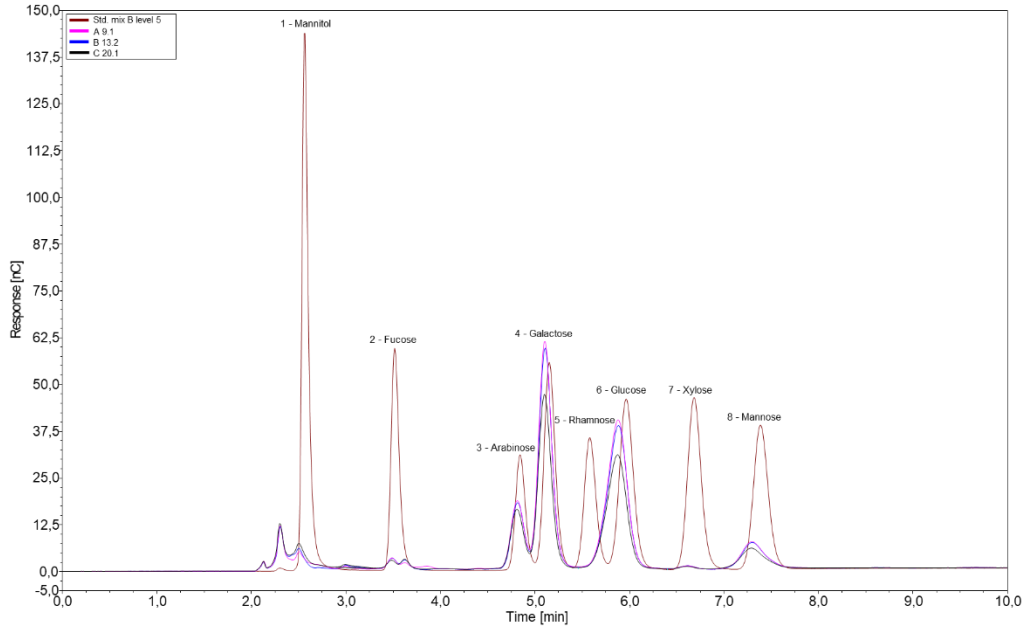

Figure 36: Chromatogram from monosaccharide analysis of *A. dichotoma*. Marked in red is Std. mix B level 5. Results obtained by HPAEC-PAD using a Dionex ISC 5000+ instrument with a 4x250 mm CarboPac SA10 column.

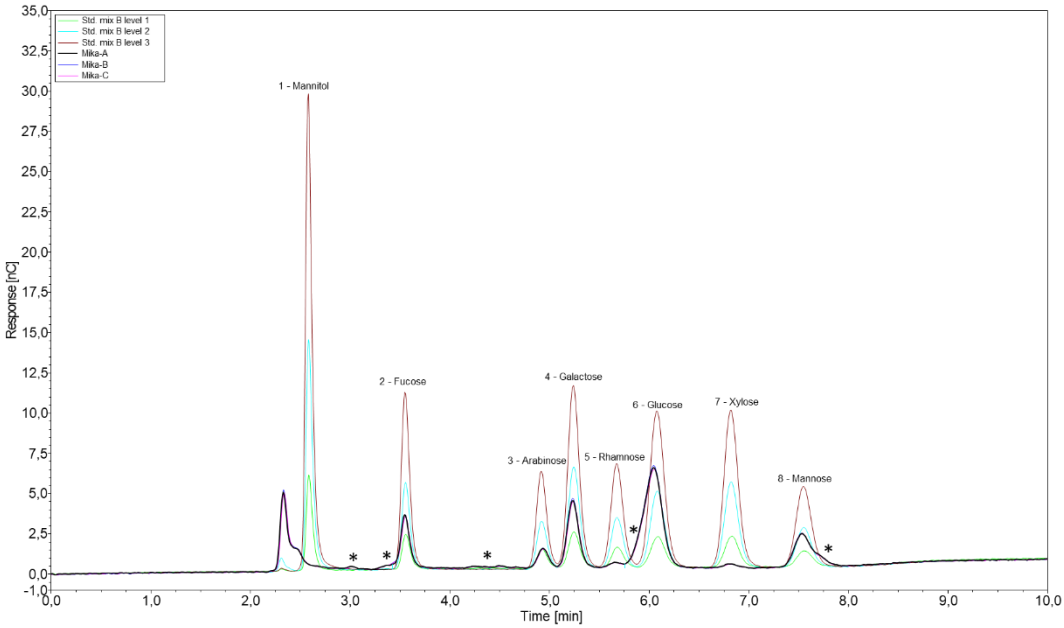

Figure 37: Chromatogram from monosaccharide analysis of *G. barretti*. The following standard mixes are shown in the chromatogram green: level 1, cyan: level 2, red: level 3. *Some signals in the chromatogram did not correspond with the monosaccharides tested for. Results obtained by HPAEC-PAD using a Dionex ISC 5000+ instrument with a 4x250 mm CarboPac SA10 column.

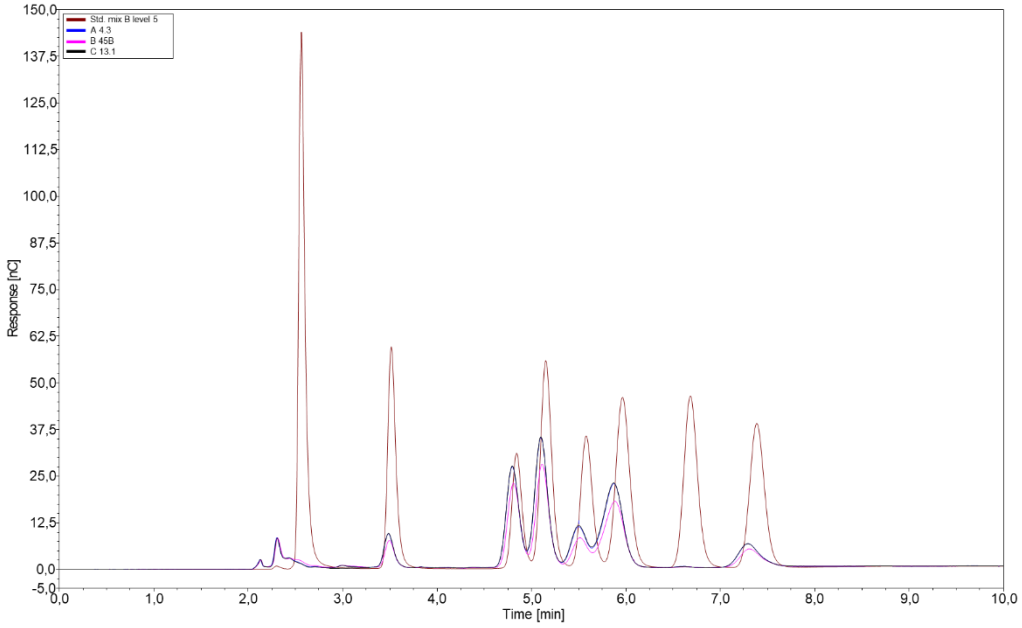

Figure 38: Chromatogram from monosaccharide analysis of *M. lingua*. Marked in red is Std. mix B level 5. Results obtained by HPAEC-PAD using a Dionex ISC 5000+ instrument with a 4x250 mm CarboPac SA10 column.

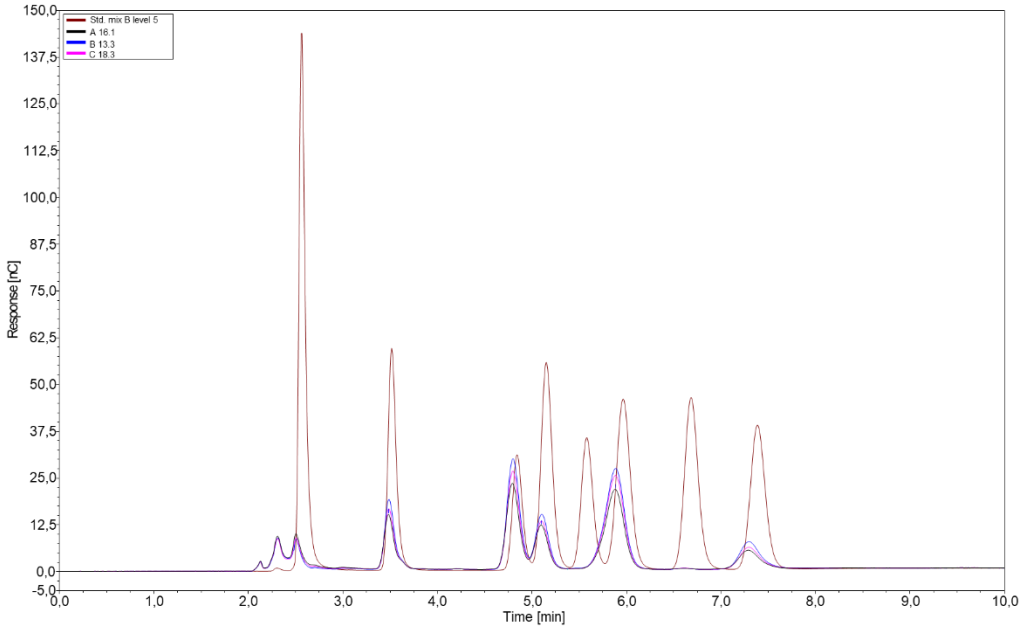

Figure 39: Chromatogram from monosaccharide analysis of *P. ventilabrum*. Marked in red is Std. mix B level 5. Results obtained by HPAEC-PAD using a Dionex ISC 5000+ instrument with a 4x250 mm CarboPac SA10 column.

Table 37: Concentrations of seven standard mixes used in neutral monosaccharide analysis.

	Concentration of given monosaccharide [mg/L]						
Level	**Mannitol**	**Fuc**	**Ara**	**Gal**	**Rha**	**Man**	**Xyl**
1	15	10	5	10	10	10	10
2	7.5	5	2.5	5	5	5	5
3	3.75	2.5	1.25	2.5	2.5	2.5	2.5
4	1.5	1	0.5	1	1	1	1
5	0.75	0.5	0.25	0.5	0.5	0.5	0.5
6	0.375	0.25	0.125	0.25	0.25	0.25	0.25
7	0.15	0.1	0.05	0.1	0.1	0.1	0.1

Appendix D Total amino acid analysis – raw data and calculations

Raw data of the total amino acid analysis of the sponge samples is shown in the following tables.

Antho dichotoma raw data

Table 38: Total amino acid analysis of *A. dichotoma*. Results obtained by HPLC using a Dionex UltiMate® 3000 HPLC+ focused instrument with a 3,9x150 mm 4 µm Nova-Pak C18 column.

No.	Peak Name	Retention Time [min]	Area [mV*min]	Height [mV]	Relative Area [%]	Relative Height [%]	Amount [µmol/l]
1	Asp	1.553	2.928	24.815	11.94	18.26	1.5355
2	Glu	2.425	1.961	8.374	8.00	6.16	0.9335
3	Asn	3.380	0.000	0.023	0.00	0.02	0.0001
4	His	4.360	0.152	1.031	0.62	0.76	0.1066
5	Ser	4.752	0.889	5.159	3.63	3.80	0.5742
6	Gln	4.965	0.020	0.309	0.08	0.23	0.3824
7	Gly/Arg	8.048	11.070	44.175	45.15	32.51	6.9073
8	Thr	8.688	0.855	3.637	3.49	2.68	0.6218
9	Ala	13.195	2.121	10.719	8.65	7.89	1.6084
10	Tyr	14.610	0.048	0.334	0.20	0.25	0.0314
11	Aba	16.445	0.176	0.965	0.72	0.71	0.0903
12	Met	18.200	0.243	1.781	0.99	1.31	0.1372
13	Val	18.500	0.854	6.932	3.48	5.10	0.4446
14	Phe	18.995	0.662	5.328	2.70	3.92	0.4037
15	Ile	19.973	0.570	5.070	2.33	3.73	0.2922
16	Leu	20.320	1.121	9.641	4.57	7.09	0.6398
17	Lys	22.018	0.850	7.607	3.47	5.60	0.5261
Total:			24.520	135.898	100.00	100.00	15.2351

Geodia barretti raw data

Table 39: Total amino acid analysis of *G. barretti*. Results obtained by HPLC using a Dionex UltiMate® 3000 HPLC+ focused instrument with a 3,9x150 mm 4 µm Nova-Pak C18 column.

No.	Peak Name	Retention Time [min]	Area [mV*min]	Height [mV]	Relative Area [%]	Relative Height [%]	Amount [µmol/l]
1	Asp	1.542	3.160	27.238	16.00	22.00	1.6570
2	Glu	2.413	2.070	9.387	10.48	7.58	0.9856
3	Asn	3.383	0.002	0.030	0.01	0.02	0.0010
4	His	4.348	0.213	1.412	1.08	1.14	0.1494
5	Ser	4.733	1.062	6.205	5.37	5.01	0.6853
6	Gln	4.953	0.020	0.328	0.10	0.27	0.3938
7	Gly/Arg	8.022	4.125	12.849	20.88	10.38	2.5741
8	Thr	8.670	1.281	5.253	6.48	4.24	0.9316
9	Ala	13.162	1.684	8.921	8.52	7.21	1.2767
10	Tyr	14.582	0.028	0.188	0.14	0.15	0.0182
11	Aba	16.395	0.017	0.140	0.08	0.11	0.0086
12	Met	18.172	0.274	2.511	1.39	2.03	0.1547
13	Val	18.472	1.448	12.319	7.33	9.95	0.7537
14	Phe	18.968	0.719	6.069	3.64	4.90	0.4384
15	Ile	19.947	1.122	9.328	5.68	7.54	0.5752
16	Leu	20.293	1.748	14.507	8.85	11.72	0.9983
17	Lys	21.995	0.780	7.093	3.95	5.73	0.4829
Total:			19.753	123.780	100.00	100.00	

Mycale lingua raw data

Table 40: Total amino acid analysis of *M. lingua*. Results obtained by HPLC using a Dionex UltiMate® 3000 HPLC+ focused instrument with a 3,9x150 mm 4 µm Nova-Pak C18 column.

No.	Peak Name	Retention Time [min]	Area [mV*min]	Height [mV]	Relative Area [%]	Relative Height [%]	Amount [µmol/l]
1	Asp	1.540	1.956	16.700	10.01	14.79	1.0258
2	Glu	2.413	1.717	7.432	8.79	6.58	0.8177
3	Asn	3.385	0.000	0.016	0.00	0.01	0.0000
4	His	4.353	0.176	1.168	0.90	1.03	0.1236
5	Ser	4.737	1.006	5.919	5.15	5.24	0.6497
6	Gln	4.948	0.034	0.352	0.17	0.31	0.6592
7	Gly/Arg	8.027	7.964	30.818	40.75	27.30	4.9698
8	Thr	8.670	0.882	3.579	4.51	3.17	0.6415
9	Ala	13.180	0.884	5.013	4.52	4.44	0.6707
10	Tyr	14.605	0.329	2.334	1.68	2.07	0.2142
11	Aba	16.413	0.076	0.596	0.39	0.53	0.0391
12	Met	18.190	0.270	2.288	1.38	2.03	0.1524
13	Val	18.488	1.025	8.187	5.24	7.25	0.5332
14	Phe	18.982	0.491	4.272	2.51	3.78	0.2995
15	Ile	19.962	0.707	6.274	3.62	5.56	0.3625
16	Leu	20.312	1.139	9.866	5.83	8.74	0.6503
17	Lys	22.010	0.889	8.076	4.55	7.15	0.5506
Total:			19.547	112.891	100.00	100.00	

Phakellia ventilabrum raw data

Table 41: Total amino acid analysis of *P. ventilabrum*. Results obtained by HPLC using a Dionex UltiMate® 3000 HPLC+ focused instrument with a 3,9x150 mm 4 µm Nova-Pak C18 column.

No.	Peak Name	Retention Time [min]	Area [mV*min]	Height [mV]	Relative Area [%]	Relative Height [%]	Amount [µmol/l]
1	Asp	1.553	2.499	20.729	12.67	17.57	1.3108
2	Glu	2.572	2.073	10.226	10.51	8.67	0.9872
3	Asn	3.525	0.003	0.018	0.01	0.02	0.0013
4	His	4.458	0.176	1.082	0.89	0.92	0.1237
5	Ser	4.842	1.070	6.145	5.42	5.21	0.6911
6	Gln	5.057	0.032	0.407	0.16	0.35	0.6172
7	Gly/Arg	8.248	6.421	24.367	32.54	20.65	4.0064
8	Thr	8.890	1.065	4.493	5.39	3.81	0.7743
9	Ala	13.265	1.267	6.753	6.42	5.72	0.9609
10	Tyr	14.637	0.284	1.989	1.44	1.69	0.1851
11	Aba	16.432	0.064	0.469	0.32	0.40	0.0328
12	Met	18.187	0.198	1.791	1.00	1.52	0.1120
13	Val	18.485	1.111	9.463	5.63	8.02	0.5784
14	Phe	18.977	0.660	5.622	3.34	4.76	0.4020
15	Ile	19.953	0.847	7.588	4.29	6.43	0.4342
16	Leu	20.302	1.296	10.760	6.57	9.12	0.7401
17	Lys	22.005	0.665	6.094	3.37	5.16	0.4119
Total:			19.733	117.996	100.00	100.00	

Amino acid content calculations

The total amino acid analysis gave an amount of µmol/L for each analyte, this was used to calculate the total weight of the amino acids combined for each of the four sponges (see Figure 12). The total % of DW in the sample represented by the individual amino acids was found using the following equation.

$$\frac{\text{Amount of AA [µmol/l]} \times 10^{-6} \times \text{sample volume [L]} \times \text{AA mW [g/mol]}}{\text{weight of starting sample [g]}} \times 100\% = \%\ \text{of sample as AA}$$

The amount of AA represents the emission of an amino acid during the analysis. A factor of 10^{-6} is used to convert µmol to mol. Sample volume is equal to the total volume of the sample if the whole sample was diluted. As this analysis had a sample suspended in 10 mL solution and diluted

1:500, the whole sample volume would be 5 L. Amino acid molecular weights used are shown in Table 42. The weights of the starting samples were 0.05 g. The following is an example of the calculation of asparagine content in *A. dichotoma*.

$$\frac{1.5355\ \mu mol/L \times 10^{-6} \times 5L \times 133\ g/mol}{0{,}05\ g} \times 100\% = 2.04\ \%$$

Combining the value for each amino acid gave a total value of amino acids in the four sponge species. This was done once assuming the Gly/Arg emission consisted of only glycine, and once assuming it only consisted of arginine.

Table 42: Amino acids detected in the total amino acid analysis, their three-letter abbreviation, and molecular weight (68).

Amino acid	Abbreviation	Molecular weight [Da]
Alanine	Ala	89
Aminobutyric acid	Aba	103
Arginine	Arg	174
Asparagine	Asn	132
Aspartic acid	Asp	133
Glutamine	Gln	146
Glutamic acid	Glu	147
Glycine	Gly	75
Histidine	His	155
Isoleucine	Ile	131
Leucine	Leu	131
Lysine	Lys	146
Methionine	Met	149
Phenylalanine	Phe	165
Serine	Ser	105
Threonine	Thr	119
Tyrosine	Tyr	181
Valine	Val	117

Appendix E NMR spectroscopy of sponge samples

This section contains NMR spectra recorded of a calcium precipitated polysaccharide extract from *G. barretti.*

H2BC

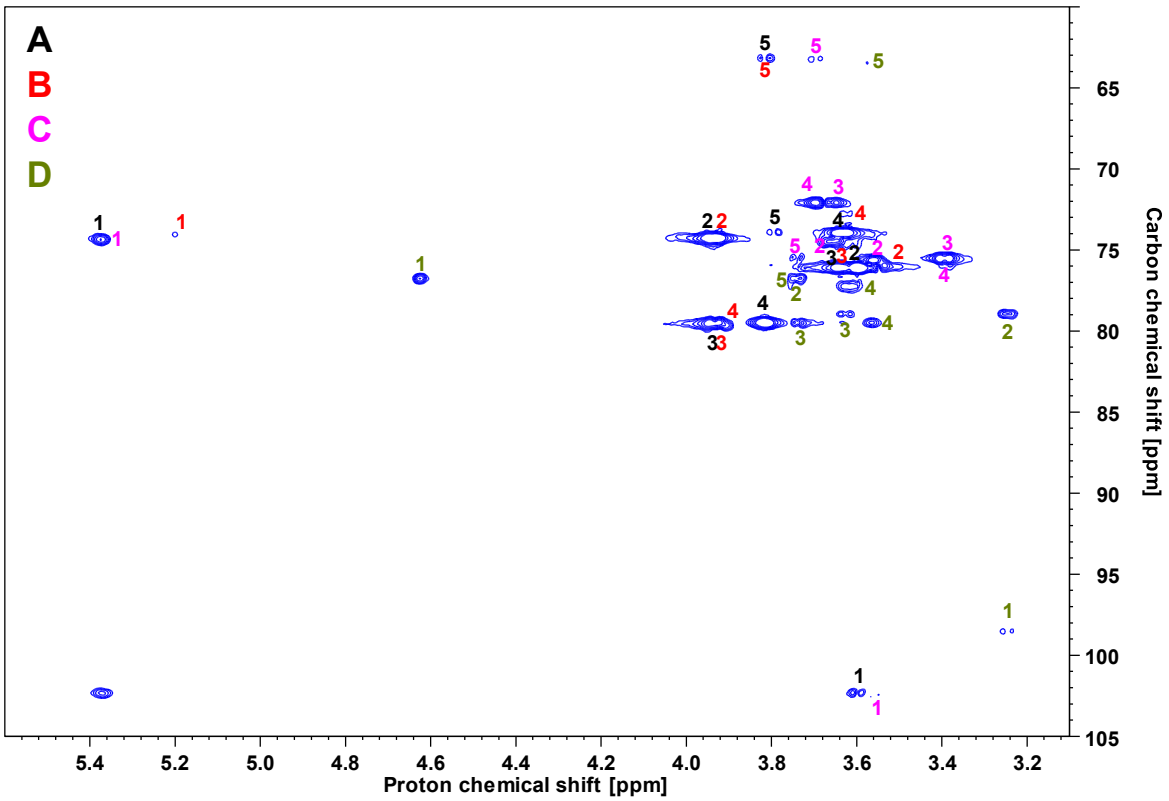

Figure 40: H2BC spectrum recoded of a calcium precipitated polysaccharide extract from the marine sponge *G. barretti*. Numbers on the spectrum correspond to which correlations were observed from a given position in the spin system. Spin systems A-D are color coded. Spectrum recorded using an 800 MHz Avance III HD instrument.

As the HMBC spectrum contains a lot more correlations than the H2BC spectrum, only correlations from spin system A were included as an example.

HMBC

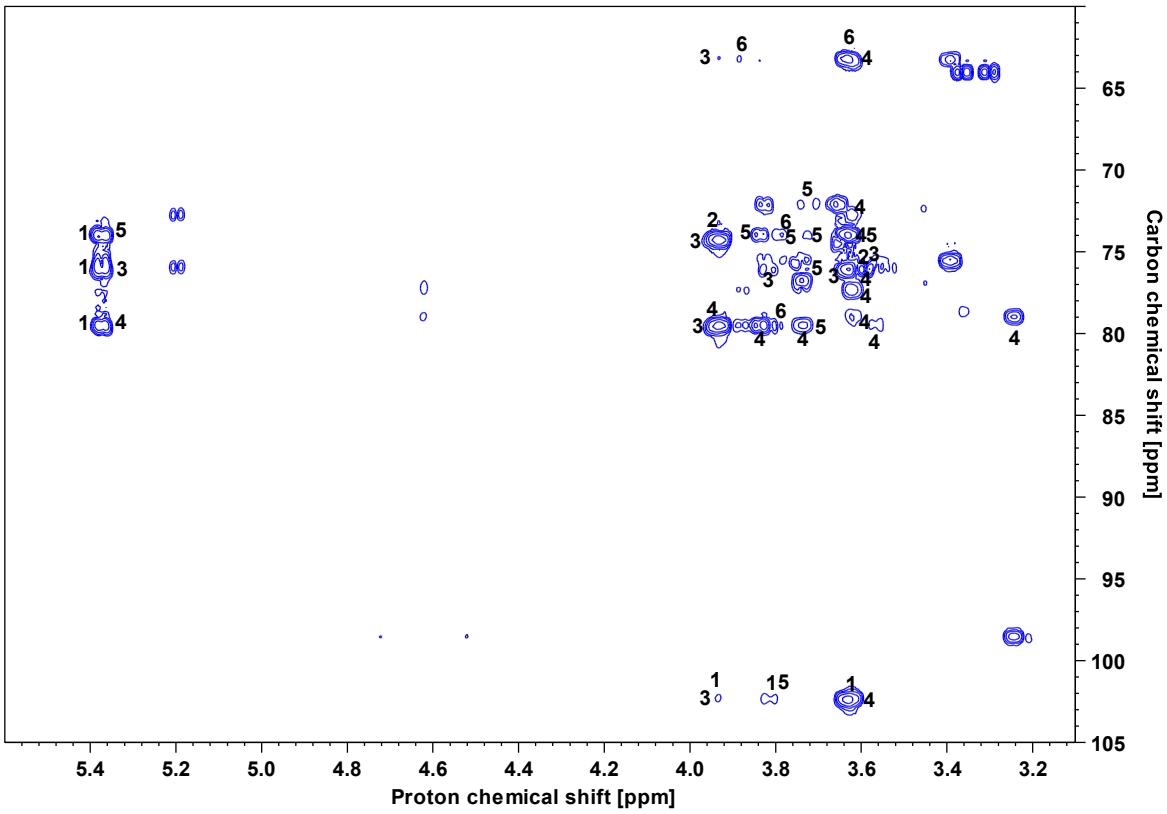

Figure 41: HMBC spectrum recoded of a calcium precipitated polysaccharide extract from the marine sponge *G. barretti*. Numbers on the spectrum correspond to which correlations could be observed from the different positions in spin system A. Spectrum recorded using an 800 MHz Avance III HD instrument.

The following tables contain observed H2BC and HMBC correlations from spin systems B, C, and D.

Table 43: H2BC and HMBC correlations for spin system B of a polysaccharide extract from the marine sponge *G. barretti*. Position corresponding to the correlation is written in parenthesis. (-) indicates the correlation does not correspond to an identified signal within the spin system.

Position in spin system B	**H2BC ^{13}C Correlations**	**H2BC ^{1}H Correlations**	**HMBC ^{13}C Correlations**	**HMBC ^{1}H Correlations**
B1(5.20 – 94.6)	74.0 (C2)	3.54 (H2)	75.9 (C3)	-
	-	-	72.6 (C5)	-
B2 (3.54 – 74.0)	75.9 (C3)	3.93 (H3)	-	3.63 (H4)
B3 (3.93 – 75.9)	79.5 (C4)	3.63 (H4)	102.3 (-)	5.37 (-)
	-	-	79.5 (C4)	3.82 (-)
	-	-	74.3 (-)	3.63 (H4)
	-	-	63.1 (-)	3.60 (-)
B4 (3.63 – 79.5)	78.9 (-)	3.91 (H5)	102.3 (-)	5.37 (-)
	77.2 (-)	3.82 (-)	78.9 (-)	3.93 (H3)
	73.9 (-)	3.74 (-)	77.2 (-)	3.87 (-)
	72.6 (C5)	3.56 (-)	76.0 (C3)	3.74 (-)
	-	-	74.0 (C2)	3.56 (-)
	-	-	72.6 (C5)	3.24 (-)
	-	-	63.1 (-)	-
B5 (3.91 – 72.6)	63.2 (C6)	3.79 (H6)	79.5 (C4)	
B6 (3.79 – 63.2)	-	3.82 (-)	79.5 (C4)	3.89 (-)
	-	-	73.9 (-)	3.63 (H4)
	-	-	-	3.39 (-)

Table 44: H2BC and HMBC correlations for spin system C of a polysaccharide extract from the marine sponge *G. barretti*. Position corresponding to the correlation is written in parenthesis. (-) indicates the correlation does not correspond to an identified signal within the spin system.

Position in spin system C	**H2BC ^{13}C Correlations**	**H2BC ^{1}H Correlations**	**HMBC ^{13}C Correlations**	**HMBC ^{1}H Correlations**
C1 (5.36 – 102.5)	74.3 (C2)	3.56 (H2)	79.5 (-)	3.63 (-)
	-	-	75.7 (C3)	-
	-	-	74.0 (-)	-
C2 (3.56 – 74.4)	75.6 (C3)	3.66 (H3)	96.5 (-)	3.66 (H3)
	-	-	79.5 (-)	3.39 (H4)
C3 (3.66 – 75.6)	72.0 (C4)	3.39 (H4)	78.9 (-)	5.36 (H1)
	-	-	74.4 (C2)	3.75 (-)
	-	-	72.0 (C4)	3.56 (H2)
	-	-	-	3.39 (H4)
C4 (3.39 – 72.0)	75.5 (C5)	3.69 (H5)	75.6 (C3)	3.82 (-)
	-	-	63.2 (C6)	3.74 (H6)
	-	-	-	3.66 (H3)
C5 (3.69 – 75.5)	63.2 (C6)	3.73 (H6)	72.0 (C4)	5.36 (H1)
	-	-	63.2 (C6)	3.82 (-)
	-	-	-	3.78 (-)
	-	-	-	3.39 (H4)
C6 (3.73 – 63.2)	79.5 (-)	3.91 (-)	75.5 (C5)	3.89 (-)
	-	-	-	3.63 (-)
	-	-	-	3.39 (H4)

Table 45: H2BC and HMBC correlations for spin system D of a polysaccharide extract from the marine sponge *G. barretti*. Position corresponding to the correlation is written in parenthesis. (-) indicates the correlation does not correspond to an identified signal within the spin system.

Position in spin system D	**H2BC ^{13}C Correlations**	**H2BC ^{1}H Correlations**	**HMBC ^{13}C Correlations**	**HMBC ^{1}H Correlations**
D1 (4.62 – 98.5)	76.7 (C2)	3.24 (H2)	78.9 (C3)	3.24 (C2)
	-	-	77.2 (C5)	-
	-	-	-	-
D2 (3.24 – 76.7)	78.9 (C3)	3.74 (H3)	98.5 (C1)	3.74 (H3)
	-	-	78.9 (C3)	-
D3 (3.74 – 78.9)	79.5 (C4)	3.63 (H4)	98.5 (C1)	4.62 (H1)
	-	-	79.5 (C4)	3.82 (-)
	-	-	76.7 (C2)	3.63 (H4)
	-	-	72.0 (-)	3.24 (H2)
D4 (3.63 – 79.5)	78.9 (C3)	3.91 (-)	102.3 (-)	5.37 (-)
	77.2 (C5)	3.82 (-)	78.9 (C3)	3.93 (-)
	73.9 (-)	3.74 (C3)	77.2 (C5)	3.87 (H6')
	72.6 (-)	3.56 (C5)	76.0 (-)	3.74 (H3)
	-	-	74.0 (-)	3.56 (H5)
	-	-	72.6 (-)	3.24 (H2)
	-	-	63.1 (-)	-
D5 (3.56 – 77.2)	63.4 (C6)	3.75 (H5)	98.5 (C1)	4.62 (H1)
	-	-	79.5 (C4)	3.63 (H4)
D6 (3.75 – 63.4)	-	-	-	-

As an example, correlations found from the anomeric signal of spin system A (5.37 ppm) are marked with a number corresponding to their position in spin system A.

TOCSY

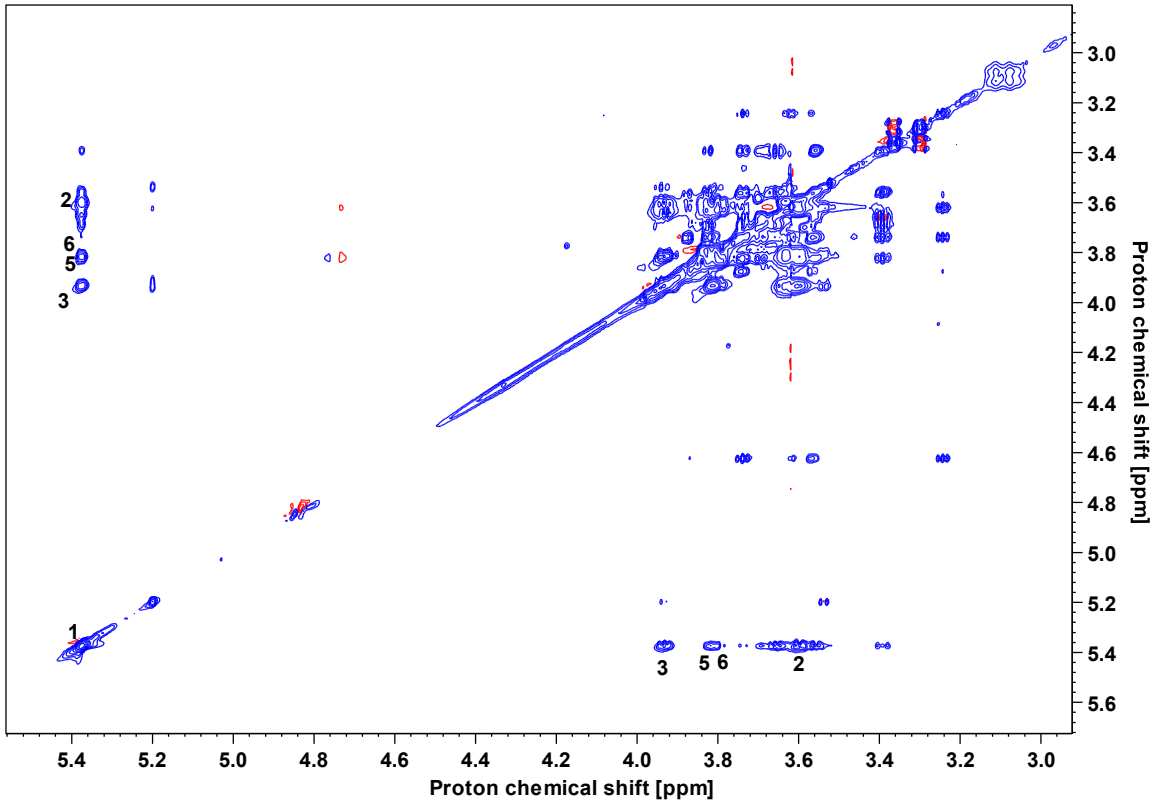

Figure 42: TOCSY spectrum recoded of a calcium precipitated polysaccharide extract from the marine sponge *G. barretti*. Numbers on the spectrum correspond to which positions in spin system A that were found using correlations from the 1 position (5.37 – 102.3 ppm). Spectrum recorded using an 800 MHz Avance III HD instrument.

Similar to the TOCSY spectrum, correlations found from the anomeric signal of spin system A (5,37 ppm) are marked with a number corresponding to their position in spin system A.

HSQC-TOCSY

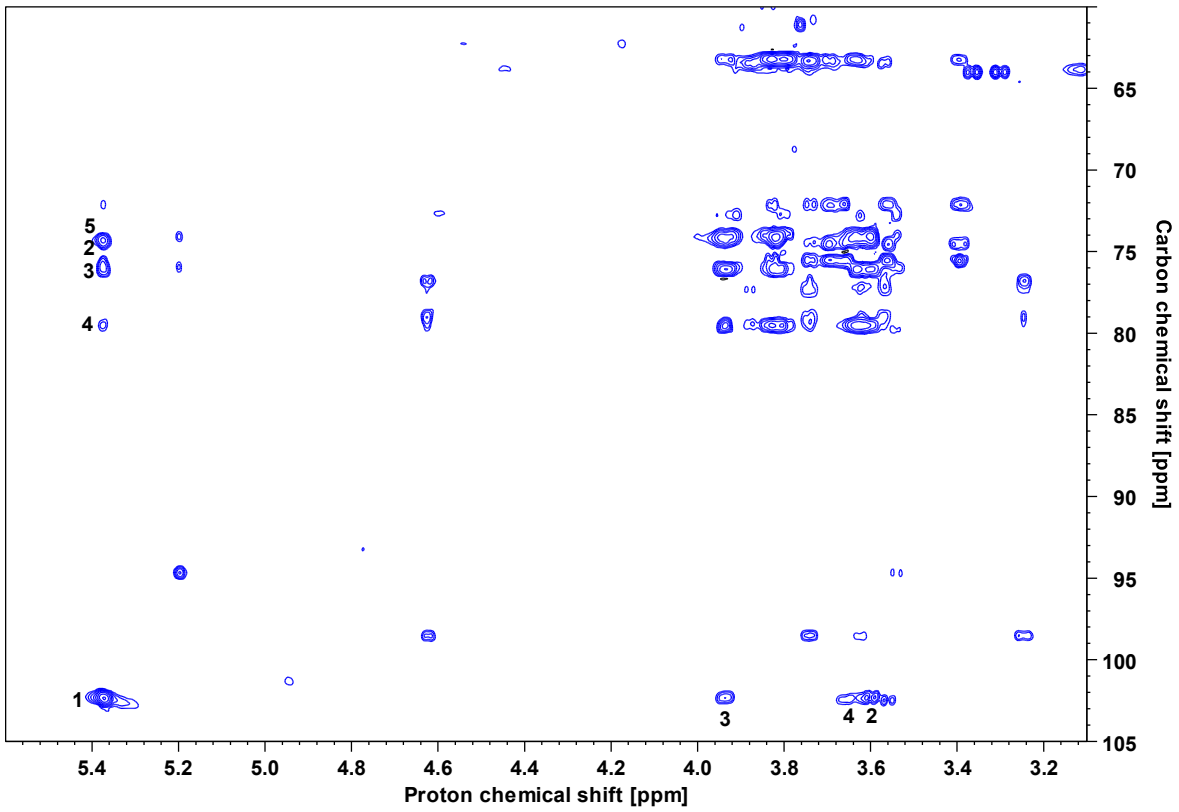

Figure 43: HSQC-TOCSY spectrum recoded of a calcium precipitated polysaccharide extract from the marine sponge *G. barretti*. Numbers on the spectrum correspond to which positions in spin system A that were found using correlations from the 1 position (5.37 – 102.3 ppm). Spectrum recorded using an 800 MHz Avance III HD instrument.

Cross peaks marked on the NOESY spectrum with their corresponding positions in the individual spin systems.

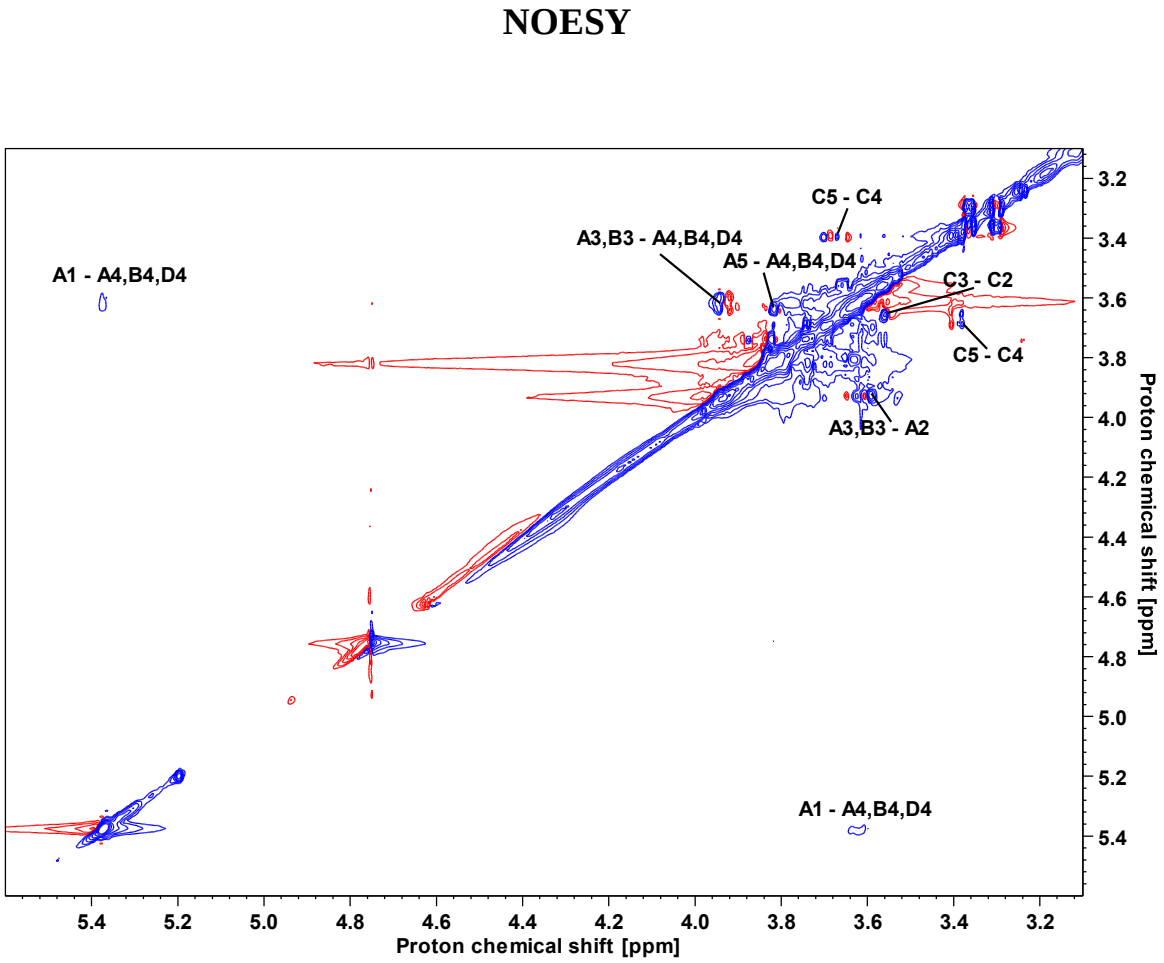

Figure 44: NOESY spectrum recoded of a calcium precipitated polysaccharide extract from the marine sponge *G. barretti*. Marked on the spectrum are cross peaks and which positions the correlations correspond to on the different spin systems. Spectrum recorded using an 800 MHz Avance III HD instrument.

Correlations from spin system A are marked in the IP-COSY spectrum.

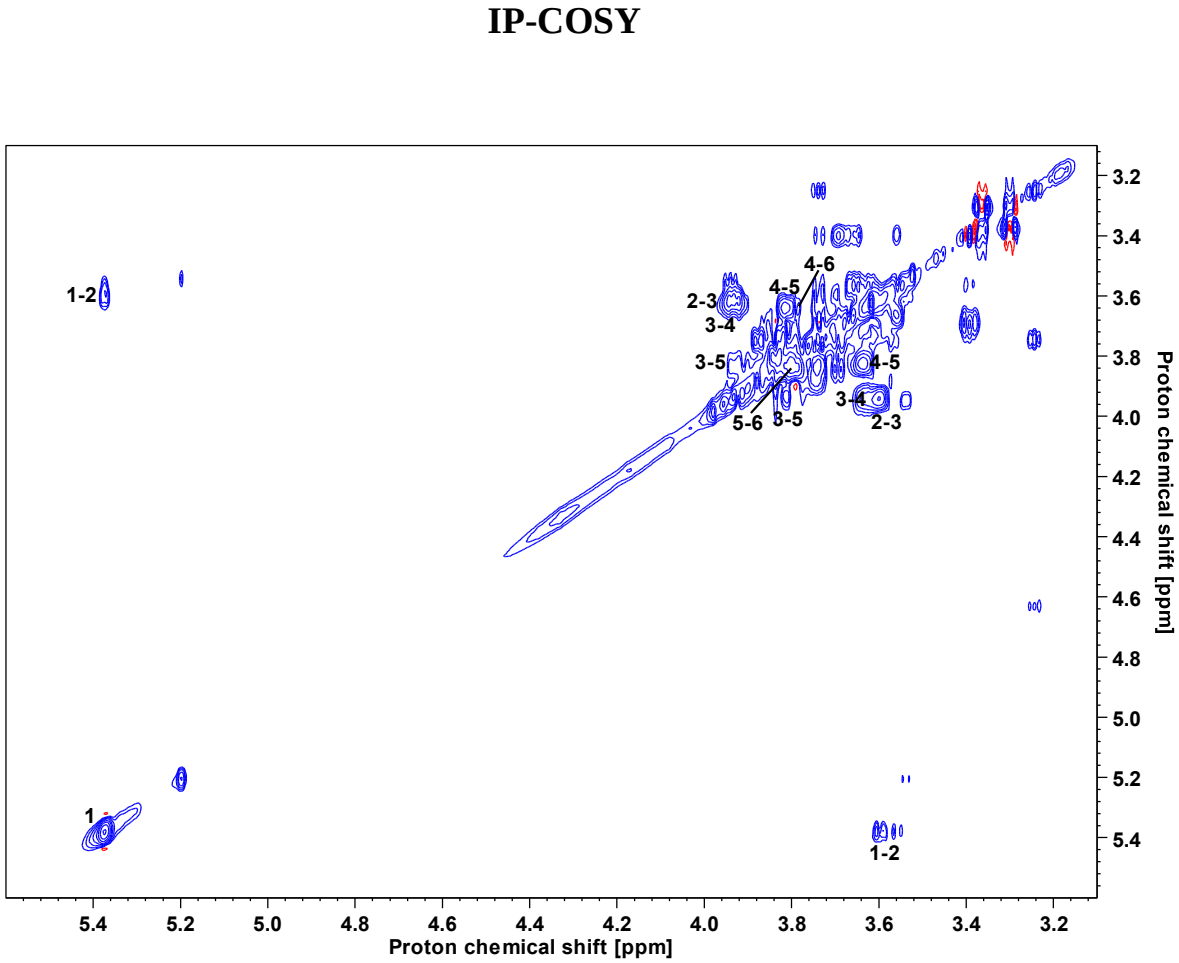

Figure 45: IP-COSY spectrum recoded of a calcium precipitated polysaccharide extract from the marine sponge *G. barretti*. Numbers on the spectrum correspond to which correlations are observed between various positions in spin system A. Spectrum recorded using an 800 MHz Avance III HD instrument.

Correlations found in the IP-COSY spectrum (Figure 45) from each of the four identified spin systems are listed in Table 46.

Table 46: IP-COSY correlations for spin systems A-D of a calcium precipitated polysaccharide extract from the marine sponge *G. barretti*.

Position and chemical shift [ppm] A	**COSY Corr. [ppm]**	**Position and chemical shift [ppm] B**	**COSY Corr. [ppm]**	**Position and chemical shift [ppm] C**	**COSY Corr. [ppm]**	**Position and chemical shift [ppm]**	**COSY Corr. [ppm]**
$1_{(A)}$	3.93	$1_{(B)}$	3.54	$1_{(C)}$	3.93	$1_{(D)}$	3.74
(5.37 – 102.3)	3.60	(5.20 – 94.6)	-	(5.36 – 102.5)	3.66	(4.62 – 98.5)	3.24
	-		-		3.60		-
	-		-		3.56		-
$2_{(A)}$	5.37	$2_{(B)}$	5.20	$2_{(C)}$	5.37	$2_{(D)}$	4.62
(3.60 – 74.3)	3.93	(3.54 – 74.0)	3.93	(3.56 – 74.4)	3.66	(3.24 – 76.7)	3.74
	-		-		3.39		3.63
$3_{(A)}$	5.37	$3_{(B)}$	5.37	$3_{(C)}$	5.37	$3_{(D)}$	3.88
(3.93 – 76.0)	3.82	(3.93 – 75.9)	3.82	(3.66 – 75.6)	3.56	(3.74 – 78.9)	3.24
	3.63		3.63		-		-
	3.60		3.60		-		-
	3.54		3.54		-		-
$4_{(A)}$	3.94	$4_{(B)}$	3.94	$4_{(C)}$	3.69	$4_{(D)}$	3.94
(3.63 – 79.5)	3.91	(3.63 – 79.5)	3.91	(3.39 – 72.0)	-	(3.63 – 79.5)	3.91
	3.82		3.82		-		3.82
	3.79		3.79		-		3.79
$5_{(A)}$	3.93	$5_{(B)}$	3.63	$5_{(C)}$	3.39	$5_{(D)}$	5.37
(3.82 – 73.9)	3.79	(3.91 – 72.6)	-	(3.69 – 75.5)	-	(3.56 – 77.2)	3.66
	3.74		-		-		3.39
	3.63		-		-		-
$6_{(A)}$	3.82	$6_{(B)}$	3.82	$6_{(C)}$	-	$6_{(D)}$	-
(3.79 – 63.1)	3.63	(3.79 – 63.2)	3.63	(3.73 – 63.2)	-	(3.75 – 63.4)	-

Appendix F Fucoidan fraction 6

IP-COSY spectrum recorded of fucoidan fraction 6. As some signals had low intensities not all correlations are visible at the selected intensity.

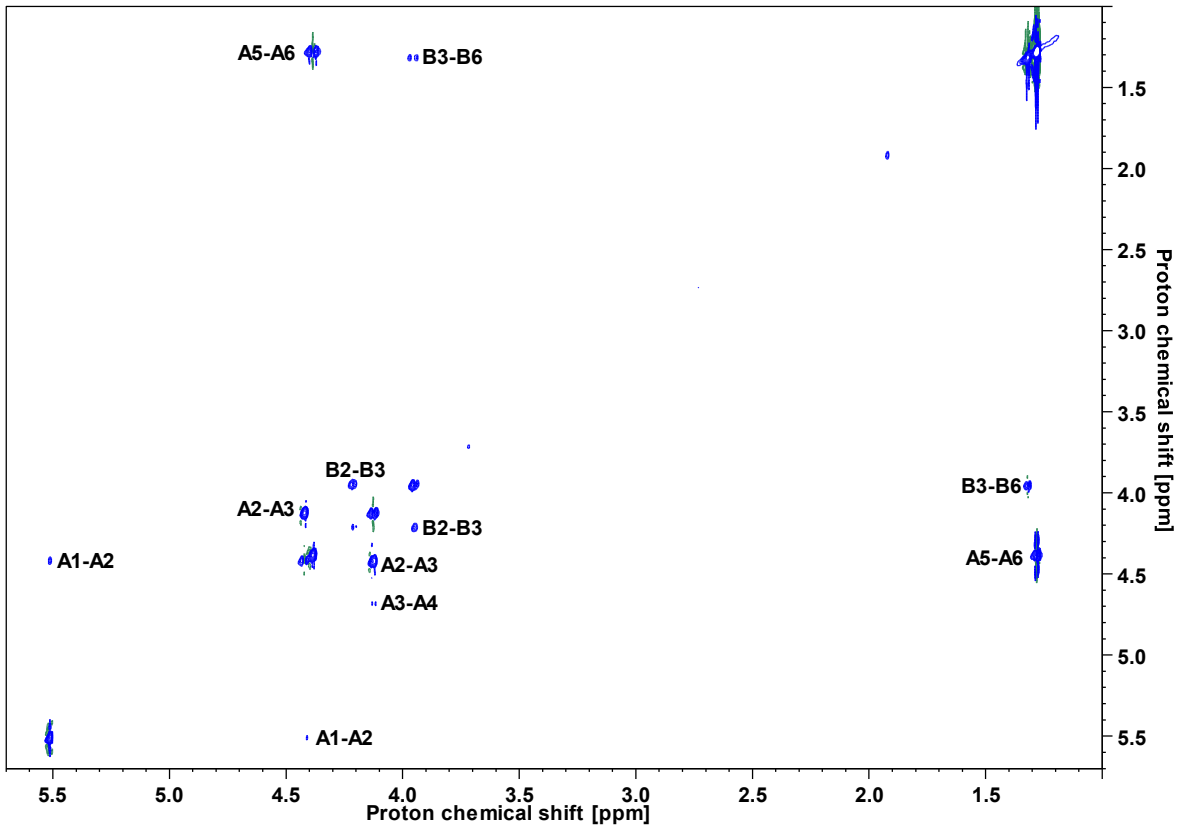

Figure 46: IP-COSY spectrum recoded of an enzymatically degraded fucoidan sample. Correlations from two spin systems (A and B) are labeled. Spectrum recorded using a Bruker Avance III HD 800 MHz instrument.

NOESY spectrum recorded of fucoidan fraction 6. Correlations are labeled with appropriate positions from spin systems A and B and marked in in red circles.

NOESY

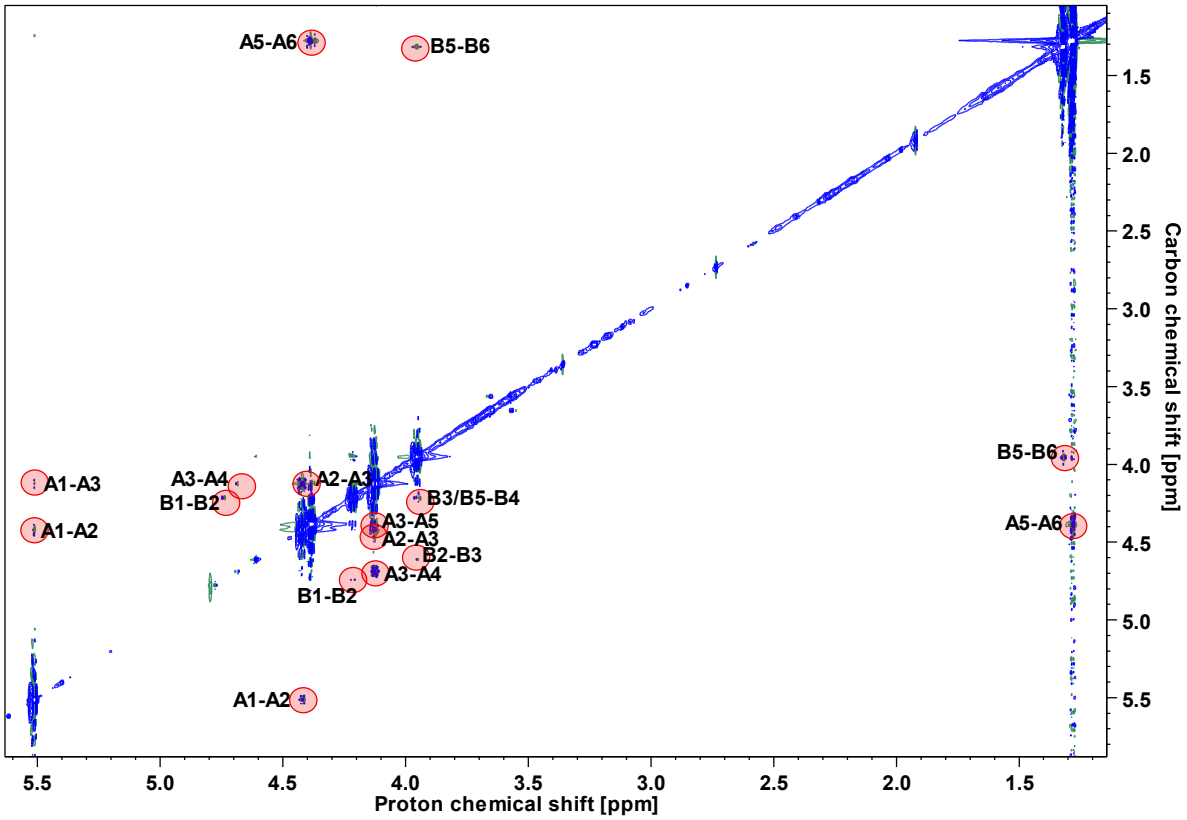

Figure 47: NOESY spectrum recoded of an enzymatically degraded fucoidan sample. Correlations from two spin systems (A and B) are labeled. Spectrum recorded using a Bruker Avance III HD 800 MHz instrument.

Appendix G Fucoidan fraction 4

H2BC spectrum recorded of fucoidan fraction 4. Marked in red circles are correlations from spin system A.

H2BC

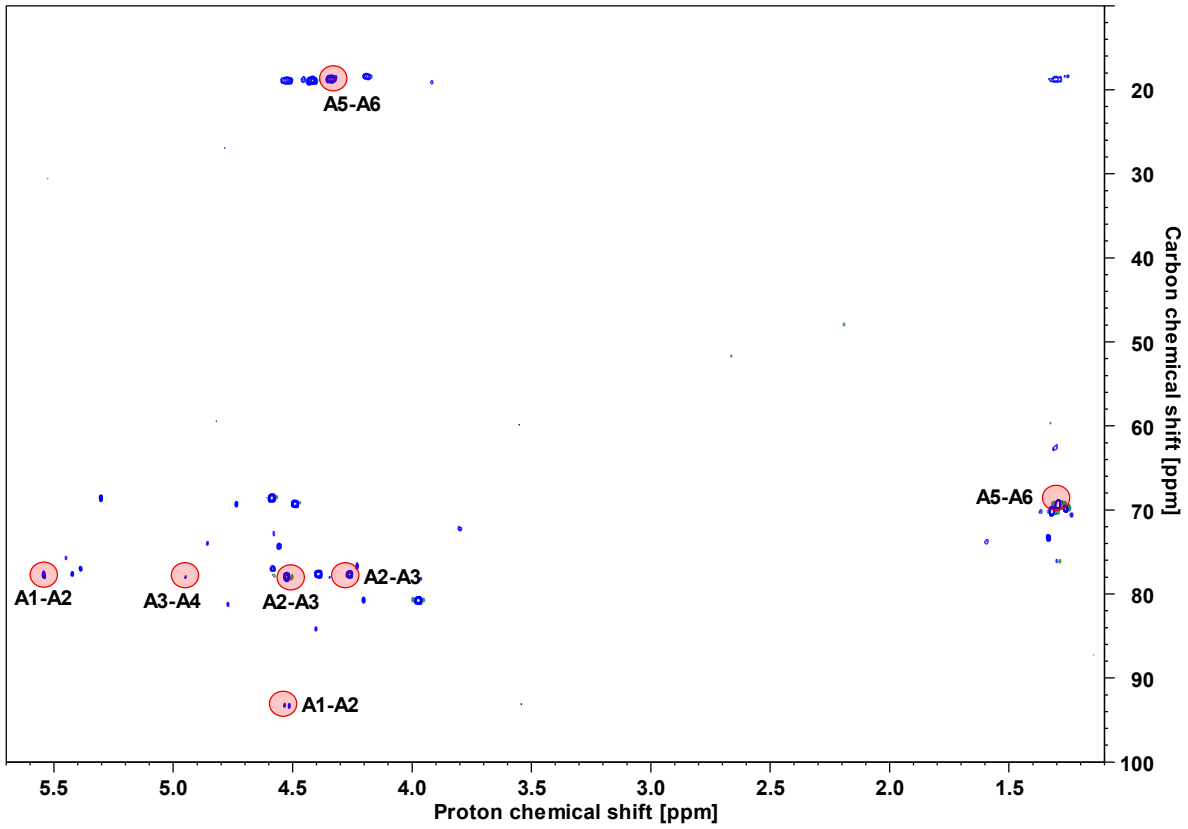

Figure 48: H2BC spectrum recoded of an enzymatically degraded fucoidan sample. Correlations from spin system A are labeled. Spectrum recorded using a Bruker Avance III HD 600 MHz instrument.

HMBC spectrum recorded of fucoidan fraction 4. Marked in red circles are correlations from spin system A.

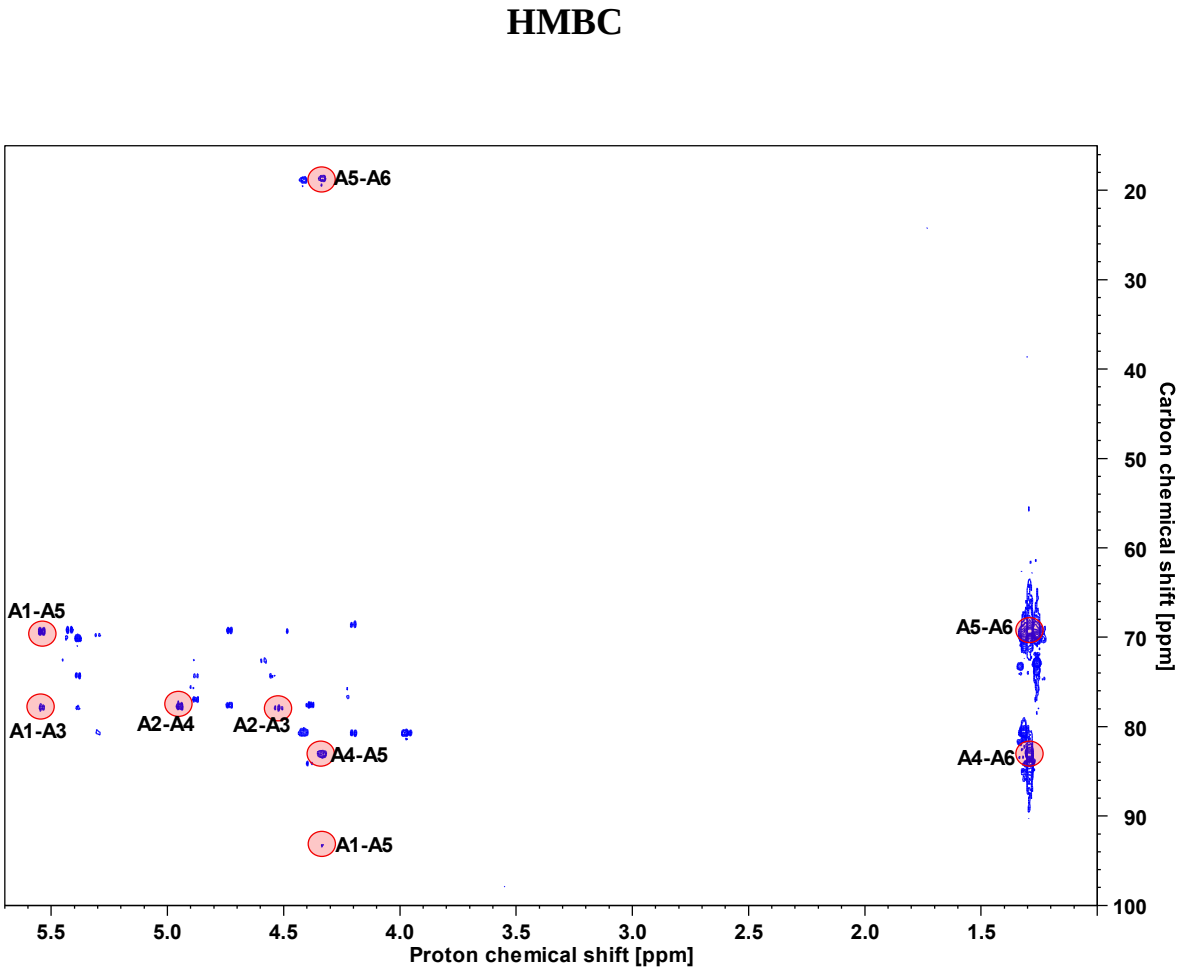

Figure 49: HMBC spectrum recoded of an enzymatically degraded fucoidan sample. Correlations from spin system A are labeled. Spectrum recorded using a Bruker Avance III HD 600 MHz instrument.

TOCSY spectrum recorded of fucoidan fraction 4. Marked in red circles are correlations from spin system A observed from the anomeric position (5.54 ppm).

TOCSY

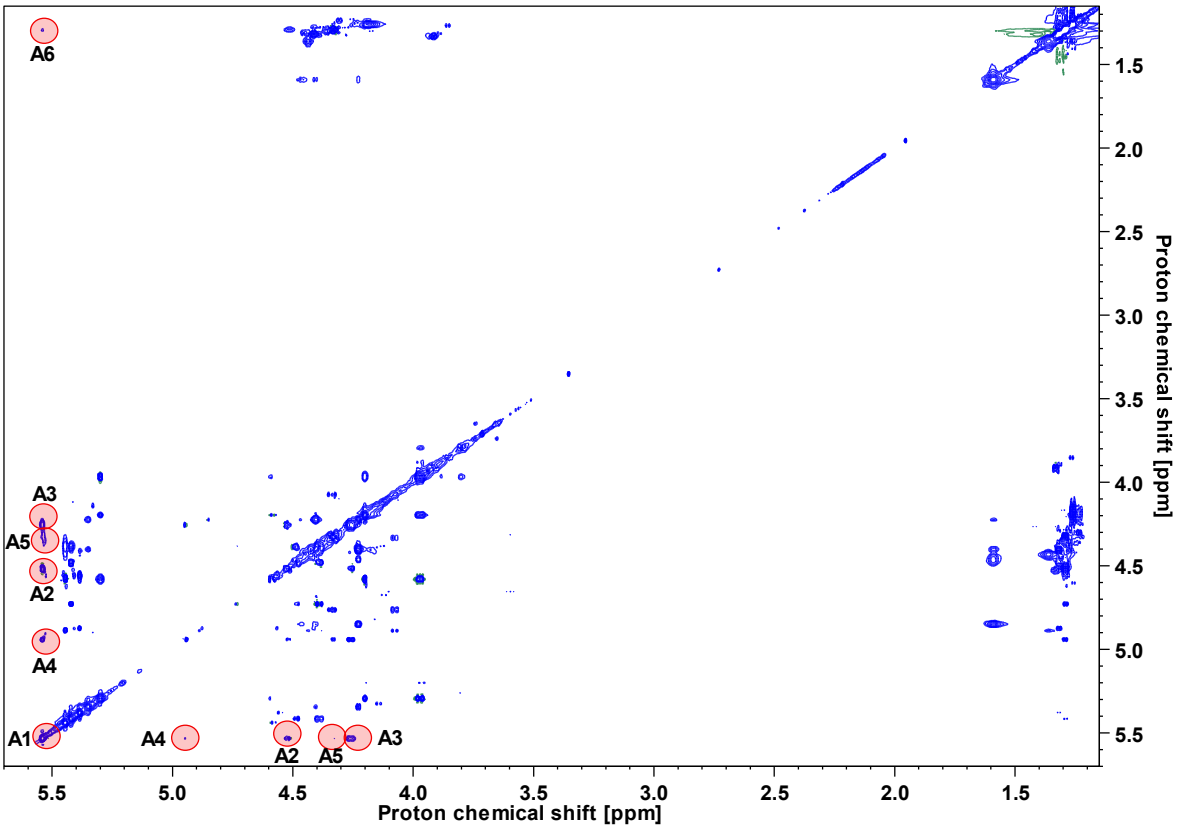

Figure 50: TOCSY spectrum recoded of an enzymatically degraded fucoidan sample. Correlations observed from anomeric position of spin system A are labeled. Spectrum recorded using a Bruker Avance III HD 600 MHz instrument.

The following tables contain observed H2BC and HMBC correlations from spin systems B-F.

Table 47: H2BC and HMBC correlations for spin system B of a fucoidan fraction. Position corresponding to the correlation is written in parenthesis. (-) indicates the correlation does not correspond to an identified signal within the spin system.

Position in spin system B [ppm]	H2BC ^{13}C Correlations [ppm]	H2BC ^{1}H Correlations [ppm]	HMBC ^{13}C Correlations [ppm]	HMBC ^{1}H Correlations [ppm]
B1 (4.77 – 97.9)	81.1 (C2)	-	-	-
B2 (4.34 – 81.1)	-	-	-	-

Table 48: H2BC and HMBC correlations for spin system C of a fucoidan fraction. Position corresponding to the correlation is written in parenthesis. (-) indicates the correlation does not correspond to an identified signal within the spin system.

Position in spin system C [ppm]	H2BC ^{13}C Correlations [ppm]	H2BC ^{1}H Correlations [ppm]	HMBC ^{13}C Correlations [ppm]	HMBC ^{1}H Correlations [ppm]
C1 (5.38 – 101.5)	77.0 (C2)	-	77.9 (-)	-
	-	-	74.3 (C3)	-
	-	-	70.1 (C5)	-
C2 (4.56 – 77.0)	74.3 (C3)	4.58 (H3)	-	4.88 (H4)
C3 (4.58 – 74.3)	-	-	-	4.88 (H4)
C4 (4.88 – 80.7)	-	4.20 (-)	77.0 (C2)	4.41 (H5)
	-	3.97 (-)	74.3 (C3)	3.97 (-)
	-	-	-	1.32 (H6)
C5 (4.41 – 70.1)	18.9 (C6)	1.32 (H6)	80.7 (C4)	5.38 (H1)
			18.9 (C6)	1.32 (H6)
C6 (1.32 – 18.9)			80.7 (C4)	4.41 (H5)
			70.1 (C5)	

Table 49: H2BC and HMBC correlations for spin system D of a fucoidan fraction. Position corresponding to the correlation is written in parenthesis. (-) indicates the correlation does not correspond to an identified signal within the spin system.

Position in spin system D [ppm]	H2BC ^{13}C Correlations [ppm]	H2BC ^{1}H Correlations [ppm]	HMBC ^{13}C Correlations [ppm]	HMBC ^{1}H Correlations [ppm]
D1 (5.30 – (-))	68.5 (C2)	-	80.7 (C3)	-
	-	-	69.8 (C5)	-
D2 (3.97 – 68.5)	80.7 (C3)	4.58 (H3)	80.7 (C3)	4.58 (H3)
	-	-	-	4.20 (H4)
D3 (4.58 – 80.7)	77.0 (-)	4.20 (H4)	72.6 (-)	5.30 (H1)
	72.9 (C4)	-	68.5 (C2)	4.42 (-)
	-	-	-	4.20 (H4)
	-	-	-	3.97 (H2)
D4 (4.20 – 72.9)	-	-	80.7 (C3)	1.26 (H6)
D5 (4.18 – 69.8)	18.4 (C6)	1.26 (H6)		1.26 (H6)
				5.30 (H1)
D6 (1.26 – 18.4)	-	-	72.9 (C4)	-
	-	-	69.8 (C5)	-

Table 50: H2BC and HMBC correlations for spin system E of a fucoidan fraction. Position corresponding to the correlation is written in parenthesis. (-) indicates the correlation does not correspond to an identified signal within the spin system.

Position in spin system E [ppm]	H2BC ^{13}C Correlations [ppm]	H2BC ^{1}H Correlations [ppm]	HMBC ^{13}C Correlations [ppm]	HMBC ^{1}H Correlations [ppm]
E1 (5.42 – 97.3)	77.6 (C2)	-	69.3 (C3)	-
E2 (4.49 – 77.6)	69.3 (C3)	4.39 (H3)	69.3 (C3)	4.95 (-)
	-	4.26 (-)	-	-
E3 (4.40 – 69.3)	84.1 (C4)	4.73 (H4)	84.1 (C4)	5.42 (H1)
	-	-	77.6 (C2)	4.73 (H4)
	-	-	-	4.49 (H2)
E4 (4.73 – 84.1)	-	-	77.6 (C2)	4.40 (H3)
	-	-	69.3 (C3)	-

Table 51: H2BC and HMBC correlations for spin system B of a fucoidan fraction. Position corresponding to the correlation is written in parenthesis. (-) indicates the correlation does not correspond to an identified signal within the spin system.

Position in spin system E [ppm]	**H2BC ^{13}C Correlations [ppm]**	**H2BC ^{1}H Correlations [ppm]**	**HMBC ^{13}C Correlations [ppm]**	**HMBC ^{1}H Correlations [ppm]**
E1 (5.45 – 100.8)	75.7 (C2)	-	72.5 (-)	-
E2 (4.58 – 75.7)	77.0 (-)	-	72.6 (-)	4.90 (-)
	72.9 (-)	-	68.5 (-)	-

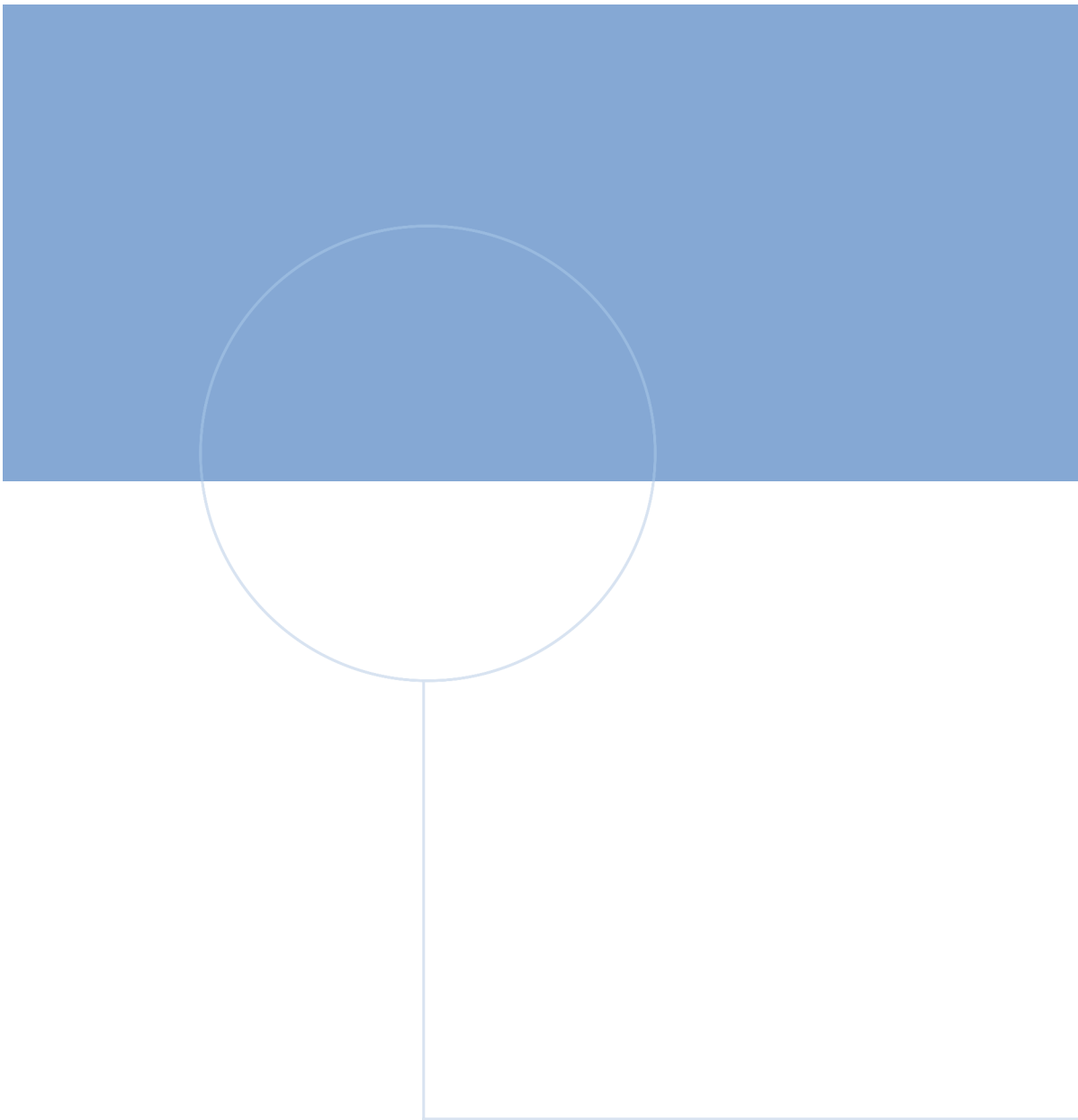

NTNU

Norwegian University of
Science and Technology